DOE-NEUP Final Report

Enhancement of the Extraction of Uranium from Seawater

Award Number
NU-15-MD-UMD-0601-02

Principal Investigator
Mohamad Al-Sheikhly
Department of Materials Science & Engineering
University of Maryland
College Park, MD 20742
Email: mohamad@umd.edu

Reporting Period
October 1, 2015 – September 30, 2018

Report Prepared by
Professor Mohamad Al-Sheikhly
Dr. Travis Dietz
Jaclyn Cua

Submitted December 31, 2018

Contents

I. Abstract

Due to the limited uranium resources available for recovery through mining and ore processing and to the environmental problems associated with these operations, the future of nuclear power depends, to a large extent, on the feasibility of recovery of uranium from the ocean. While the amounts of uranium in the ocean are sufficient to fulfill the nuclear industry for many thousands of years, recovery of uranium from the ocean is hampered by its low concentration (3.3 parts per billion) and the presence of many other solutes in seawater at comparable or much higher concentrations. Thus, the only hope for economically viable recovery of uranium from the ocean lies in the development of adsorbents with high capacity and high selectivity for uranium as present in the seawater environment (pH 8.1, U(VI) oxidation state, anionic carbonate complexes). Moreover, it is quite unlikely that economically viable recovery of uranium could be achieved if the adsorbent could be used only once. Thus it is essential to develop adsorbents that can be used through multiple cycles of uranium adsorption followed by elution of the uranium to regenerate the adsorbent without significant degradation of their capacity and selectivity for uranium. Adsorbents used in the large majority of studies aimed at recovery of uranium from seawater are based on the use of radiation grafting to produce polymeric supports, in particular polyethylene, with attached amidoxime groups. This configuration has been concluded to offer the best candidate for use in recovery based on studies which were performed in the early 1980's. Substantial progress has been made in improving the amidoxime-based adsorbents.

The basic approach undertaken by the authors of the proposal, on the other hand, has been to test ligands which have not been included in the scoping studies of the 1980's or have been developed since then. So far, 18 such ligands have been tested, of which three, including B2MP (an organic phosphate), DAOx (an organic oxalate), and Br-PADAP (an azo compound) have been selected for further investigation. In addition, Winged Nylon 6 has been identified as a promising polymeric support in view of its large surface area and high chemical stability. Furthermore, improved grafting techniques intended to achieve high grafting density under "green chemistry" conditions, i.e., in aqueous media, have been developed. These techniques include the use of surfactants to enhance the solubility of ligands in water and the use of a homopolymerization inhibitor to promote grafting rather than homopolymerization. Furthermore, unlike amidoxime-based adsorbents, which require a chemical treatment step following the radiation grafting to convert a nitrile group to amidoxime, the adsorbents developed by the authors do not require an additional step after grafting. Highly effective regeneration has been demonstrated for the phosphate-grafted polymeric adsorbent over at least 21 adsorption/elution cycles without significant loss of capacity.

The currently proposed study is intended to build upon the progress made so far in developing alternative systems for removal of uranium from seawater. It will focus on the following objectives:

1. Continued searches will be conducted for high-capacity, high-selectivity ligands based on systematic characterization of structural features favorable to uranium adsorption. (For instance, phosphates have been found to be much more effective than the corresponding phosphonates). At the same time, development and testing of the three ligands selected so far will continue, focusing on issues such as high grafting densities and effective regeneration.

2. Testing will be conducted in non-spiked sweater (3.3 µg/L U) and lightly spiked seawater (up to 10 µg/L U). The authors have recently been able to refurbish an ICP-MS spectrometer for this purpose.
3. Improved grafting techniques will be developed and refined for specific ligands. These techniques will include the use of surfactants to allow grafting of ligands with low solubility in water, the use of homopolymerization inhibitors, modifying the chemical structure of ligands to introduce C=C bonds, investigating possible modification of the surface of the polymeric support, and mechanistic analysis of the effects of grafting conditions, in particular accumulated dose and dose rate.
4. Improvements in the characterization of adsorbents before and after contact with seawater will be implemented using techniques such as XPS, SEM-EDS, and zeta potential measurements to investigate the mechanism of uranium adsorption.
5. Effective techniques of multi-cycle regeneration of promising adsorbents without degradation of their performance will be developed and refined through testing of mild, preferably near-neutral eluant solutions.
6. The kinetics of adsorption and desorption of uranium will be investigated. This study is of great operational value and it will also greatly contribute to improved understanding of adsorption/desorption mechanism on promising adsorbents.

II. Scope and Aims of Proposed Work

The proposed study builds upon results of research carried out by the authors of this proposal over the past 3 1/2 years with a focus on developing novel technologies for extraction of uranium from seawater through the use of adsorbent fabrics. While the large majority of efforts in this area have been aimed at improving the performance of adsorbents synthesized by the grafting of amidoxime groups onto polyethylene fabrics[1–8], the approach taken by the authors of this proposal has consisted of studying alternative systems by identifying and investigating other possible ligands, polymeric supports, grafting methods, regeneration techniques, etc.

In particular, the proposed study is intended to identify and characterize ligands that will have advantageous properties with respect to capacity and selectivity for recovery of uranium from seawater, amenability to grafting onto polymeric supports from "green" aqueous media without need for post-grafting reactions such as amidoximation, and high multi-cycle regenerability without significant loss of capacity for uranium adsorption. The scope of the study includes completion of the investigation of three ligands already selected out of 18 candidate compounds on the basis of initial test results. The three selected ligands are bis(2-methacryloxy)ethyl phosphate or B2MP, diallyl oxalate or DAOx, and 2-(5-bromo-2-pyridylazo)-5-(diethylamino)phenol or Br-PADAP. In addition, further ligands will be selected for testing based on structural trends observed during the initial screening of all 18 candidate compounds tested to date.

The scope of the proposed research will also include use of polymeric supports with large surface areas such as winged fibers. Another area which will be studied is enhancement of grafting densities through the use of surfactants to increase ligand solubility in water and through the use of homopolymerization inhibitors to promote grafting rather than homopolymerization. Development of effective multi-cycle regeneration techniques for the new adsorbent fabrics

through identification of effective, non-destructive eluants is also a part of the proposed study. Testing of the new polymeric adsorbents will be performed with lightly spiked and non-spiked seawater to provide a realistic evaluation of adsorbent performance in service environments. The experimental data will be used to develop structural models for ligand optimization and kinetic models for grafting and extraction.

1. High-Capacity Ligands

Adsorbents used in the large majority of studies aimed at recovery of uranium from seawater are based on the use of radiation grafting and chemical processing to produce polymeric supports, in particular polyethylene, with attached amidoxime groups. This configuration has been concluded to offer the best candidate for use in uranium recovery based on studies which were performed in the early 1980's. Substantial progress has been made in improving the characteristics of amidoxime-based adsorbents[8]. At the same time, a number of potential candidates have not been included in the scoping studies of the 1980's or have been developed since then. During earlier stages of the study we have explored 18 such candidates, including eight organic phosphorous compounds, three oxalates, three amines, two azo compounds, one oxime and one ketone. The testing procedure consisted of two stages. During the first stage, the candidate ligands were sorbed on activated carbon and tested for their capability to remove uranium from seawater. Ligands that did not perform well were removed from consideration, but the results obtained for all ligands proved to be very useful in providing guidance for the search for additional candidate ligands. Three ligands have been concluded so far to merit further study. These ligands are again (bis[2-(methacryloxy)ethyl] phosphate or B2MP, diallyl oxalate or DAOx, and 2-(5-bromo-2-pyridylazo)-5-(diethylamino)phenol or Br-PADAP. For their chemical structures see Table 1.

Table 1 – Description of Ligands

Ligand	Ligand Structure
B2MP	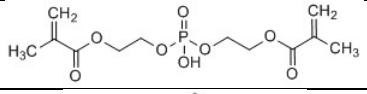
DAOx	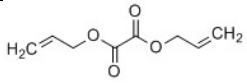
Br-PADAP	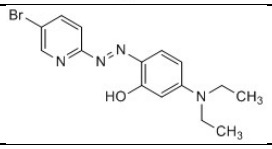

The selection of candidate ligands for testing has not been random, but based on a systematic approach of searching for trends. Thus, B2MP was identified following an observation that among organic phosphate compounds screened in preliminary tests phosphates performed much more effectively than the corresponding phosphonates. DAOx was selected for testing following the identification of ammonium oxalate as an effective regenerant of B2MP-grafted Nylon 6 which had adsorbed uranium from seawater. Br-PADAP was selected for testing as a result of a survey of uranium complexants for use in the development of a rapid and sensitive spectrophotometric test for uranium. During this survey it was noted that, of various color reagents that have been considered, Br-PADAP is particularly suitable for use at the pH range of seawater.[9] It is intended to continue such systematic search for highly effective ligands while focusing on improving the performance of the three compounds already identified as promising candidates by optimizing the grafting techniques for these compounds.

The second stage of the testing program consisted of efforts to graft the promising candidates onto Nylon 6, using an aqueous medium as a solvent during the radiation-induced grafting process. In the case of B2MP, the main problem has been the limited solubility of B2MP.

Several approaches have been tried in order to overcome this difficulty, including addition of a small volume fraction of an alcohol, rapid stirring to maintain the B2MP in suspension, and the use of food-grade surfactants. At 120% grafting density, the highest uranium loading of 10 mg U/g adsorbent was obtained upon testing 15-mg samples of adsorbent fabric with 10 mL of 10 mg/L U in seawater, and when the volume of the solution was raised to 100 mL the observed loading increased to 44 mg/g U.

Low grafting densities (around 10%) have been the main issue in the case of DAOx. A dramatic increase in grafting densities (to 100% and above) has been recently achieved through the addition of Mohr's salt [$(NH_4)_2Fe(SO_4)_2$] as a homopolymerization inhibitor.[10] At that grafting density, a uranium loading of 3 mg U/g adsorbent was observed using 14-mg samples of adsorbent fabric with 10 mL of 10 mg/L U in seawater.

In the case of Br-PADAP, recently obtained results with this ligand sorbed on activated carbon are indicative of high selectivity and high loading. Thus, a uranium loading of 6 mg U/g adsorbent was observed using 15-mg samples of adsorbent fabric with 10 mL of 10 mg/L U in seawater. When the concentration of uranium was lowered to 0.2 mg/L and the volume was kept constant at 10 mL, the observed loading fell to 0.1 mg U/g adsorbent, but when the volume of the 0.2-mg/L U solution was increased to 100 mL the observed volume increased to 0.7 mg U/g adsorbent, indicating that the falloff of the observed loading with concentration was largely due to depletion of the test solution with respect to uranium, and that higher loadings can be expected if the volume of the dilute U solution in seawater is further increased. However, the absence of double bonds from the molecule has to be addressed in order to make it possible to graft the Br-PADAP ligand onto a polymeric support. The major approach being currently studied includes the synthesis of derivatives of Br-PADAP with C=C bonds. Activation of the surface of the polymeric support by grafting it with surface-active moieties, such as graphene oxide, could also be used to attach the Br-PADAP ligand. Formation of graphene coatings on the surface through thermal treatment or CVD may also be used for modification of the polymeric surface. Other ligands with structural similarities to the three mentioned above have already been identified and they will be used in future testing.

2. Testing in lightly spiked and non-spiked seawater

Initial testing of the adsorbents was performed with seawater spiked with 10-20mg/L U due to the use of ICP-AES in the analysis. Recently, our ICP-MS was refurbished, permitting us to run tests with non-spiked (≤10 μg/L U) seawater. Future testing will be conducted in this medium, since extrapolation from results obtained with higher concentrations of uranium is complicated by the fact that at such high concentrations the ratio of uranium levels to those of competing ions is much higher than it is in actual seawater.

Testing will also include studies of seawater variables, in particular temperature, on the performance of the various adsorbents in terms of their loading capacity of the various adsorbents for uranium.

3. Improved surface grafting techniques

In order to support the efforts to optimize the preparation of the novel adsorbents, a major effort towards quantitative modeling of the mechanism and kinetics of the pertinent reactions will

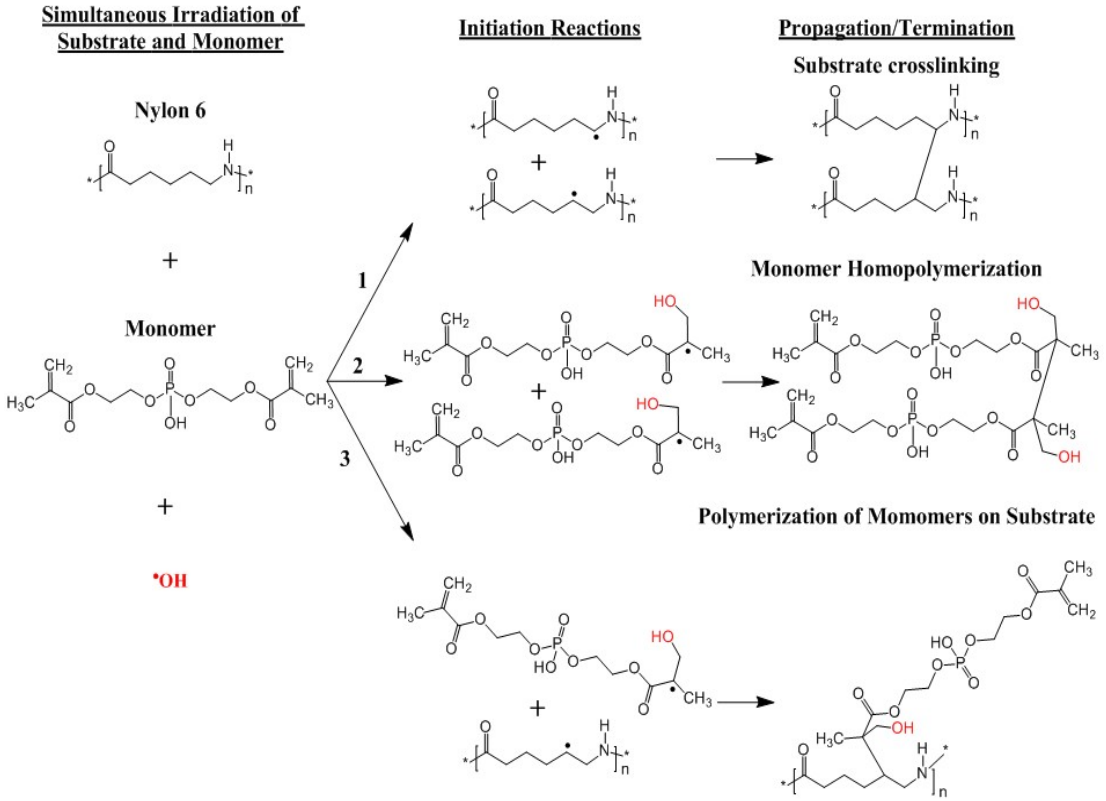

Figure 1 - The reactions of radiolytically-produced hydroxyl radicals (•OH) with Nylon 6 and B2MP: (1) substrate crosslinking, (2) monomer homopolymerization, and (3) polymerization of monomers on the substrate.

be undertaken. The synthesis of the adsorbent fabrics is based on radiation-induced grafting, in which ionizing radiation is used to attach desirable functional groups onto a durable polymeric substrate. The most important factor controlling the capacity of the adsorbent for uranium is the grafting density of the monomer onto the polymer (ultra-high surface area Winged™ Nylon 6). See Figure 1 for the reaction schema for the reactions between Nylon 6, the monomer (in this case, B2MP), and the hydroxyl radical. It is proposed to use mechanistic analysis of the relevant reactions to maximize this density. Two approaches to the grafting of the active monomer on the polymer were tested in preliminary experiments. The first was *indirect grafting*, consisting of irradiating the Nylon 6 polymer in the absence of oxygen and then placing it in an oxygen-free B2MP solution in order to cause addition of the radiolytically produced carbon centered radicals (Nylon•) to the double bonds of the B2MP to initiate the grafting.

However, the best results to date have been obtained using *direct grafting*, where the Nylon is immersed in aqueous, oxygen-free B2MP solution during irradiation. The proposed set of reactions for direct grafting is based on the fact that under the irradiation conditions to be used and in the absence of oxygen, the •OH radicals, which are produced upon radiolysis of the aqueous medium, add to the unsaturation sites of the B2MP and abstract H-atoms from the backbone of the Nylon polymer, producing •B2MP—OH radicals and Nylon(-H) radicals, respectively.

In the case of DAOx, experiments performed so far again indicate that the key to achieving high grafting densities is to make the grafting process more competitive with undesirable homopolymerization processes. For this purpose, Mohr's salt ($(NH_4)_2Fe(SO_4)_2$) has been added, resulting in dramatic improvements in grafting density.[10] The exact mechanism through which this improvement is achieved is still under investigation.

As described in the previous paragraph, the use of homopolymerization inhibitors, in particular Mohr's salt, can lead to very large improvement of grafting densities of candidate ligands, such as DAOx, onto a polymeric support, such as Nylon 6. This result indicates that the addition of Mohr's salt might be useful in grafting other ligands as well onto the polymer support. However, no significant presence of Fe(III) following the irradiation of the polymer/DAOx system has been found using XPS spectroscopy, and this finding is not compatible with existing explanations of the role of Mohr's salt, which attribute the suppression of homopolymerization to electron transfer between the Fe^{2+} ion and the propagating polymer radical.[10] It is planned to continue the study of the effect of Mohr's salt and extend it to other substances reported to act as homopolymerization inhibitors, such as copper(II) sulfate, in order to identify the mechanism accounting for their effect on grafting densities. The issues of non-uniform distribution of Fe(II) in the grafted polymer and of the effect of the presence of such ions on the loading capacity have to be investigated, although present results indicate that the latter effect is not overly detrimental.

Studies performed on polymeric adsorbents synthesized by grafting of B2MP or DAOx on Nylon 6 have shown that at low grafting densities the uranium loadings increased with increasing grafting density, but loadings reached their highest values once grafting densities reached approximately 100% and showed a decrease at higher grafting densities.

While Winged™ Nylon has been determined to be the most effective polymeric substrate of all the fabrics tested, future work will involve the grafting of additional fabrics with B2MP, DAOx and Br-PADAP to investigate whether a new fabric may show greater radiation resistance, improved mechanical properties and a higher spin concentration than Winged™ Nylon. Proposed fabrics for testing include, but are not limited to, polyethylene and additional ultra-high surface area Winged™ fibers. EPR will be used to study the formation and reactions of radicals. The various fabrics will also be tested in grafting experiments to compare grafting densities.

While the optimization of grafting conditions for B2MP onto winged nylon has been mostly completed, the grafting procedure for all promising ligands will continue to be varied and adjusted to maximize adsorbent efficiency and to reduce complexity and cost. Emphasis will be placed on maintaining the standards of “green chemistry”, including the elimination of organic solvents and minimizing the formation of waste.

4. Improvements in the characterization of sorbents

Little information has been reported so far regarding the characteristics of the adsorbent fabrics and of the changes in these characteristics resulting from the contact with seawater and the uptake of uranium. However, such information can be very valuable in gaining better insight into the adsorption process, thus laying the ground for further optimization of the adsorbent. This information is also essential for assessing the effects of the exposure to seawater on the structure of the adsorbent and the implications of such effects on the durability of the adsorbent and the potential for regeneration.

Accordingly, it is proposed to undertake a series of measurements aimed at characterizing experimental adsorbents developed for enhanced extraction of uranium before and after contacting them with seawater.

XPS is a powerful tool that can provide critical information about bonding between the polymeric adsorbent and adsorbed species such as uranium and vanadium. Until now, the amount of information available regarding the nature of this bonding has been limited. XPS measurements will provide data that will describe the elemental concentrations, speciation, and bonding of the monomer, uranium, and other adsorbed species.

The uptake of potentially competing cations, e.g. vanadium, on the adsorbents can be measured, and the important question as to whether they compete for the same of the sites on which uranium is adsorbed can be resolved by adding controlled concentrations of such metal ions to the uranium-containing solution used in the adsorption experiments and determining the effects of such additions on the uranium uptake. Energy-dispersive x-ray spectroscopy (EDS) in combination with scanning electron microscopy (SEM) can be used to establish the distribution of competing ions on the adsorbent. Furthermore, EDS can provide direct information regarding the relative amounts of various adsorbed ions on the adsorbent.

5. Optimization of elution/regeneration processes

It is generally recognized that economically viable recovery of uranium from seawater requires the development of a technology based on the use of multiple cycles of uranium adsorption followed by elution/regeneration without significant deterioration in the performance of the polymeric adsorbent. In the case of B2MP-grafted Nylon 6, subjecting the adsorbent to at least 21 consecutive cycles, each consisting of contacting a 17.5-mg sample of the polymeric adsorbent with a 5 mL of seawater containing 10 mg/L U followed by elution of the uranium with a saturated (approximately 0.4 M) solution of ammonium oxalate in water, exhibited no change in the loading capacity for uranium within experimental error. The good regenerability of the adsorbent has been attributed to the fact that the regenerant solution provided effective removal of the uranium although it had a near-neutral pH which ensured that the binding sites for B2MP on the polymer would not be destabilized during the regeneration process. Regeneration studies on Nylon 6 supports grafted with DAOx are planned to start once the grafting methodology is optimized. As mentioned above, grafting of Br-PADAP is still in the design stage.

6. Investigation of the adsorption/desorption kinetics

The kinetics of the adsorption and elution processes is of great scientific interest as well as critical economic importance. Results reported in the literature regarding the performance of amidoxime-grafted polyethylene fabrics in actual ocean environments indicated that the adsorption process was quite lengthy. The time required for the adsorption process to take place is a combination of the time it takes for dissolved uranium to reach the adsorption sites on the surface of the adsorbent and the time required for the adsorption to take place. In laboratory experiments on the performance of B2MP-grafted Nylon 6, see Figure 2 below, carried out with and without subjecting each of two 23-mg samples to rotation in the aqueous medium (50 mL of seawater spiked with 20 mg/L of uranium), it was observed that the loading level reaches about 50% of the ultimate loading (taken to be the loading reached in 7 days) by the end of the first day and about 90% by the end of the second day. While not as long as the time periods reported in the ocean

experiments, these times, recorded in a confined system, subject in the dynamic case to rotation at 30 rpm, are quite long in comparison with the times commonly required for full loading to be achieved in removing minor constituents from aqueous environments by means of ion exchange or the use of sorbents such as activated carbon.

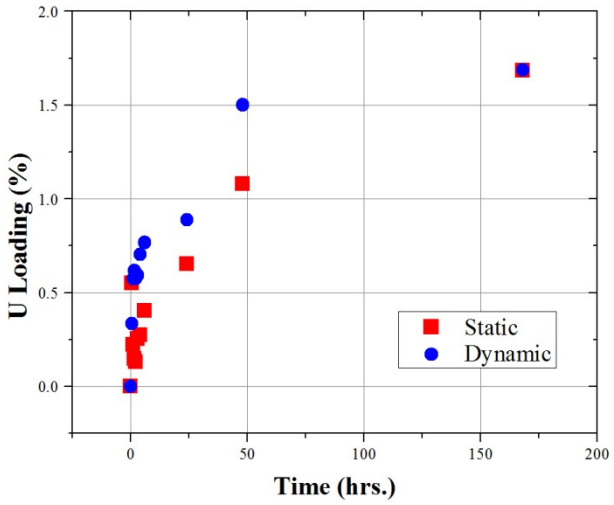

Figure 2 – U Loading on B2MP-Grafted Nylon 6 Fabric

The relatively long times required for approaching full loading of uranium may be due to a more complex adsorption mechanism operating in the case of removal of uranium from seawater, where only very small concentrations of UO_2^{2+} ions exist at equilibrium with much higher concentrations of $UO_2(CO_3)^{2-}$ and $UO_2(CO_3)^{4-}$ ions. In this case longer time is necessary for substantial fractions of uranyl ions to be released from the carbonato complexes so that they can attach to the adsorbent. Another reason for the relatively slow adsorption is that it is likely that other cations, which have lower distribution coefficients but are present in seawater at higher concentrations than uranium may become attached to the adsorption sites on the surface of the polymeric adsorbent when the adsorbent is first contacted with seawater. Subsequently, these are slowly replaced by uranium due to a high distribution coefficient with respect to the uranyl ion, but this replacement may be a much slower process than the initial uptake of various cations.

Detailed studies of the adsorption kinetics are planned for adsorbents based on all three of the currently selected ligands. These experiments will be used to elucidate the adsorption mechanism and to obtain important information for the eventual upscaling and commercialization of the process.

Experiments are also planned to study the elution kinetics of uranium from the polymeric adsorbent using selected regenerant solutions (see previous section).

A mathematical model describing the kinetics of adsorption and desorption will be developed and the rate constants of these two processes will be developed based on the experimental results of the kinetic studies on these two processes. For instance, if the adsorption is the rate-determining step and it is first order with respect to the concentration of uranium, the overall rate of uranium recovery from seawater, R, will be given by $R = Q/T = C_0[1 - \exp(-k_a t_a)]V/t_a$, where Q is the total amount of uranium removed from the water, T is the total time of one cycle, V is the volume of the seawater contacted with the adsorbent, C_0 is the concentration of uranium in the seawater before contact with the adsorbent, t_a is the time allowed for the adsorption process, and k_a is the rate constant of the adsorption process. According to this equation, R will be very low if t_a approaches zero or becomes very long (in which case the amount of uranium recovered during each cycle is maximized, but overall uranium recovery slows down). There is an intermediate value of t_a, which can be obtained by differentiation of the equation, which will yield the highest possible value of R. (Of course, if the rate constant of desorption, k_r, is not much higher than k_a,

the time allowed for desorption, t_d, will also have to be taken into account in calculating the maximum value of R; furthermore, the expression needs to be modified if the adsorption and desorption are not simple first order processes.) This model will be applied to interpreting data to be obtained in multi-cycle semi-continuous adsorption/desorption tests.

III. Technical Summary of the Work Accomplished

Radiation Synthesis of Uranium Extracting Materials Using Artificial Polymers

Primarily, uranium extracting fabrics were produced for this project via radiation induced graft polymerization. The following two images provide pictorial representations for the two different radiation grafting methods used in this work, direct grafting, see Fig. 3, and indirect grafting, see Fig. 4.

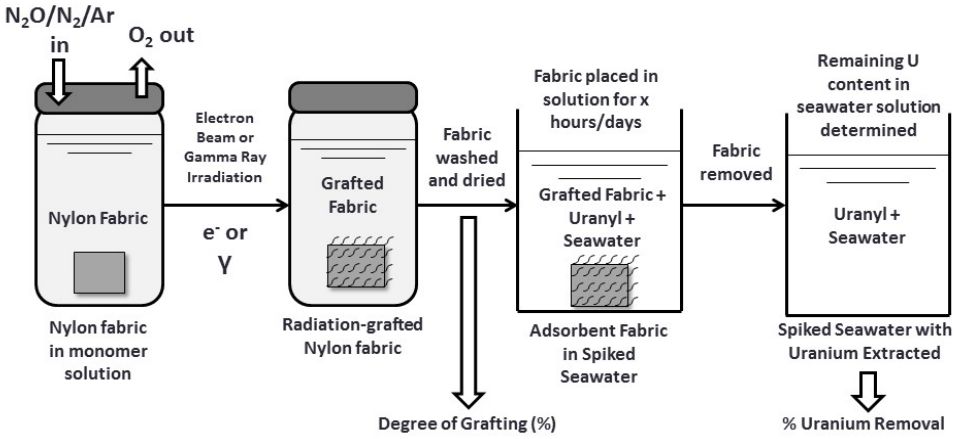

Figure 3 – A schematic of the processing steps required for direct grafting of a uranium extracting monomer to the surface of a substrate and the subsequent testing procedure.

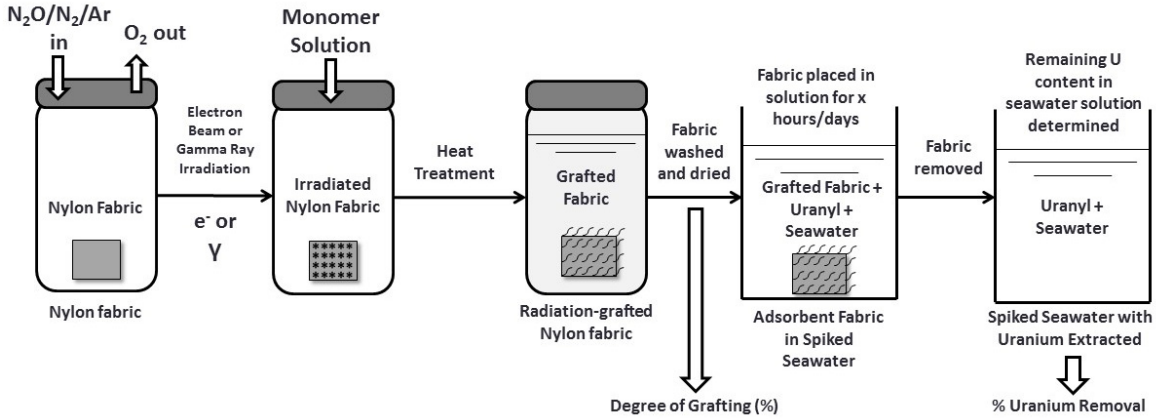

Figure 4 - A schematic of the processing steps required for indirect grafting of a uranium extracting monomer to the surface of a substrate and the subsequent testing procedure.

3.1 Substrate Selection

3.1.1 Activated carbon

Candidate monomers for uranium extraction needed to be tested prior to radiation grafting in order to ascertain their ability to extract uranium successfully in a seawater environment. By using activated carbon powder doped with the candidate monomer, the difference in adsorption capacity of the doped versus undoped activated carbon is used as an estimate for the ligand's performance once grafted to a fabric substrate.

3.1.2 Nylon 6

While many previous and current studies on the extraction of uranium from seawater have focused on the use of polyethylene fibers as the substrate for radiation grafting, this work has mainly relied on the use of nylon 6.[7,11–14] The chemical structure of this compound is shown in Fig. 5 and an SEM image of the polymer as a fiber is shown in Fig. 6. Throughout the radiation grafting experiments and chemical treatments performed on this substrate material, nylon 6 has shown resistance to degradation which is supported by the material's resistance to many types of chemical attack, not including strong acids.[15]

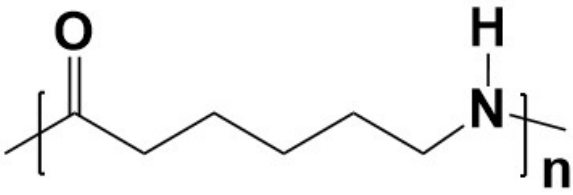

Figure 5 – The chemical structure of nylon 6.

Figure 6 – An SEM micrograph of a nylon 6 fabric produced by the 3M Company.

3.1.5. Winged Polymers

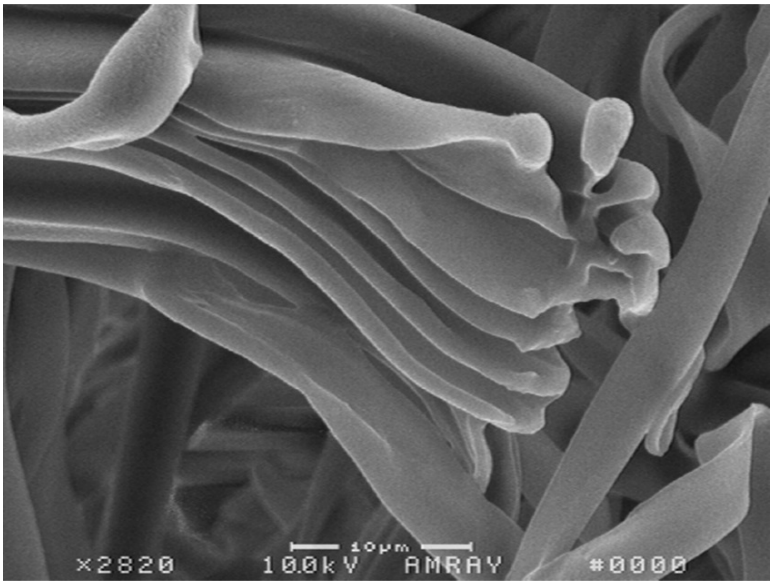

Figure 7 – An SEM micrograph of winged nylon 6 fabric. This view shows the end of one of the "winged" fibers.

Winged fibers were obtained from Allasso Industries and were preferred, as they provide (i) higher surface areas upon which to graft both uranium extracting monomer and (ii) a greater surface area upon which uranium extraction could occur. The channels seen in Fig. 7, of width one micron or less, are possible locations for the growth of grafted monomer chains. This patented fiber design has already been suggested for use in purification/separation systems with an average specific surface area of about 140,000 cm^2/g.[16]

3.2 Sample Preparation

The general procedure for fabric sample preparation prior to irradiation grafting can be described as follows. Square pieces of fabric were cut from larger swathes of sample nylon-6. The cut pieces of fabric were trimmed until their mass fell within a specified range, 0.020 – 0.021 g or 0.045 – 0.046 g. Mass ranges were selected to reduce any impact that sample size might have on the total grafting of the final sample. The magnitude of the mass range (1 mg) was selected based on the accuracy of the scale used to physically weigh each fabric. These numbers were also chosen as they would allow for the highest accuracy of the ranged balanced combined with the ease of cutting the samples, such that their masses would fall in aforementioned specified range.

Once samples had been cut and massed, they were placed in labeled sample vials, the majority of which were capped with silicone septa. In both direct and indirect grafting this allowed for the subsequent purging of the atmosphere and/or the solution inside the vial with inert gas.

Following the preparation of the fabric samples, the monomer solutions were prepared per the concentrations of different monomers and solvents described for each independent experiment. All monomer solutions were prepared in ambient air. In all cases, complete mixing was insured through stirring and/or sonication. Following solution preparation in the case of direct grafting, 10 mL of monomer solution was transferred to each sample vial. These vials were then purged with an inert gas, either nitrogen or argon, or with nitrous oxide in the case of some aqueous monomer solutions.

3.3 Co-60 Irradiation for Sample Fabrication

3.3.1 National Institute of Standards and Technology Co-60 Irradiator Set-up

Fabrics have been irradiated using two Co-60 irradiators located at the National Institute of Standards and Technology (NIST), each of which can provide a different dose rate, specifically 5 kGy per hour and 1 kGy per hour.

3.3.2 Dosimetry

Dosimetry for the NIST Co-60 irradiators was carried out using pellets of alanine. These pellets are composed of alanine and a binder and are roughly half a centimeter in diameter. The alanine pellets are irradiated to a number of different doses. Subsequently, the pellets are analyzed in an EPR spectrometer, which is able to measure the change in the absorbance of a microwave in the sample which is absorbed by the splitting of the unpaired electrons generated in alanine during their irradiation. The specific relationship between dose and the area of the peaks generated in the EPR is dependent on a number of factors, including the geometry of the pellet in the EPR. The determination of the radical concentration-peak area relationship using a ruby standard, and knowledge of the amount of energy required to produce an unpaired electron in alanine. Based on the alanine dosimetry and the assumption that the gamma rays completely penetrate through both the container inside the irradiator (assuming negligible attenuation) and the glass vials in which the fabric samples sit, the dose and dose rate of a Co-60 irradiation can be determined for all samples. The assumption that there is negligible attenuation of the gamma rays due to the glass vials is founded on the significant penetration power exhibited by this neutrally charged, highly energetic particle.

3.4 Linear Accelerator – Radiation Grafting & Medical, Industrial Radiation Facility (MIRF)

The majority of irradiations were performed at the MIRF facility using a pulsed electron beam LINAC with a fixed pulse repetition rate (100 Hz per 6 μs pulse) and electron energies from 7-32 MeV, however all irradiations were carried out at about 10 MeV. This energy was chosen for a number of reasons. For example, the accelerator has difficulties operating at energies below this value and any energy values greater than 10 MeV have a greatly increased probability of activating the samples. Due to the high energy of the electrons and variable current that it can operate at, in comparison to the fixed rate of the Co-60 irradiatior, this facility is ideal for polymer modification at intermediate to very high dose rates.

A number of different sample irradiation configurations were used with the MIRF LINAC, one of which is shown in Fig. 8. These different configurations can be separated into two qualities: (i) the ability to irradiation samples at a desire temperature and (ii) the ability to irradiate multiple samples at one time using a rotating table. One or two samples could be placed at the front of the rotating sample table to allow for higher dose rates.

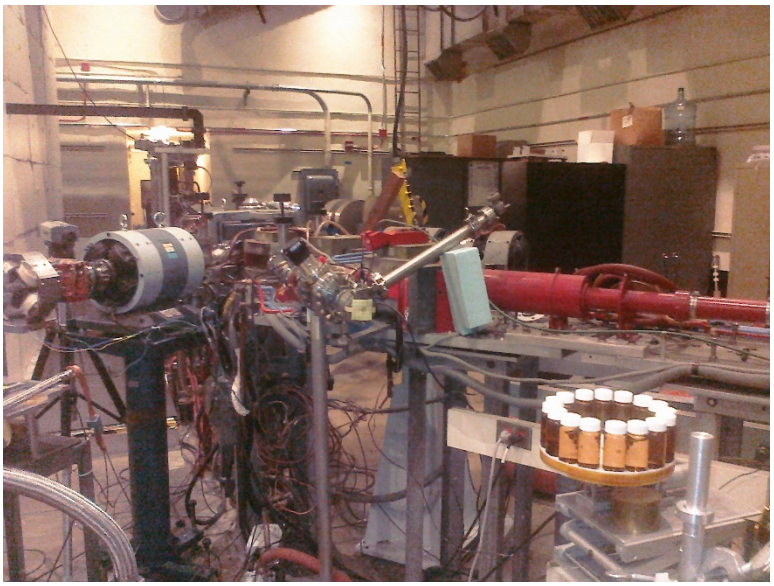

Figure 8 – The sample stage on which the sample vials are irradiated can be seen in the bottom right of this image. The exit port of the electron beam can be seen at the center of the image.

Figure 6 shows the initial irradiation set-up, where the vials were not irradiated in a temperature controlled chamber. The circular stage with white-capped vials on top of it was used as a means to irradiate a larger number of samples with a relatively even dose without having to irradiate each sample individually. In this particular configuration, 16 (though depending on vial size, this number could change) 20 mL vials fit around the edge of the rotating platform. The platform performs a full rotation approximately twice every minute. The platform was operated through the mechanism of a mechanical motor beneath the platform and was powered by an external voltage supply present in the control room of the LINAC facility.

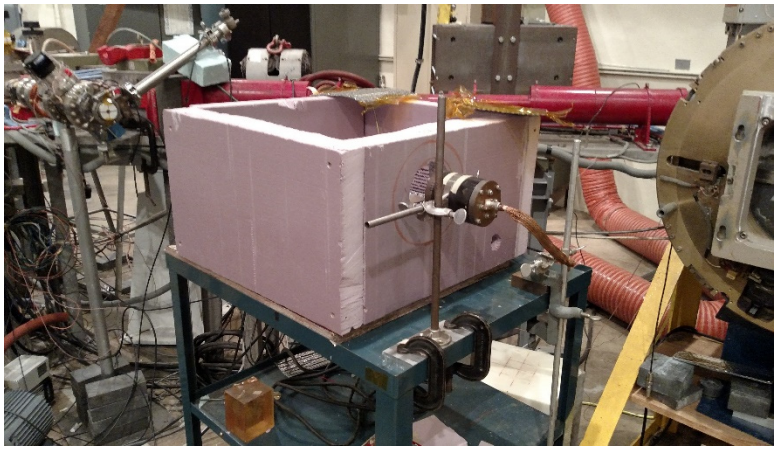

Figure 9 – The outside of the insulated irradiation chamber for controlling temperature during irradiations.

Figure 10 – The inside of the insulated irradiation chamber for controlling temperature during irradiations.

The two pictures above, Figs. 9 and 10, show the exterior and interior of an insulated box that was used for temperature control of the samples. Two holes were cut out of the box in order to allow for the electron beam to enter and exit the box unimpeded by the foam walls.

The method of heating the box (direct grafting), and cooling it (indirect grafting), varied slightly. Copper piping extended into the box (though this is not shown in the above photo). This copper piping was attached to a source of pressurized air. To cool the box, dry ice was placed in the bottom of the chamber and air was blown into the box. This allowed for irradiation temperatures of about -20 °C. Prior to an irradiation, the box was allowed to cool to a more stable temperature and also to let the sample vials reach temperature equilibrium with the surrounding box. During the irradiation, the sample vials would most likely begin to heat up due to the energy that is introduced by the electron beam, however the air flow in the chamber kept this from having a significant effect. For heating the chamber, a heating tape is wrapped around the outside of the copper tube, air inlet prior to entering the sample chamber. When turned on, the heated air passing through the tubing was able to heat the box to the desired temperature. In a similar fashion to the cooling process, the external temperature of the vials during the irradiation was higher than the temperature of the box, which was monitored through the use of two thermocouples at different locations in the box.

3.4.1 Dosimetry

The accurate determination of the dose reached by the irradiated samples was a fundamentally important aspect of the grafting experiments. Dose measurements are reliant on the geometry and physical state of the system being irradiated. Therefore, individual dosimetry measurements had to be performed for a number of different sample irradiation configurations, direct and indirect grafting, and for both the rotating platform and the higher dose rate direct irradiation configurations. In all cases, BioMax Alanine Dosimeter Films, were attached to calibration sample vials prior to the irradiation of any actual samples.

These reference vials did not contain sample fabric nor did they contain a monomer solution. For indirect grafting experiments, where the fabric is by itself in the sample vial, the calibration vials would be filled with air. For direct grafting experiments, the calibration vials would be filled with water to the same height as what would be characteristic of the monomer

solution level in actual sample vials. During the rotating platform experiments, three to four sample vials would have alanine films stuck onto their outer surface, two per vial. The alanine strips would be oriented in such a way so that when the sample is in the direct path of the electron beam the alanine strip would be parallel to the electron beam. Alanine strips would be placed on vials around the platform at even intervals.

For the higher dose rate irradiations where either one or two vials would be placed directly in the beam path, one alanine strip would be placed on each side of the vial(s), parallel to the beam path. The alanine strips were both oriented vertically, so the alanine strip was running up and down the vial, or horizontally around the bottom of the vial. These two orientations were selected as a means of more accurately referencing the beam profile that would be observed by the sample for that particular dosimetry.
The BioMax alanine strips have a limited calibrated range and so the strips could not be irradiated to doses above roughly 80 kGy or below 3 kGy otherwise there could be significant deviations. Based on previously measured doses/dose rates and assuming an increase or decrease in dose rate based on the configuration of the samples, a time was chosen for the irradiation of the samples (about five minutes in most cases). Following the irradiation of the calibration vials and the alanine strips, the strips were taken to a Bruker Alanine Dosimeter Reader.

This alanine dosimeter reader is an EPR spectrometer capable of reading the unpaired electron signal generated in the alanine on the strip during the irradiation. By integrating the area under the peaks in the alanine spectra and comparing the values to an internal standard, the dose received by the strip can be determined. The doses received by the various strips during the irradiation are then averaged. This final dose was used for the determination of the counts/kGy of the sample configuration tested. It is assumed that the average of the dose received on the front and back side of the sample vial could be used to estimate the dose received inside the vial. Since the greatest attenuation of the electrons from the LINAC would be from the glass, especially for the indirect-grafted sample vials, the dose inside the vial can be estimated to be the average of the dose entering and leaving the vial. The high energy electrons leaving the LINAC would have enough energy wherein there would not be a significant loss of electron energy through particle interactions. The difference between the average value of the two exterior alanine strips and the one interior alanine strip was minimal. Using the calculated dose, the time of the irradiation, and the total counts received via the Faraday cup allowed for an accurate and rigorous prediction of time of irradiation to reach a desired dose for the actual fabric samples. While sample irradiations could not be stopped at a specific number of counts, the irradiations could be stopped well within 1% of the desired dose, especially for larger doses. Dosimetry was used as an initial calibration step; therefore, it was not performed every time a sample irradiation was carried out and was only performed if the sample configuration was changed. However, all evaluations of the standard error of the dose measurement (under the same irradiation conditions), $\sigma_{tot,}$ can be considered to have less than 4% error based on the individual contributions to the standard error from both the accuracy of the measurement from the dose reading off the alanine strips ($\leq$ 1%), $\sigma_{alanine}$, and the standard error value for the distribution of doses obtained from the placement of the alanine strips on the irradiation stage at different positions ($\leq$ 3%), $\sigma_{location}$, per equation 1[17]:

$$\sigma_{tot} = \sqrt{\sigma_{alanine}^2 + \sigma_{location}^2} \quad (1)$$

3.5 Post-radiation processing of samples

Following the irradiation of the sample vial, the fabric had to be processed through a number of extra experimental steps to prepare the samples for uranium extraction experiments.

3.5.1 Directly Grafted Samples

Following the irradiation of vials containing both the monomer and fabric solution, in some cases the vials were left overnight at about 60 °C. This heat treatment was shown to increase the DoG of the substrate in many cases. Once the heat treatment was completed, the grafted substrate would have to be cleaned of any excess monomer. This was often carried out through multiple washes with an appropriate solvent, such as methanol, water, dichloromethane (DCM), etc. Samples would be sonicated and rinse multiple times. Once the washing was completed, the sample would be dried in an oven at 60 °C. The final mass of the sample would then be obtained with the use of a mass balance once the sample had cooled back to room temperature.

3.5.2 Indirectly Grafted Samples

For samples grafted through the indirect process, the monomer solution needs to be added very quickly after the initial irradiation. This is to make sure that the decay of radicals is limited as much as possible following the irradiation. Immediately following the irradiation, sample vials containing only the substrate material are moved into a glove bag along with purged vials of monomer solution. This glove bag is sealed and purged with argon gas to prevent any oxygen penetration into the sample vials as this would further decrease the radical concentration in the samples. The monomer solution is then transferred to the sample vials via syringe or pouring. Once the monomer solution has been transferred, the vials are shaken to ensure the complete penetration of solution into and around the substrate and they are moved into an oven at 60 °C where they remain at least overnight. This heat treatment is believed to allow for increased radical mobility inside the substrate material, thereby allowing the radicals to react more readily with the vinyl groups in the monomer solution. Following the heat treatment step, the indirectly grafted substrates are washed, dried, and massed in similar fashion to the directly grafted samples.

3.5.3 Azo group attachment

Once samples had been grafted with the VBC precursor, they subsequently had to have the selected azo compound chemically bound to their surface. The samples chosen for azo attachment were placed into polypropylene baskets and individually labeled. A mixture of sodium carbonate, dimethyl formamide, and the azo compound were mixed together in a flask under nitrogen. There were roughly 8 equivalents of azo compound to the estimated molar quantity of chlorine groups on the surface of the VBC grafted fabric. This mixture was stirred at 40-50 °C for 30 minutes. The fibers in their baskets were then added one by one. Once all the baskets had been added, the mixture was heated and stirred under nitrogen for 3-4 days.

Following this time period, the samples were removed from reflux, washed of excess reactant using methanol and water repeatedly, and then dried in an oven overnight at 60 °C. The dried fabrics cooled and their final masses were obtained.

3.6 Linear Accelerator – Pulse Radiolysis

Pulse radiolysis measurements were carried out at facilities at Brookhaven National Laboratory (BNL). Sample solutions were prepared in the laboratories at BNL. No pulse radiolysis experiments were performed with substrates, only solutions of monomer were irradiated.

3.6.1 Van de Graaff and FTIR

In order to study the decay of specific vibrational modes of monomer correlating to the polymerization of the monomer under ionizing radiation, a combination of a 2 MeV Van de Graaff accelerator and time resolved FTIR was used. Different concentrations of a specific monomer were prepared in solutions and placed in vials like the one in Fig.11.

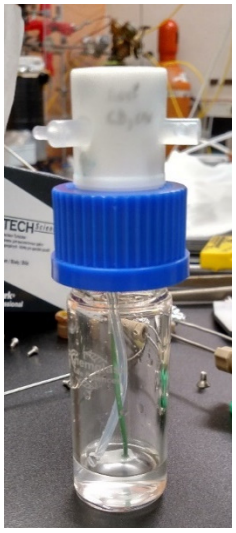

Figure 11 – The reservoir bottle from which monomer solution was drawn for Van de Graaff pulse radiolysis experiments. The cap of this bottle allows the solution to be sparged with a gas while sample is withdrawn using a syringe pump.

These vials allowed for the purging of the monomer solution with an inert or N_2O atmosphere (which in aqueous solution irradiations quenches the production of aqueous electrons in solution while doubling the amount of hydroxyl radicals), while also allowing for the solution to be pumped into a thin cell window, shown below.

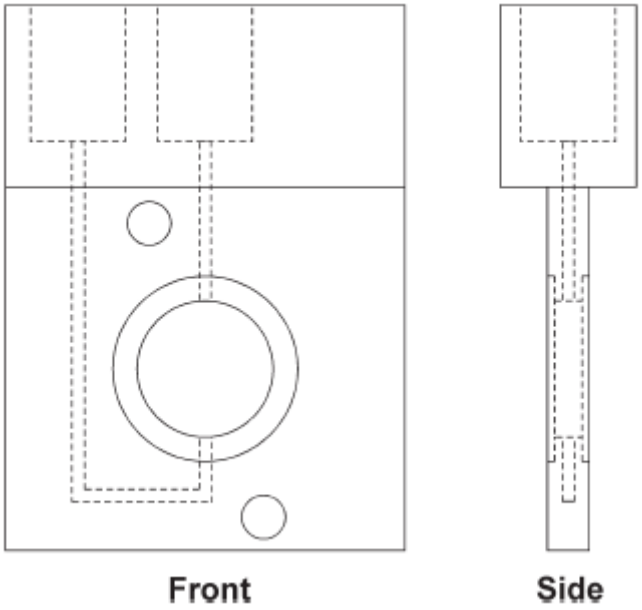

Figure 12 – This schematic illustrates the inlet and outlet of the IR window used during pulse radiolysis experiments. From the front, the electron beam is allowed to pass through the circular quartz window where it can interact with a thin film of monomer solution. From the side, the FTIR beam can pass through the irradiated sample for sample data collection.[18]

This thin cell window, shown in Fig. 12, allows for the electron beam generated by the Van de Graaff accelerator to pass through a window which is composed of a thin layer of monomer solution sandwiched between two quartz windows. The set-up as it was used during the experiments is shown in Fig. 13.

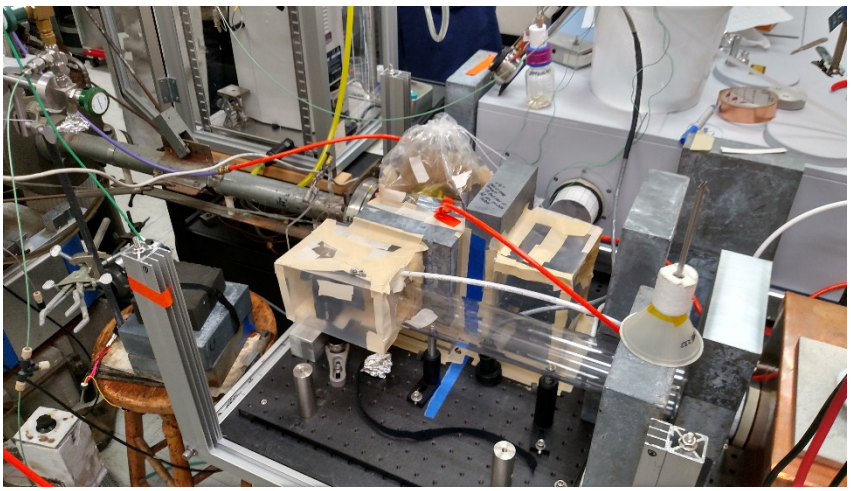

Figure 13 – This image illustrates the FTIR pulse radiolysis set-up. The beam tube and exit port of the Van de Graaff can be seen on the left side of this image. In the center of the image, within the plastic bag, is the FTIR cell window containing the monomer solution. In the back right of the image, the FTIR spectrometer can be seen.

During and following the irradiation of the monomer solution, the fluctuating chemistry inside the cell window is monitored through the use of real-time FTIR. Once FTIR measurements are completed, the cell is purged of the irradiated solution through the use of a syringe pump. Once a fresh solution is in the cell, a new irradiation run can be carried out.

3.6.2 Linear Electron Accelerator Facility (LEAF)

The decay of a number of free radical species, such as the aqueous electron and the hydroxyl radical, can be studied through the use of ultrafast UV-Visible spectroscopy coupled with a pulsed electron beam. The decay of these free radical species provides valuable insight into the mechanism and rate of polymerization of a selected monomer species. The LEAF facility is capable of nanosecond spectroscopy measurements, with absorbance measurements taken at intervals of 0.5 ns. For these experiments, a number of solutions are prepared depending on the desired dominant radical species.

For hydroxyl radical production, a solution of monomer in water in a quartz cuvette is purged with nitrous oxide before being placed in a sample holder. This sample holder, shown as a yellow square in the above image of the facility is incident both to the pulsed electron beam and a UV-Visible laser pulse. An initial electron pulse is produced when the high-energy laser pulse is directed towards a metal plate. Through the photoelectric effect, a packet of electrons is ejected from the plate and accelerated down a beam line using a series of sequential, alternating electric fields. The laser pulse that past the beam splitter is time delayed before hitting the aqueous sample so that the absorption of the sample at the specific laser wavelength can be measured following the initial electron excitation, but still fast enough to monitor transient radical species.

For aqueous electron production, an aqueous solution of monomer with 20 wt. % tert-butyl alcohol is prepared. The procedure remains the same as that described for the N_2O purged solution.

3.6.3 Dosimetry

Dosimetry of the Van de Graaff accelerator was not specifically determined. The dose received by any sample was estimated based on previous knowledge by the facility of the dose received by aqueous solutions in the IR cell. The dose received by the aqueous solutions in the LEAF facility were obtained through the use of thiocyanate dosimetry.

3.6.3.1 Thiocyanate dosimetry

In order to determine the inherent dose upon the sample in the LEAF facility, a thiocyanate dosimeter was used. The thiocyanate dosimeter is a 10 mM solution of potassium thiocyante in water and purged with N_2O. This solution is irradiated with the pulsed beam and the absorbance of a 480 nm light pulse in the sample is recorded over time. An example of a trace of the absorption of a 10 mM thiocyanate solution is shown in Fig. 14.

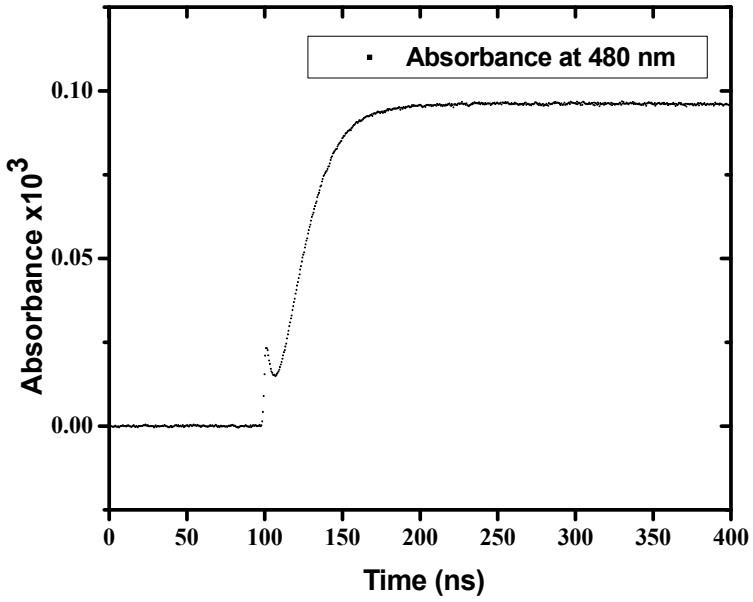

Figure 14 – A trace of the absorbance of the thiocyante solution at 480 nm after an electron pulse showing the production and quenching of the aqueous electron at about 100 ns and the continued production of the $(SCN)_2^{\bullet -}$ following.

The adsorption of thiocyante at 480 nm is due to the $(SCN)_2^{\bullet -}$ species which is formed via the following reaction pathway shown in equations 2 and 3 upon interaction of the thiocyante ion with the hydroxyl radical[19,20]:

$$^{\bullet}OH + SCN^- \rightarrow SCN^{\bullet} + OH^- \quad (2)$$

$$SCN^{\bullet} + SCN^- \rightarrow (SCN)_2^{\bullet -} \quad (3)$$

The dose per pulse of pulse radiolysis experiments is obtainable through the use of the following equation, eq. 4:

$$D_D = \frac{\Delta A}{\Delta \varepsilon l \rho G(P)} \quad (4)$$

where D_D is the dose (per pulse, in the case of pulse radiolysis), ΔA is the change in adsorption at 480 nm following the electron pulse (unitless), $\Delta\varepsilon$ is the difference in molar adsorption coefficient between the reactant and product at 480 nm ($m^2\ mol^{-1}$), l is the path length (m), ρ is the density of the solution ($kg\ m^{-3}$), and G(P) is the radiation yield of the product molecule ($mol\ J^{-1}$)[21]. If the units of the radiation yield of the product are in molecules/100 eV, then the numerator of the equation will be multiplied by 9.648×10^6, $\Delta\varepsilon$ will be in $M^{-1}cm^{-1}$, density will be in $g\ cm^{-3}$, and path length will be in centimeters to obtain the same units.

Within the thiocyanate system used in this dissertation, with $\Delta\varepsilon \times G(CNS)_2^{\bullet -} = 2.23 \times 10^{-4}\ m^2J^{-1}$, l = 0.010 m, and $\rho \cong 1000\ kg/m^3$, the dose per pulse can be calculated based on the average adsorption of initial pulse radiolysis adsorption measurements of a 10 mM solution of thiocyanate. With an average adsorption value of 0.095 ± 0.00049 of the different runs, the average dose per pulse of the LEAF facility during the pulse radiolysis experiments of DAOx was 42 ± 0.22 Gy/pulse.

3.6.4 Reaction Kinetics Analysis

The determination of the reaction kinetics of the aqueous-monomer systems through the data recorded from the pulse radiolysis experiments described throughout section 3.6 was carried out by fitting the data to the appropriate rate constants. In particular, the pulse radiolysis data obtained for the 1697 cm^{-1} and 1798 cm^{-1}- B2MP peaks and the transient absorption of DAOx at 480 nm were fit to first order, second order, and pseudo-first order rate constants respectively.

In particular for the build-up of product at the 1798 cm^{-1} peak during and following the irradiation of B2MP solution in D_2O special consideration must be made for the evaluation of the second order kinetics. As the product is adsorbing, i.e. the product of the second order reaction is what is being monitored, not the decay of the reactants, the reaction rate cannot simply be fit to a trend of the inverse of the absorbance versus time. In order to obtain a useful relationship, an equation relating the slope of the inverse of the change in absorbance versus time to the rate constant of the reaction if the adsorption coefficient, ε, and path length, l, are known for the investigated system[22]. For a system where the product adsorbs and the reaction is predicted as a reaction between two identical radical species as portrayed in the following reaction, eq. 5:

$$A + A \rightarrow M \tag{5}$$

where A is the radical species and M is the product of the reaction between the two radical species. In this case, if we let x = [M] and by stoichiometry $[A] = [A]_\circ - 2x$, then we obtain the following, equations 6-8, if only M absorbs:

$$\frac{d[M]}{dt} = k[A]^2 \tag{6}$$

$$\int_0^{[M]_t} \frac{dx}{([A]_\circ - 2x)^2} = \int_0^t k dt \tag{7}$$

$$\frac{1}{2([A]_\circ - 2[M]_t)} - \frac{1}{2[A]_\circ} = kt \tag{8}$$

Assuming the reaction essentially goes to completion, then we will obtain equations 9 and 10

$$[A]_\circ \cong 2[M]_\infty \tag{9}$$

$$\frac{1}{4([M]_\infty - 2[M]_t)} - \frac{1}{4[M]_\infty} = kt \tag{10}$$

Assuming Beer's Law holds ($A = [M]\varepsilon l$) then we obtain equation 11

$$\frac{1}{A_\infty - A_t} = \frac{4kt}{\varepsilon l} + \frac{1}{A_\infty} \tag{11}$$

Therefore plotting $[A_\infty - A_t]^{-1}$ vs. t should give a straight line with equation 12

$$Slope = \frac{4k}{\varepsilon l} \tag{12}$$

3.7 Sample Characterization

Following the grafting of uranium extraction monomer to the surface of various substrates, multiple characterization techniques were employed to (i) determine the attachment of the monomer (ii) examine the surface morphology of the substrate, and (iii) examine the concentrations of various elements on the surface.

3.7.1 Gravimetric analysis

Gravimetric analysis was performed on all fabrics following the cleaning and drying stage of the sample preparation. Samples were massed on a MS205DU Mettler-Toledo scale. These measurements were performed in order to obtain the mass difference of substrates following grafting to provide information on the total DoG of the monomer on the polymer backbone.

3.7.2 FTIR-ATR

All FTIR-ATR measurements were carried out using a Thermo Nicolet NEXUS 670 FTIR with a SMART Endurance ATR attachment in place. The ATR attachment was purged for at least 15 minutes before any samples were run. Samples were run from 4000 to 650 cm^{-1} with a resolution of 2 cm^{-1} with 48 scans per sample. Background spectra were obtained prior to each different sample number and the surface of the ATR module was cleaned with organic solvent and dried prior to starting the next sample analysis. These measurements were carried out at random space intervals throughout the sample, with usually three measurements on one side of a fabric substrate and three more on the other side.

3.7.3 SEM-EDS

A scanning electron microscope (SEM) equipped with an energy dispersive spectroscopy (EDS) detector was used to characterize the morphology of the adsorbent fabric and to identify the chemical species extracted by it. Adsorbent samples that have been exposed to Atlantic Ocean seawater during the adsorption experiments were dried overnight in a vacuum dessicator and mounted on a SME aluminum stub for EDS analysis. The EDS detector was part of a Hitachi S-3400 variable pressure SEM.

3.7.4 XPS

XPS measurements were carried out using a Kratos Axis 165 spectrometer using monochromatic Al radiation (at a power of 280 W) with a vacuum level at or below 5 x 10^{-8} torr throughout the data collection process. Due to the insulating nature of the nylon 6 samples, charge neutralization was required to minimize sample charging. All survey spectra were collected with a pass energy of 160 eV and all high resolution spectra with a pass energy of 20 eV. All spectra were calibrated to C-C/C-H bonding at 284.8 eV. Samples were prepared by attaching the grafted fabric directly to the metal stage using copper tape.

3.7.4.1 Uranyl binding to azo compounds

Binding of uranyl to a number of azo compounds was carried out using XPS. Equivalent molar quantities of an azo compound and uranyl acetate were dissolved in separate solutions of methanol. Once dissolved, these solutions were mixed and stirred. The methanol was then allowed to evaporate off and the precipitate was collected for testing in the XPS.

3.7.5 Zeta Potential Measurements

Microparticle solutions were prepared using pieces of nylon 6 grafted fabric via the “solvent in water” precipitation method. Samples were first dissolved in acetic acid at 80°C, at a concentration of 20 mg/mL to form the diffusing phase (organic phase). This phase was then added drop by drop into filtered deionized water, which is the dispersing phase (aqueous phase), under moderate magnetic stirring. The formation of microparticles was instantaneous and the solution

was kept under mild agitation for 4 h to allow for particle stabilization. Small aliquots from each microparticle solution were diluted in DI water and titrated to pH 8.3, pH 4.5, and pH 3 using sodium hydroxide and hydrochloric acid solutions prior to surface charge characterization. The zeta potential of nylon 6 microparticles was assessed by means of electrophoretic light scattering (Zetasizer nano-ZS90; Malvern instruments; Westborough, MA).

3.7.6 Electron Paramagnetic Resonance Spectroscopy

EPR spectroscopy is a powerful technique for detecting the spin of unpaired electrons, also known as free radicals, in a material. In a magnetic field, the magnetic fields of the unpaired electrons will align parallel to the generated magnetic field. During a measurement, photons of a range of frequencies in the microwave region are supplied to the sample. These photons can be adsorbed by the aligned, unpaired electrons causing the alignment of the electron's magnetic field to become antiparallel to the generated magnetic field. The relationship between the microwave energy and the energy required to flip the spin of the electron is described by the following equation, eq. 13:

$$\Delta E = \hbar\nu = g\mu_{\circ}B \tag{13}$$

where ΔE is the energy required to flip the spin of the electron, ħ is the reduced Planck's constant, 1.055×10^{-34} J ● s, ν is the frequency of the microwave inherent upon the sample, g is the g-factor which is approximately 2, $\mu_{\circ}$ is the Bohr magneton, 9.264×10^{-24} J●T^{-1}, and B is the magnitude of the magnetic field in gauss[23].

When an EPR spectra is obtained, a constant microwave frequency is applied to the sample and the magnetic field is swept over a range of strengths. The intensity of the adsorption of the microwave is recorded by the EPR, however the first derivative of this adsorption spectrum is often what is reported. The generated spectrum contains many subtleties regarding its behavior and shape. For example, in many samples the free radical is located close enough to an unpaired nuclear spin, i.e. a hydrogen atom, which will apply a small but measureable magnetic field to the free radical along with the magnetic field from the EPR. Therefore the resulting magnetic field applied to the unpaired electron will actually be a sum of these two magnetic fields, shown in equation 14:

$$B = B_{\circ} \pm B_I \tag{14}$$

where B is the total field strength applied to the unpaired electron, $B_{\circ}$ is the field strength from the EPR magnet, and B_I is the magnetic field strength contribution from the local unpaired nuclear spin. B_I can be positive or negative, similarly to the orientation of unpaired electron being antiparallel or parallel to the EPR magnetic field. Since there are now two different magnetic fields affecting the orientation of the unpaired electron spin, the adsorption peak will be split into two identical peaks. Known as the hyperfine interaction, the magnitude of this interaction follow's Pascal's triangle.

When interpreting an EPR spectrum (reported as the first derivative of the actual adsorption spectra), the number and splitting of the peaks present in the spectrum are directly related to the local chemical environment of the free radical. Nomenclature of EPR dictates that the atom that is bound to the free radical is the α atom, while the nearest neighbor atoms are the β atoms.

Figure 15 – An example image of a Bruker Elexsys Spectrometer.[24]

EPR spectroscopy was carried out at NIST on a Bruker Elexsys, shown in Fig. 15, using an EPR spectrometer equipped with a Bruker 4119 cavity and operating in the X-band. The spectral recording parameters utilized for the measurements in this dissertation were as follows: 12.7 mW microwave power; 10 mT field sweep; 0.4 mT modulation amplitude; 20 ms conversion time; 20 ms time constant; and a spectral resolution of 1024 data points. This instrument and these instrument parameters were used to study the behavior of radical decay in irradiated polymer substrates. The intensity of the peaks in the EPR spectrum will be directly correlated to the concentration of unpaired electrons in the measured material. Within the context of this dissertation, the main source of unpaired electrons within an irradiated substrate material, like nylon 6, would be the result of an irradiation. The experiments associated with this were aimed at determining the radical decay time inside nylon 6 to validate the indirect grafting method and to improve the understanding of the grafting mechanism.

Substrate samples were irradiated at MIRF under 10.5 MeV electrons to varying doses, particularly doses that would reflect normal grafting procedures, i.e. 150-250 kGy. These samples were irradiated in inert atmosphere conditions at dry ice temperatures. Following the irradiation, the vials containing the substrate samples were moved inside an argon purged glove bag while still in contact with dry ice, where the fabric was removed from the vial and transferred to quartz EPR tubes. These tubes were sealed with parafilm to limit the presence of oxygen in the tubes since oxygen would promote separate paths for radical decay separate from the monomer-substrate radical interactions that would be present during the indirect grafting process.

3.8 Uranium Extraction Testing

3.8.1 Rotator

Test solutions of uranium in seawater were prepared by dissolving a suitable quantity of uranyl acetate dihydrate in Atlantic Ocean Seawater. In each test, the adsorbent sample was added to a desired volume of a solution of uranium in seawater and the combination of test solution and solid adsorbent was rotated for a desired period of time, usually seven days, at 30 rpm in a rotating agitator. An image of the rotator is shown in Fig. 16. At the end of this period, the solution was

separated from the adsorbent and analyzed to determine the amount of uranium remaining in the solution.

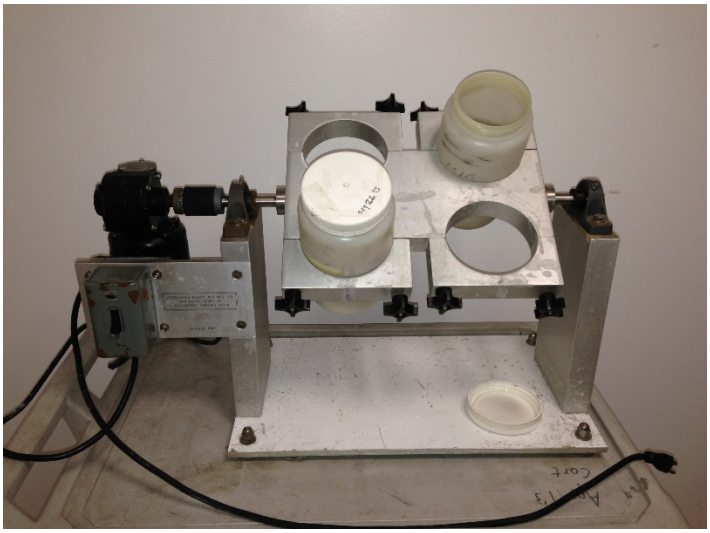

Figure 16 – The sample rotator used for agitating solutions of doped seawater in contact with grafted fabric samples.

3.8.2 Flow loop

In order to improve the testing conditions for the extraction samples, a separate testing system was manufactured to resemble the testing facilities at Pacific Northwest National Laboratory[25]. This flow loop design is shown in Figs. 17 and 18. Flow columns were obtained from PNNL which were then attached to a plastic tube via quick-connect fittings. A pump drives undoped seawater from a large reservoir through the four columns. Flow rate meter along with needle valves at the end of the columns allow for precise control over the flow rate in the columns. Samples are packed into glass wool and then placed among plastic beads inside the columns to make sure the uranium extraction sample remains in place throughout the entirety of the experiment. The flow loop reservoir was filled using Nutri-SeaWater saltwater, which is ocean water that has been filtered and replenished with certain trace elements, including uranium. Once samples were in place in the flow columns, the system was run for two weeks at ~0.4 gpm.

Figure 17 – The front view of the flow system designed to test fabrics under conditions similar to the testing performed at PNNL.

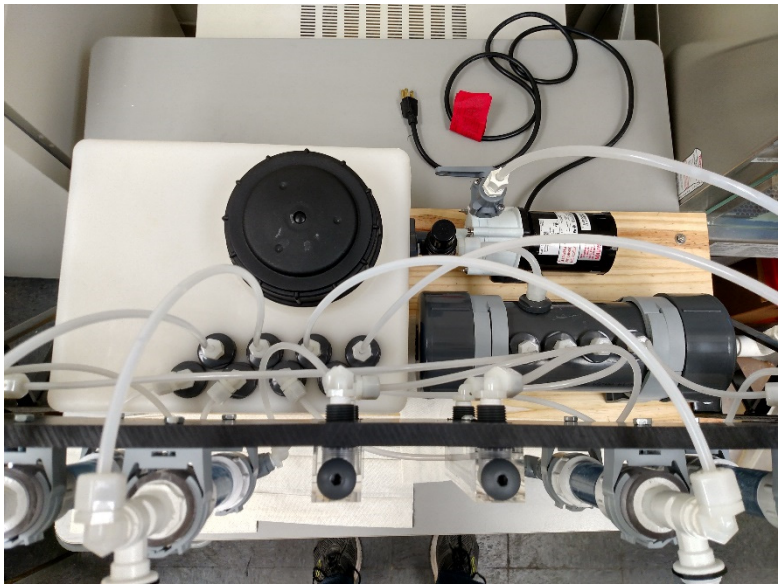

Figure 18 – A top down view of the flow system showing a clearer view of the seawater reservoir, the pump, and the pressure manifold.

3.8.3 Determination of Uranium Extraction

Fundamental to the development of materials capable of extracting uranium from seawater is the determination of their capacity for extraction. A number of different experimental methods were employed for the determination of a sample's extraction efficiency following exposure to uranium-doped seawater.

3.8.3.1 Inductively Coupled Plasma Atomic Emission Spectroscopy (ICP-AES)

ICP-AES was used for the determination of the concentration of uranium in the test solutions following the extraction period. This instrument, the Perkin Elmer Plasm 400 was capable of 1 ppm U resolution and, therefore, test solutions of less than 1 ppm were not analyzed with this technique. Prior to testing solutions, a series of uranium standards were made at varying concentrations. These standards were evaluated using the standard addition method to extrapolate uranium adsorption signal back to 0 ppm concentration. The standard addition method was used due to the complexity of the seawater matrix present in the test solution. Solutions of uranium in seawater following the extraction period were run through the spectrometer. The fraction of the uranium taken up by the adsorbent was calculated from the difference in concentration of uranium in the test solution resulting from the contact with the adsorbent.

3.8.3.2 Spectrophotometric

Uranium detection sensitivity was improved for later experiments through the use of a spectrophotometric procedure for the determination of uranium in solution. This technique has a detection limit of 0.2 ppm U, one order of magnitude better than ICP-AES measurements, thus, enabling test solutions to be used which are closer to the natural concentration of seawater in the ocean. The fundamental chemical required for this procedure is Arsenazo III, the structure of which is shown in Fig. 19.

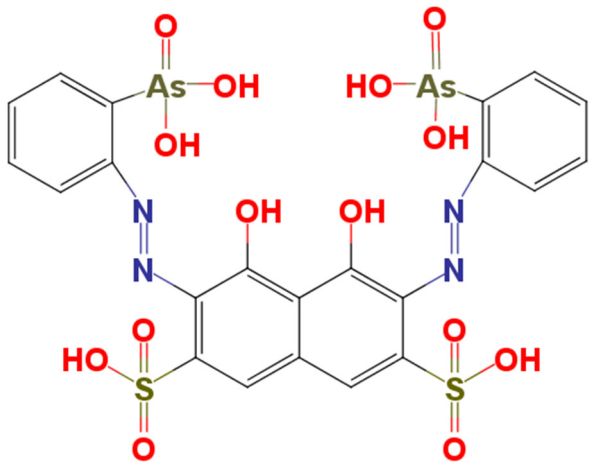

Figure 19 - The chemical structure of Arsenazo III.

Arsenazo III forms a complex with uranium with an absorption peak at 651 nm. An aqueous solution of this chemical along with a masking agent, triethylenetetraminehexa-acetic acid (TTHA), were combined with seawater samples and tested for their absorbance at 651 nm using a Cary 3 UV Spectrometer.

A 0.05 wt. % solution of Arsenazo III in ultra-high purity, deionized H_2O and a 5 wt. % TTHA were created. 2 mL of each of these solutions were added to 1 mL of uranyl solution in seawater or simulated seawater. In order to improve the sensitivity of the Arsenazo III compound, the pH of the resulting solution was adjusted to 1 using different concentrations of hydrochloric acid. Once the appropriate amount of acid was determined in order to adjust the pH of this solution

to 1, 2 mL of 0.05 wt. % Arsenazo III solution, 2 mL of 5 wt. % TTHA solution, and 1 mL of varying concentrations of uranium in a representative seawater solution were created. The seawater solutions containing specific concentrations of uranium were generated through the volumetric dilution of a standard stock solution of uranium. These solutions sat for at least one hour to allow the solutions to come to equilibrium. Afterwards, the solutions were tested for their absorbance at 651 nm in the UV-Vis spectrometer. The absorbances for the standard solutions were used as the standard reference for the test samples. Once the concentration of the uranium in the final solution was determined, the fraction of the uranium taken up by the adsorbent was calculated from the difference in concentration of uranium in the test solution resulting from the contact with the adsorbent.

3.8.3.3 Inductively Coupled Plasma Mass Spectrometry

While the prior characterization techniques provided reliable quantitative results for the concentration of uranium in extraction test solutions, they do not provide the required resolution of uranium concentration in seawater to match the concentration present in the actual ocean (3.3 ppb). In order to provide some insight into how the manufactured fabrics perform in lower concentrations of seawater, ICP-MS can be used.

3.8.4.3.1 Solution based

In order to process the fabric samples using ICP-MS that had been exposed to a solution of uranium in seawater, the uranium first had to be dissolved into an acidic solution. While an acidic solution would dissolve the Nylon 6, its complete dissolution would ensure that the entirety of the uranium present on its surface was in solution. While it was found that 2 % nitric acid could not dissolve the nylon fabrics by itself very quickly, a concentrated solution of nitric acid heated to 80 °C overnight was used to digest the fabric. Following this digestion, the concentrated nitric acid was boiled off and the remaining compound in the Teflon container which held the remaining fabric particles and metal ions was re-dissolved in 2 % nitric acid, which is the desired concentration for ICP-MS solution processing.

The uranyl test solution was processed using an ELEMENT 2 ICP-MS. After being loaded into a syringe pump, the sample solution was sent into an argon plasma where the elements in solution were ionized and accelerated through a series of cones to a bending magnet which separated the evaporated ions according to mass and charge. The concentration of uranium in the test solution was determined with the use of a standard solution of uranium. The counts per second read by the detector in the ICP-MS was correlated to varying concentrations of uranium and other elements. This relationship was then used to determine the concentration of uranium in the test solution. Since the volume of the test solution was known, the mass of uranium in the solution could be determined which could then be used to calculate the mass of uranium present on the fabric prior dissolution.

3.8.3.3.2 Laser Ablation

In order to look at uranium concentration at varying locations in the fabric, laser ablation ICP-MS can be performed. Instead of completely dissolving the uranium exposed fabric to obtain a bulk measurement, this experimental technique uses a laser to ablate a sample material. This ablated material is then blown into the ICP using a stream of helium gas.

Prior to the ablation of samples, a calibration standard was ablated to provide a reference for determining the concentration of uranium in ppm. Orchard leaves were doped with specific concentrations of uranium and vanadium. The orchard leaves acted as an analogue to the nylon 6 fabric as the carbon composition of both compounds were similar. These orchard leaves were then ablated and the carbon to uranium ratio was used to establish a calibration for the uranium in any samples where the carbon content is known, which is shown in Fig. 20.

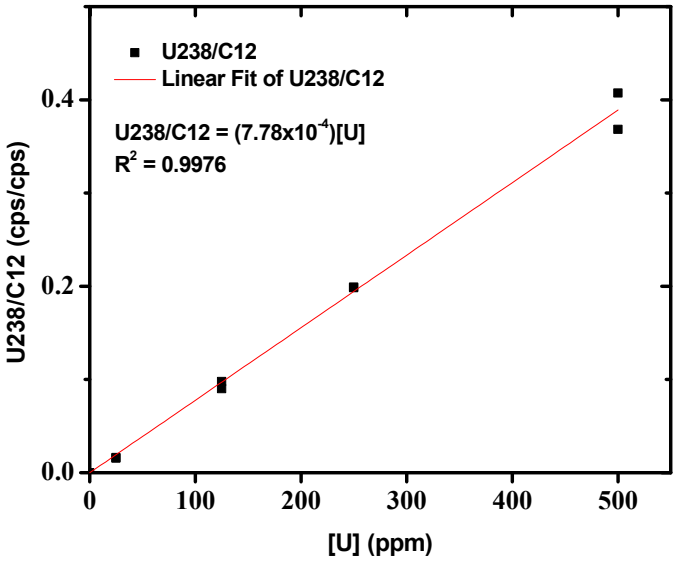

Figure 20 – The calibration curve for the ration between U-238 and C-12 counts from the mass spectrometer versus the concentration of uranium in the orchard leaf calibration standard.

For the polymer substrate samples, the carbon content is based on the knowledge of the chemical structure of the polymer samples and the mass of the initial fabric prior to uranium extraction testing.

Fig. 21 shows the control and uranium exposed samples on the sample holder for the laser ablation unit. The samples were placed on double-sided sticky tape onto a glass slide. This sample compartment was then placed inside the laser ablation unit and left for at least 15 minutes to allow for the helium to purge the internal atmosphere of the compartment of air.

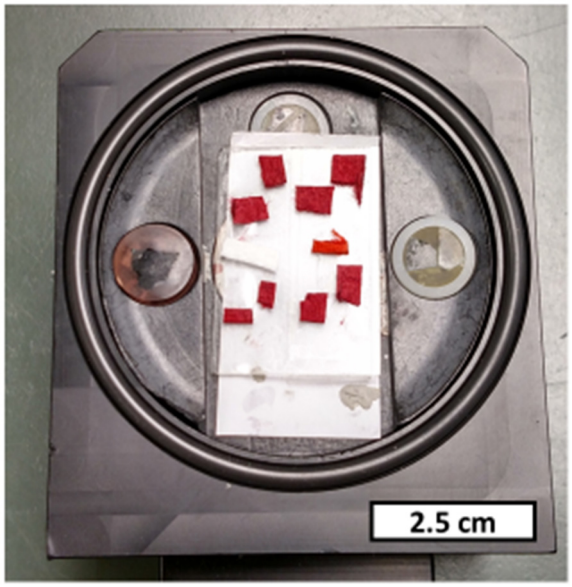

Figure 21 – Sample positioning on the laser ablation unit sample holder. A glass slide with double-sided sticky tape was used to hold the samples in place.

The fabric samples were then exposed to various beam conditions involving different beam diameters, dwell times, and laser shot frequency rates. Data collection for each run was started 20 seconds prior to the firing of the laser and was continued for about 30 seconds to one minute after the laser beam stop was removed.

3.9 Results and Discussion

Over the course of this project numerous monomers and radiation grafting techniques were utilized in an effort to fulfill the listed objectives. Testing involved the evaluation of a monomer repertoire that included eight organophosphorus compounds (including phosphates, phosphonates, three oxalates, four amines, one ketone, and four azo compounds. The preliminary studies in order to determine whether or not these compounds could actually remove uranyl from seawater were performed by incorporating the compound onto the surface of activated carbon. These doped samples would then be exposed to a solution of uranyl in seawater under different concentrations and exposure times. The compounds which had the best extraction performance would then be used in grafting experiments as possible candidates for a successful uranium extraction monomer. Throughout this work, standard error is used for the values of the error bars unless otherwise noted.

3.9.1 Substrate Selection

Throughout this project, the substrate used for the majority of grafting experiments was a high surface area, nylon 6 fabric purchased under the name winged nylon 6. An SEM image of a sample piece of fabric in Fig. 24. This fabric was chosen for its high surface area and its chemical resilience, which would assist with increasing grafting densities and regenerability following extraction respectively.

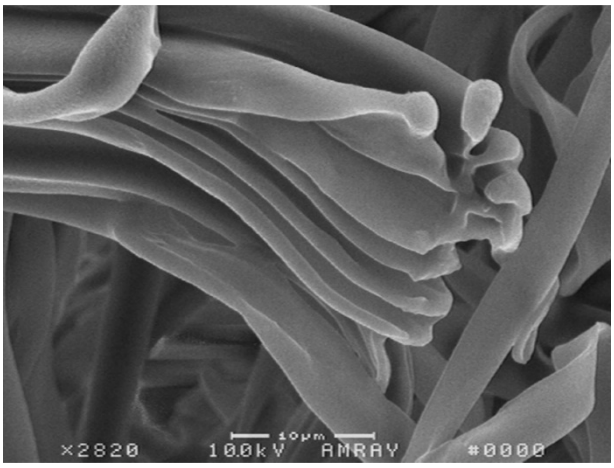

Figure 24 –SEM image of the fibers that compose the fabric.

In order to better characterize the response of the fabric to irradiation, EPR spectroscopy was performed on the nylon fabric following irradiation. This technique can be used to elucidate the lifetime and location of the radicals on the polymer backbone. Fig. 25 provides an example of the decay of the nylon radicals over the course of 2.5 hours following an irradiation to 150 kGy.

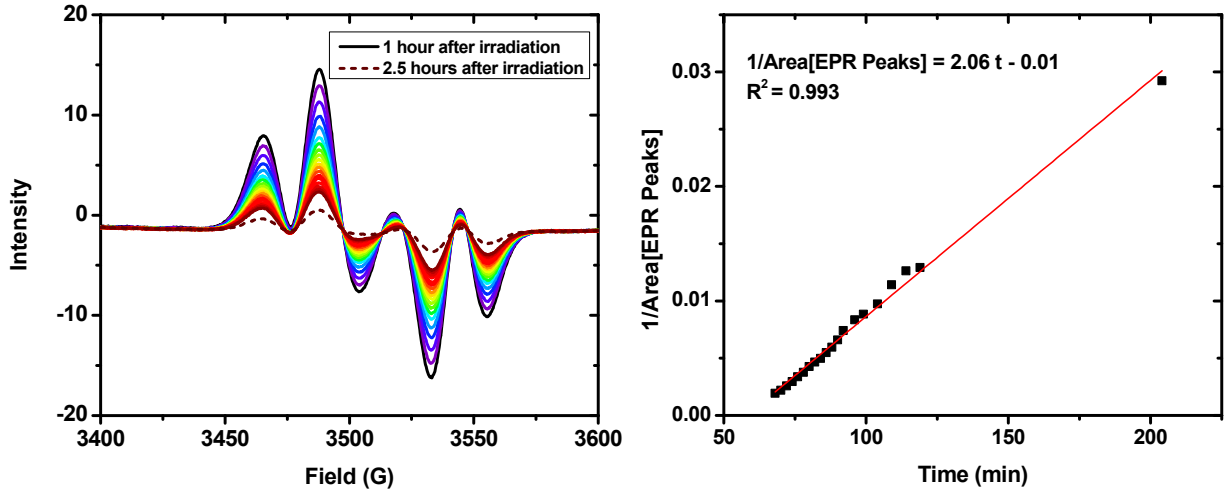

Figure 25 – **(a)** The EPR signal of winged nylon 6 irradiated to 150 kGy under electron beam. Time dependent spectra are shown from one hour after irradiation to 2.5 hours after irradiation. **(b)** The second order fit of the area of the EPR peaks for winged nylon 6 irradiated to 150 kGy.

Based on previous studies, the radical generated by irradiation of nylon 6 should be dominantly located on the carbon next to the amine that is not the carbonyl, see Fig. 26.[26,27]

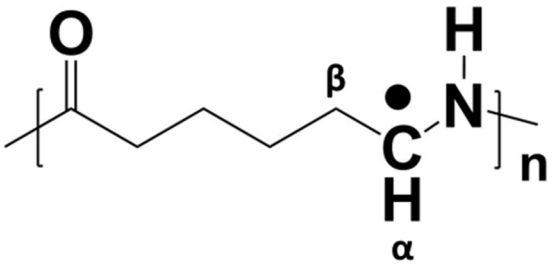

Figure 26 – The most likely position of the nylon 6 radical generated during irradiation. α and β signify the locations of the respective protons seen in the EPR spectrum.

The position of this radical matches the EPR spectra recorded. This free radical has two identical β protons, which create a triplet peak with intensity ratios 1:2:1. These peaks are further split by the single α proton, thereby forming a 1:3:3:1 intensity ratio of the peaks. The magnitude of the splitting should be 28 gauss for the β proton and 22 gauss for the α proton.[27] Fig. 27 shows the collected EPR spectra with the regions labeled with their respective intensity ratios.

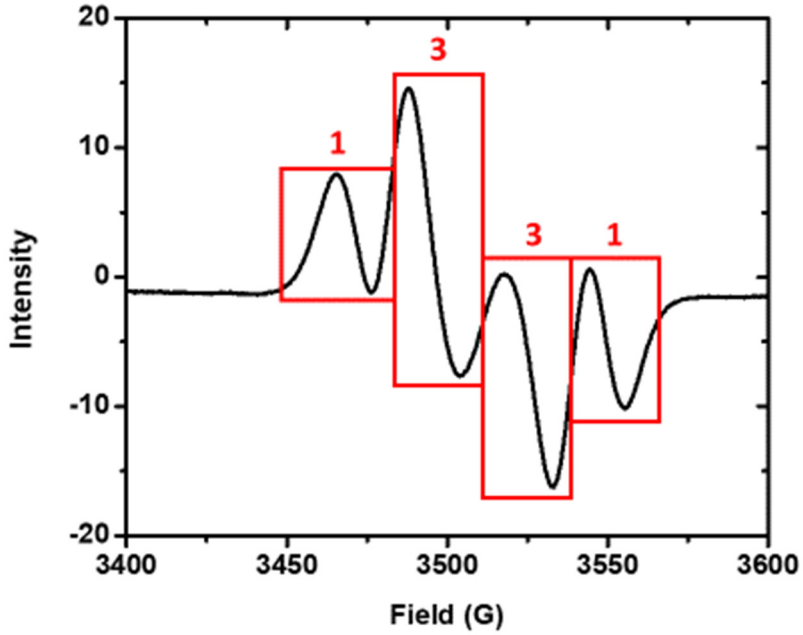

Figure 27 – The red boxes highlight the location of the 1:3:3:1 peaks associated with the overlap of the α and β proton splitting of the nylon 6 radical.

The decay of the nylon 6 radical most likely proceeds via a second order reaction through the following scheme:

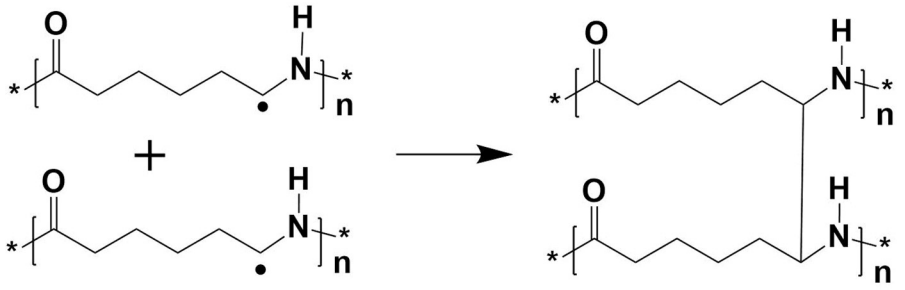

This conclusion is further corroborated by the kinetics of the decay of the radical, where the data is shown to have a significantly better fit to second order kinetics behavior in Fig. 28.

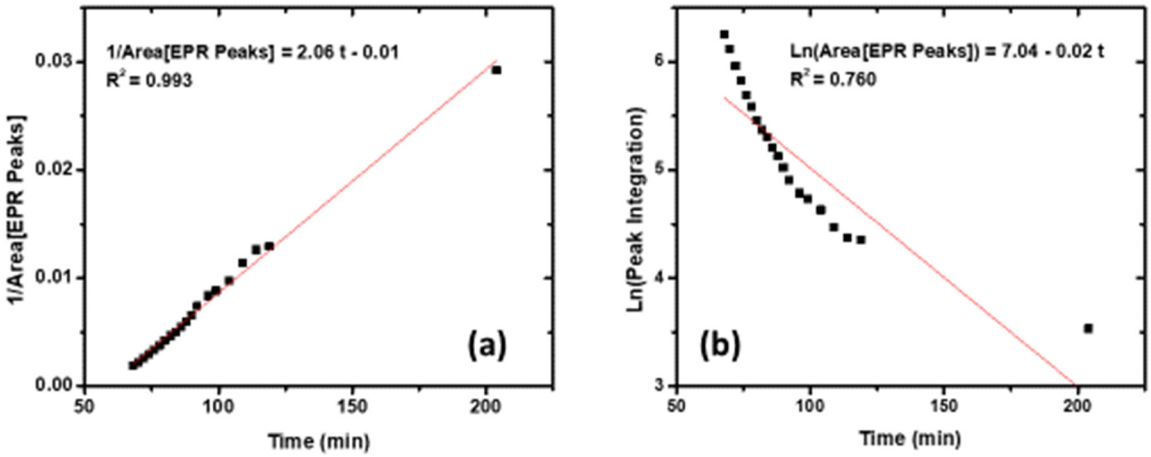

Figure 28 – The second order (a) and first order (b) fits for the nylon 6 radical decay.

3.9.2 Phosphate Compounds

The ubiquitous relationship between phosphates and uranyl ions has been well established, particularly in both geological deposits, with phosphate mine being a significant source of uranium, as well as in industrial separations of uranyl and other actinides from aqueous solutions, in the case of the PUREX process. Phosphates were initially explored as an option for the extraction of uranium from seawater based on this relationship.

3.9.2.1 Selection

Initial efforts to extract uranium from seawater were focused on obtaining allyl or vinyl functionalized phosphate derivatives. Phosphates have previously been used for the extraction of uranium from aqueous solutions and have been found complexed with uranium in natural ore deposits.[28] Commercially available ligands that matched these parameters were found and vetted using the activated carbon exposure method in order to determine which group was able to adsorb the most uranium from seawater in the shortest amount of time. The results of this initial experiment revealed bis-(2-methacryloxyethyl) phosphonate (B2MP) as the most successful candidate for extraction, see Table 2.

Table 2 – All listed monomers were γ-irradiated at 5 kGy/hr for one hour onto winged nylon and tested for their ability to extract uranium which is exhibited by their K_D value (given in mL/g, K_D

is equivalent to the mass of uranium adsorbed by the fabric per mass of the fabric given in g/g, divided by the concentration of uranium in the solution given in g/mL).

Monomer	Structure	k_D
Diethyl allyl phosphonate	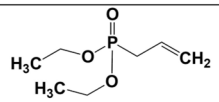	116.9
Vinylphosphonic acid	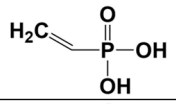	168.0
Diethylvinylphosphonate	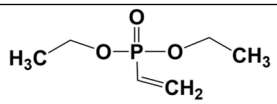	354.1
Dimethylvinylphosphonate	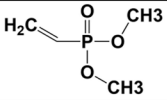	185.1
Bis(2-methacryloxyethyl) phosphonate	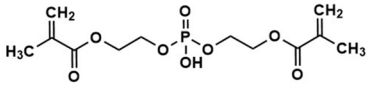	46980.1

3.9.2.2 Grafting

Initial grafting experiments were focused on establishing a baseline of grafting parameters to use with B2MP. The kinetics of the radiation-induced polymerization reactions of B2MP in aqueous solutions were measured using a pulse radiolysis setup with an FTIR detection system at the BNL 2 MeV electron Van de Graaff.

Radiolysis of D_2O yields a mixture of oxidizing, reducing, and neutral species with the following radiation- chemical yields in μmole per joule[21]:

$$G(^{\bullet}OD) = 0.294$$
$$G(e_{aq}^{-}) = 0.307$$
$$G(D^{\bullet}) = 0.045$$
$$G(D_2) = 0.037$$
$$G(D_2O_2) = 0.068$$

D_2O solutions of 5 mM to 25 mM of B2MP were saturated with N_2O to convert the e_{aq}^{-} to $^{\bullet}OD$ as follows, eq. 15:

$$N_2O + e_{aq}^{-} + D_2O \rightarrow {}^{\bullet}OD + N_2 + OD^{-} \quad (15)$$

Hence, the total G ($^{\bullet}OD$) is 0.603 μmole per joule. The solubility of N_2O in aqueous solutions is about 25 mM.

The polymerization reaction would be initiated by the addition of $^{\bullet}OD$ onto the carbon-carbon double of B2MP, giving rise to the formation of the OD-B2MP$^{\bullet}$ adducts, shown in equation 16:

$$^{\bullet}OD + B2MP \rightarrow OD\text{-}B2MP^{\bullet} \quad (16)$$

The reaction rate constant of the addition of $^{\bullet}OD$ to the double bond of the B2MP is expected to be in the order of 1-5 x 10^8 $M^{-1}s^{-1}$. Taking into account that the [B2MP] concentration is, for example, 20 mM, and a reaction rate constant of ~ 1 x 10^8 $M^{-1}s^{-1}$, one would expect the half-life

of this reaction to be about 0.3 x 10^{-6} s. Therefore, this reaction cannot be detected when electron pulses of 4 μs pulse width are used.

It should also be mentioned that the D-atoms with G (D) = 0.045 add to the double bonds or abstract H atoms from the B2MP producing DB2MP•, and B2MP•(-H), respectively, equations 17 and 18:

$$D^{\bullet} + B2MP \rightarrow DB2MP^{\bullet} \quad (17)$$

$$D^{\bullet} + B2MP \rightarrow B2MP^{\bullet}(-H) + HD \quad (18)$$

The initiating C-centered free radicals, OD-B2MP•, DB2MP• and B2MP•(-H), react relatively fast with the monomer, B2MP, via an addition reaction, triggering the propagation reaction.

As an example of the FTIR data, Figure 29 shows a series of FTIR difference spectra, recorded relative to the initial spectrum of 20 mM B2MP in N_2O-saturated D_2O, during and following irradiation of the solution with 4 ms electron pulses. Twelve consecutive pulses were used, separated by approx. 10-20 s, with each pulse depositing about 130 Gy/pulse for a total of 1.56 kGy. An FTIR spectrum was recorded immediately after each pulse, and then spectra were recorded at intervals as the polymerization reaction propagated. As shown in Figure 429, there is a decrease of the 1697 cm^{-1} n(C=O) and 1635 cm^{-1} n(C=C) absorption bands as a function of time. This is a strong indication that through the propagation reaction, the double bonds in the B2MP have reacted via the addition reactions of OD-B2MP•, DB2MP• and B2MP•(-H) radicals, leading to the formation of more C-centered radicals. Figure 29 also shows the gradual increase of the peak at 1728 cm^{-1} as a function of time. This gradual increase may be related to the formation of the methyl 2-hydroxypropanoate structure within the dimerization of the B2MP radicals.

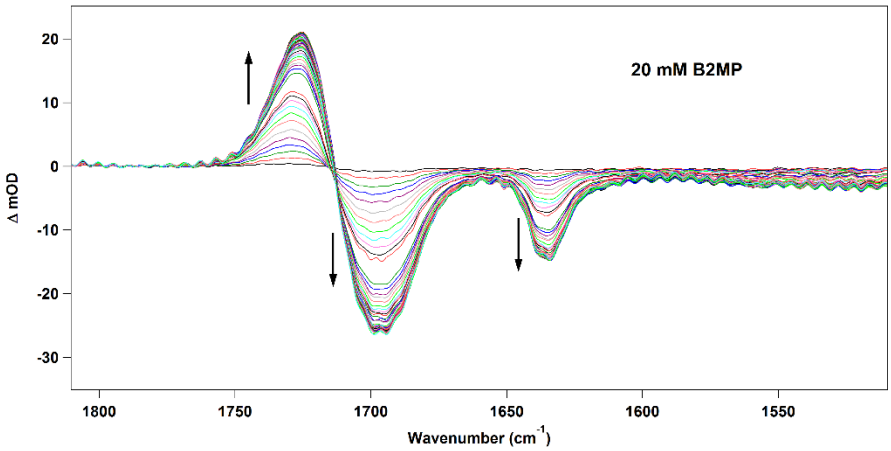

Figure 29 – The change in optical density of the 20 mM B2MP solution over the course of about seven hours. The new peak grew at 1728 cm^{-1} while the peaks at 1697 and 1635 cm^{-1} decayed following the irradiation.

Figure 30 illustrates some of the most significant radiation grafting reaction pathways that can occur during the radiation grafting of B2MP to nylon 6. Out of the five reactions illustrated, only one reaction is truly desirable: the grafting of monomer on the surface of the nylon 6 through the nylon 6 radical species. All the remaining reactions are undesired as they quench radicals produced by radiation without producing grafted material. There are tiers to desirability however. Monomer-substrate radical termination does produce a grafted material, however it does no produce high DoGs. Monomer dimerization and homopolymerization do produce polymers of the

monomer that could still attach to the substrate if a substrate radical reacts with a carbon-carbon double bond in the homopolymer or dimer. Finally, substrate crosslinking is completely undesired as this leads not only to the loss of radicals available for grafting, but it can also detrimentally alter the material properties of the substrate.

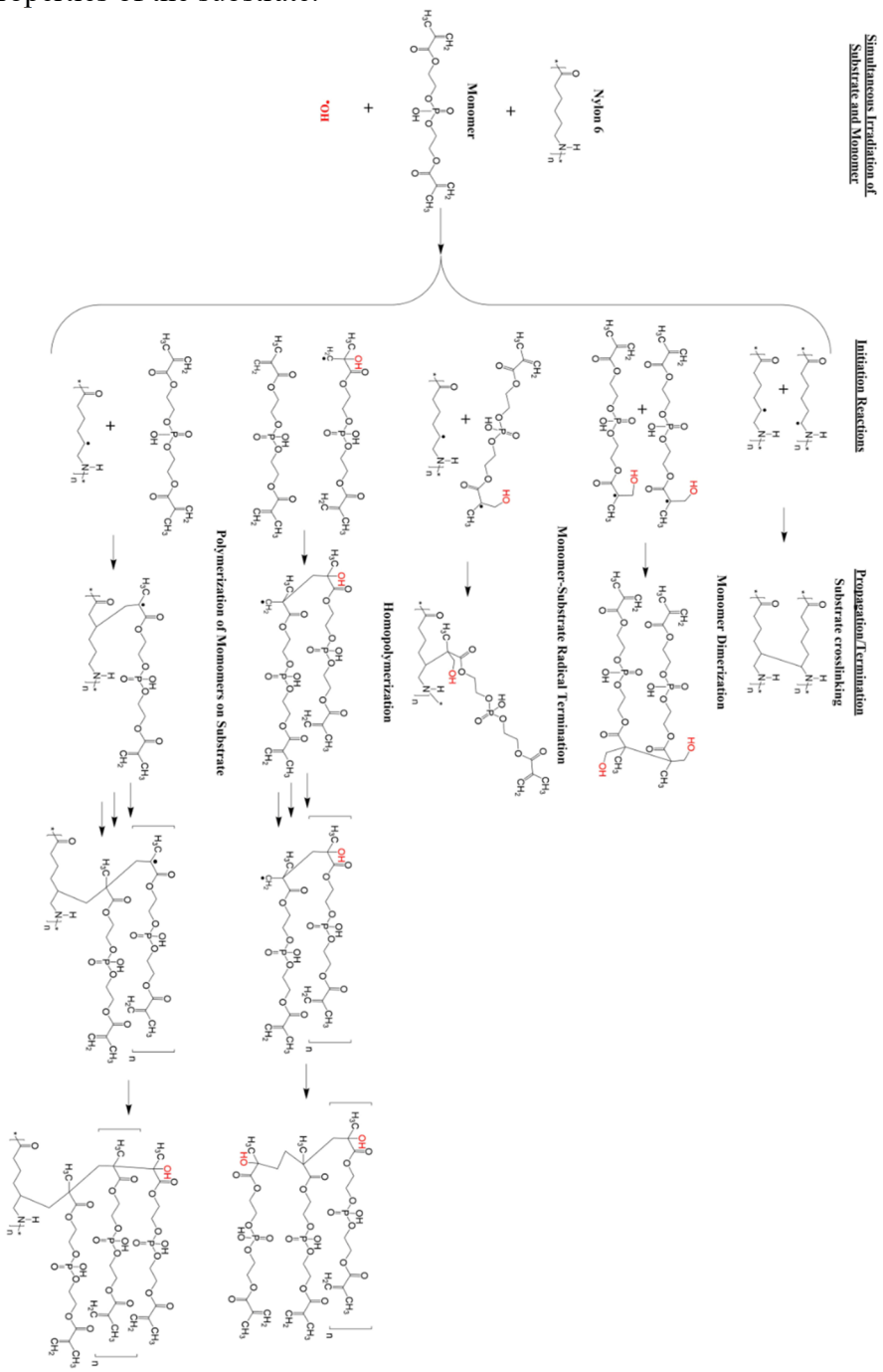

Figure 30 – The different radical reactions that would occur during the irradiation of nylon 6 fabric exposed to a solution of B2MP.

The propagation reaction kinetics were monitored by integrating the areas of the 1635, 1697, and 1728 cm^{-1} bands, and plotting them as a function of time. Figure 31 shows typical kinetic

traces obtained from this procedure, following the pulsing of a N_2O-saturated [20 mM] B2MP D_2O solution. The very sharp-fast decrease/increase in absorption within the first ~120 s (indicated by the red dash-lined box in Figure 31) is caused by the 12 successive electron pulses during the irradiation period.

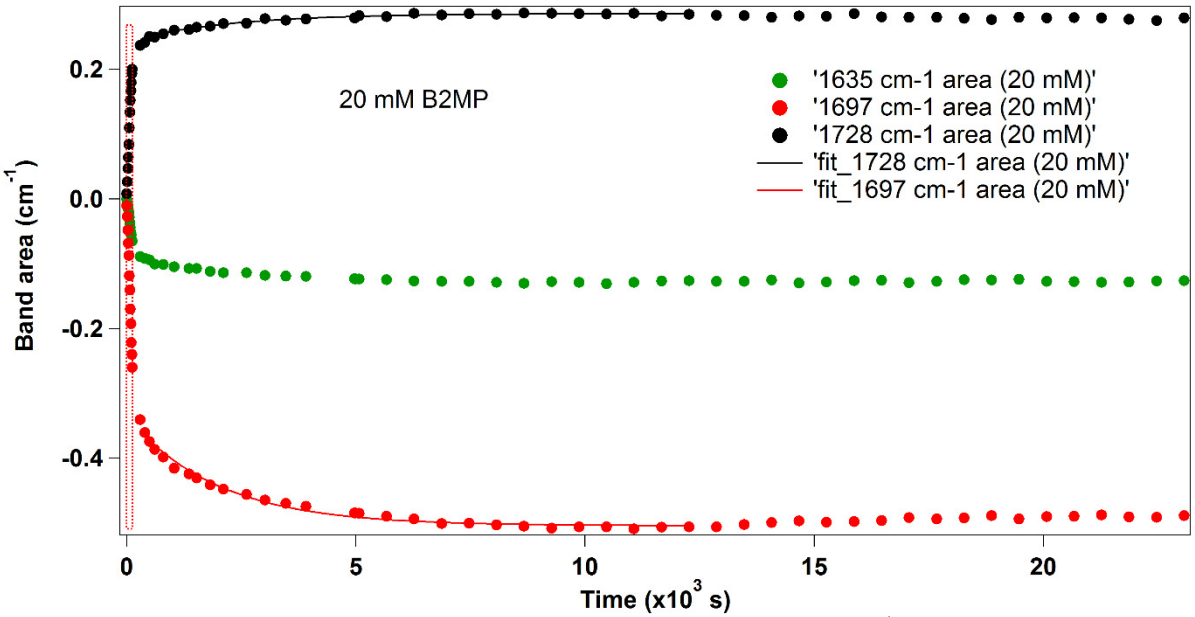

Figure 31 – The growth and decay of the 1635, 1697, and 1728 cm^{-1} peaks in the FTIR spectra of a 20 mM B2MP solution in D_2O.

The reaction rate constant of the decay at 1697 cm^{-1} was measured as a function of [B2MP] concentration. Since the data did not fit well to a single exponential function at the higher concentrations of B2MP, double exponential fitting of the kinetic traces was performed, always starting from the first time point immediately after the last electron pulse. Of the two rate constants obtained from the double exponential fits, only the higher rate constant showed a significant dependence on [B2MP]. Therefore, a pseudo-first-order plot of these rate constants as a function of [B2MP] was prepared (Figure 32). These results represent the kinetics of the propagation reactions, where the propagating C-centered radicals add to the double bonds of the B2MP, equations 19-21:

$$\text{OD-B2MP}^{\bullet} + \text{B2MP} \rightarrow \text{OD-B2MP-B2MP}^{\bullet} \quad (19)$$

$$\text{DB2MP}^{\bullet} + \text{B2MP} \rightarrow \text{DB2MP-B2MP}^{\bullet} \quad (20)$$

$$\text{B2MP}^{\bullet}\text{(-H)} + \text{B2MP} \rightarrow \text{B2MP-B2MP}^{\bullet}\text{(-H)} \quad (21)$$

The second-order reaction rate constant of the propagation reaction is the slope in Fig.32, which was found to be 0.2 ± 0.04 $M^{-1}s^{-1}$.

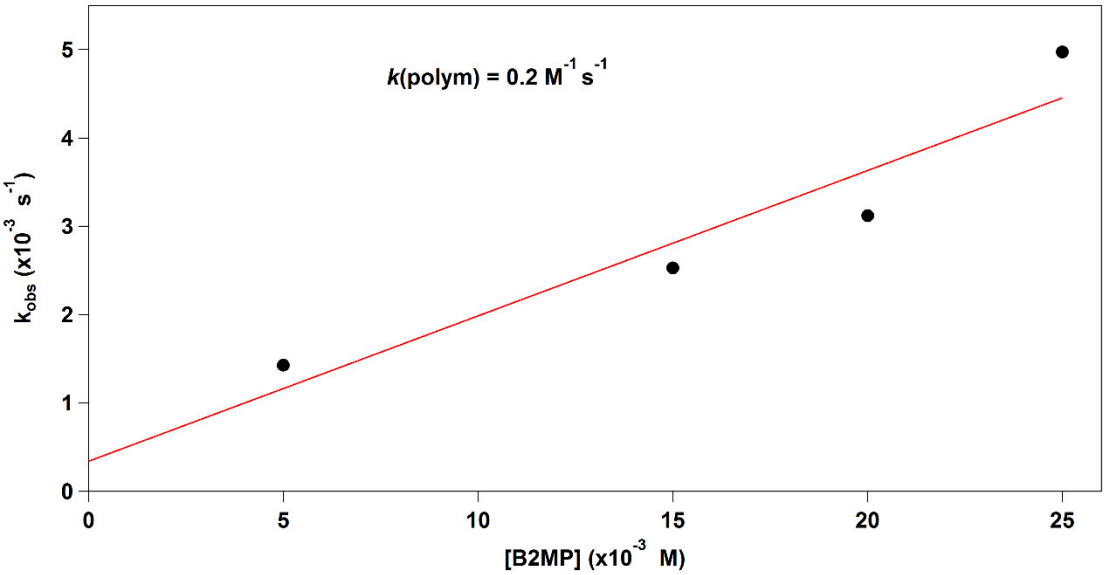

Figure 32 – The linear regression of the trend in rate constant versus the concentration of B2MP in solution to obtain the actual second order rate constant of this propagation reaction.

As for the second-order buildup of the 1728 cm^{-1} absorption band, this can be explained by the fact that under these pulse radiolysis conditions, where the dose per pulse is relatively high, one expects that the second-order dimerization reaction of the B2MP radicals competes with the propagation reaction. Figure 33 shows the buildup of the 1728 cm^{-1} absorption band at various [B2MP] concentrations.

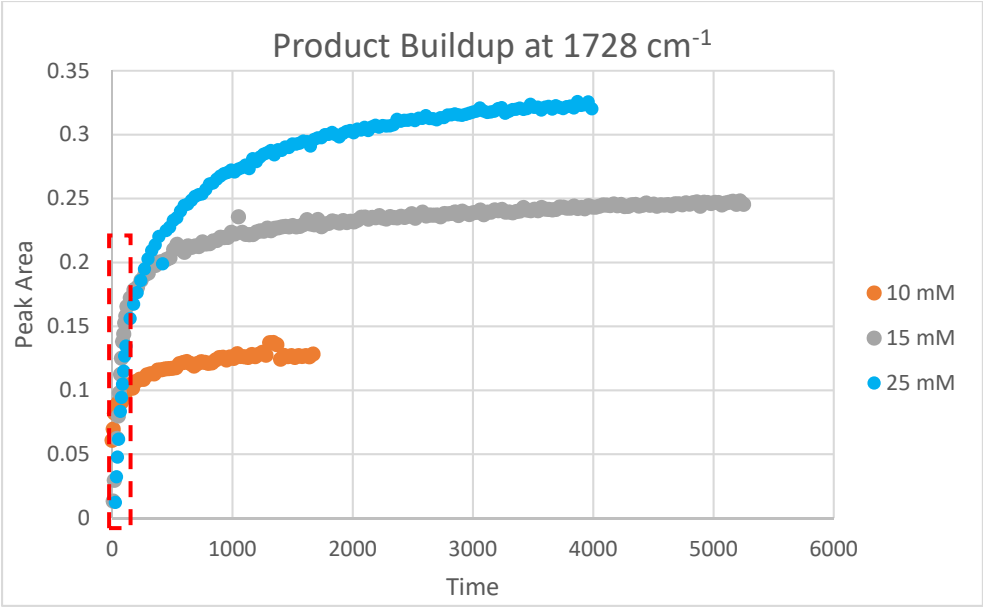

Figure 33 – The buildup of the product shown by the increase in absorbance of the B2MP solutions at 1728 cm^{-1}. The red box surrounds data points taken during the irradiation of the solution, which are ignore in the kinetics calculations.

The following kinetics equation, eq. 22 can be used to determine the reaction constant, k, from the results shown in Fig. 33,

$$\frac{1}{D_\infty - D_t} = \frac{4kt}{\varepsilon_{1728\,cm^{-1}}\, l} + \frac{1}{D_\infty} \tag{22}$$

where D_t is the optical absorbance at time, t, D_∞ is the final absorbance, k is the second-order rate constant of dimerization, e is the molar extinction coefficient of the absorbing chemical (in this case the B2MP dimer), and l is the optical path length of the IR cell. Figure 34 depicts the plot of $\frac{1}{D_\infty - D_t}$ vs. t. Hence the second-order rate constant, k, is calculated via the following equations, equations 23 and 24:

$$Slope = \frac{4k}{\varepsilon_{1728\,cm^{-1}}\, l} \tag{23}$$

$$k\ (M^{-1}s^{-1}) = \varepsilon^{1728}\ (M^{-1}cm^{-1}) \bullet slope\ (s^{-1}) \bullet \ell\ (cm)\ /\ 4 \tag{24}$$

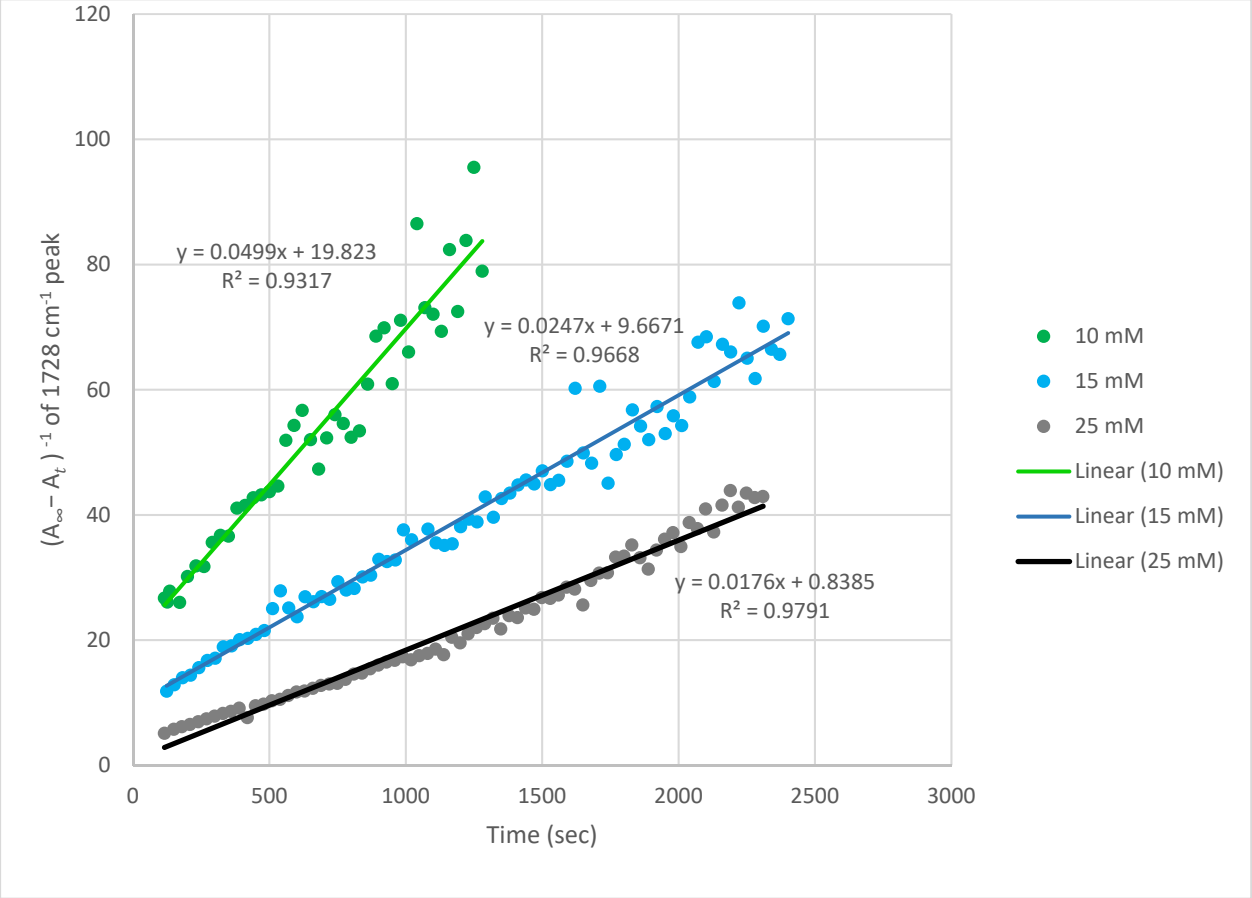

Figure 34 –The various fits of the increase in absorbance at 1728 cm^{-1} for different concentration of B2MP in solution.

Since we do not know the value of e_{1728}, it is not possible to determine the actual second-order rate constant, *k,* for the dimerization reaction. However, the slopes in Figure 34 are proportional to *k*. As in the case of any free radial polymerization reaction, the free radical dimerization reactions are independent of the initial monomer concentration, [B2MP]. They are only dependent on the dose per pulse and pulse repetition. However, as shown in Figure 35, which plots the slopes of the Figure 34 graphs versus [B2MP], the dimerization (termination) reaction rate constant of the B2MP$^{\bullet}$ radical decreases as the initial [B2MP] concentration increases. This decease may be related to the increase in the viscosity of the B2MP polymer chain in solution. As the initial [B2MP] concentration increases, the chain polymerization reaction enhances, which leads to an increase in the viscosity.

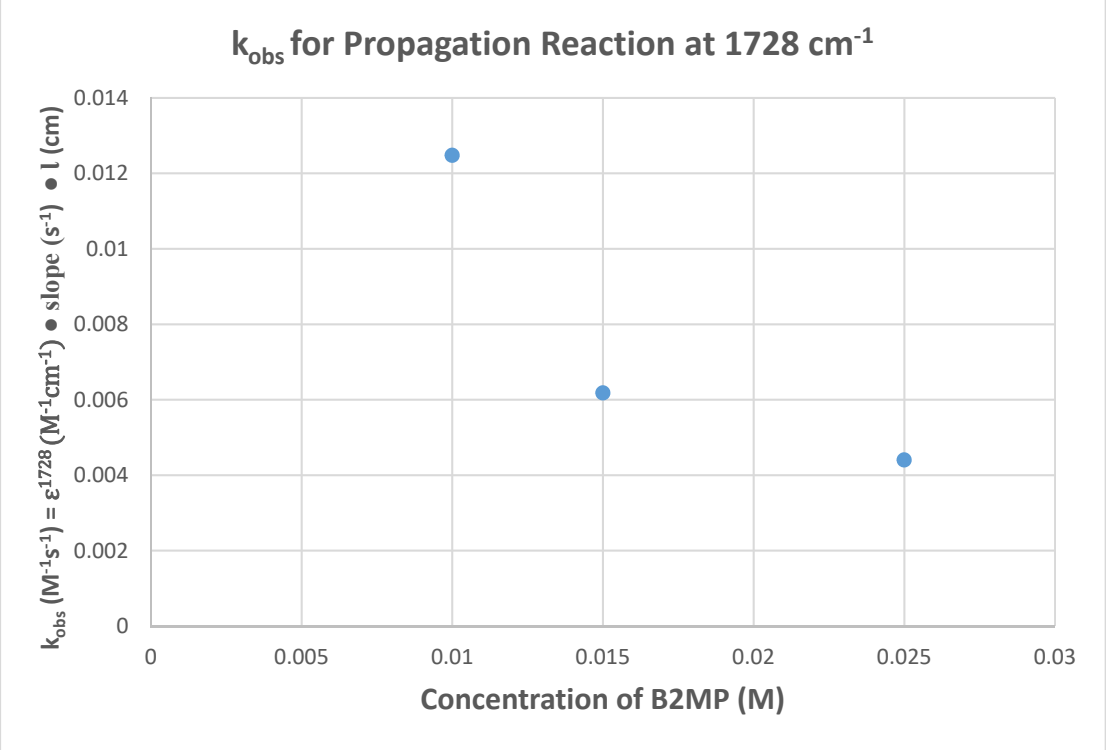

Figure 35 – The trend in rate constants of the propagation reaction occurring at 1728 cm^{-1} with concentration of B2MP.

3.9.2.3 Characterization

The attachment of B2MP to the surface of the winged nylon 6 fabric was evaluated through the use of FTIR-ATR. Fig. 36 illustrates a comparison between the clean winged nylon 6 and a B2MP-grafted winged nylon 6 sample. Of particular importance are the strong peaks emergent in the B2MP spectrum associated with the attachment of the phosphate group. The peak at ~979 cm^{-1} is most likely the P-O-C stretching vibration while the peak at ~1030 cm^{-1} is most likely the P=O stretching vibration[29,30].

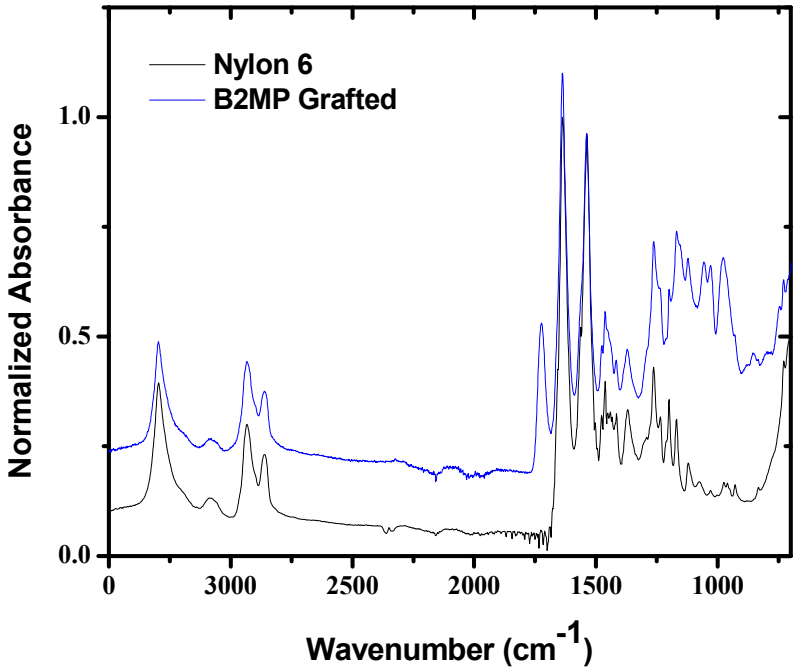

Figure 36 – The FTIR spectra of both a clean, ungrafted winged nylon 6 sample and a B2MP-grafted winged nylon 6 sample.

3.9.3 Oxalate Compound

3.9.3.1 Grafting

Initial DAOx grafting experiments were performed with aqueous solutions. Irradiations proceeded using 5.54 kGy/hr Co-60 irradiations to 10, 20, 30, and 40 kGy. These samples only achieved a maximum of 8% DoG. Due to the fact that the DAOx samples were sonicated for only about an hour, it was assumed that the DAOx was not completely dissolved in solution upon irradiation. After irradiation, the water in the DAOx was cloudy most likely indicating homopolymerization.

Initial experiments with the electron beam used the same 56 mM concentration of DAOx as in the prior Co-60 experiment, but used doses from 60-120 kGy and a dose rate of roughly 160 kGy/hr. This irradiation resulted in negligible degrees of grafting, however this is most likely due to the lack of proper dissolution of the monomer in solution along with a lack of the use of purging to make the atmosphere in the sample vials inert.

Experiments with DAOx in pure ethanol generated DoGs of about 10%, not significantly higher than the DoGs obtained in previous experiments. Direct radiation grafting of DAOx onto nylon 6 was performed in the absence of oxygen in neat (where neat refers to a system that contains no solvent) liquid DAOx and also in aqueous solutions in the presence of a surfactant.

The following experiments were able to use pure aqueous solutions of DAOx at 56 mM without a co-solvent as long as the solution was stirred overnight. This led to the complete dissolution of the monomer.

In response to the lower DoGs seen with alternate monomer-solvent systems of B2MP, methanol was used as a partial solvent. Different amounts of methanol were added to 1 mL of

B2MP in contact with fabric in order to slow down the process of homopolymerization that led to the solidification of the monomer by itself during irradiation. These samples also completely solidified upon irradiation even at doses as low as 10 kGy. Winged nylon 6 fabric was also grafted using pure monomer solution. Compared to the B2MP solutions, which saw complete solidification of the monomer in a polymer matrix within 20 kGy, the DAOx did not experience any amount of solidification and merely increased in qualitative viscosity. However, this was coupled with DoGs between 3 and 22%, indicating that grafting with pure monomer would be a possible pathway towards higher DoGs with the optimization of the grafting process.

An attempt was made to perform indirect grafting, however indirect grafting with pure monomer only yielded DoGs less than 10%. It was believed that the method for indirect grafting had to be improved as the monomer solution injections were carried out in air and the fabrics were irradiated at room temperature. This most likely led to an introduction of oxygen to the sensitive radical system and a rapid decrease in radical concentration in the fabric following the irradiation, respectively.

Higher doses at high dose rates similar to those of previous experiments led to higher DoGs. The large amount of homopolymerization present in these solutions after irradiation suggests that by altering the dose rate, temperature, and other factors of the irradiation conditions this homopolymerization can be reduced and higher degrees of grafting can be obtained. The size of the homopolymerization might also lend itself to adjusting the surfactant concentration even further to obtain micelles of sizes that promote higher DoGs. Based on experiments with neat DAOx as the monomer solution during irradiation, DAOx grafted samples with high DoGs can be consistently obtained through the use of neat monomer grafting.

The reaction rate constant of the hydrated electron, e_{aq}^- with DAOx, under anaerobic conditions, was determined by monitoring the decay of e_{aq}^- as it reacted with DAOx. Under our experimental conditions, radiolysis of water will yield the following oxidizing, reducing, and stable species, with their radiation-chemical yields given in μmole per joule[21]:

$$G(^{\bullet}OH) = 0.29$$
$$G(e_{aq}^-) = 0.29$$
$$G(H) = 0.06$$
$$G(H_2) = 0.\ 04$$
$$G(H_2O_2) = 0.08$$

Prior to the pulse radiolysis experiments, DAOx aqueous solutions were purged with Ar to remove the dissolved oxygen. This is a very important step to prevent the scavenging of e_{aq}^- by oxygen according to the following very fast reaction, eq. 25,

$$e_{aq}^- + O_2 \rightarrow O_2^{\bullet -} \quad (25)$$

which has a reaction rate constant of 2×10^{10} $M^{-1}s^{-1}$.

In the radiation chemistry of aqueous solutions, t-butanol can be used routinely to scavenge $^{\bullet}OH$ radicals in order to permit measurement of the reactions of e_{aq}^- with other solutes. Hence, in all of these experiments, 0.2 M t-butanol was added to the DAOx aqueous solutions in order to scavenge the $^{\bullet}OH$ radicals, eq. 26,

$$^{\bullet}OH + (CH_3)_3COH \rightarrow H_2O + {}^{\bullet}CH_2(CH_3)_2OH \quad (26)$$

with a reaction rate constant of 6 x 10^8 $M^{-1}s^{-1}$. $^{\bullet}CH_2(CH_3)_2OH$ is very unreactive, and does not interfere with the radiation chemistry of the other solutes. Another advantage of $^{\bullet}CH_2(CH_3)_2OH$ is that it does not interfere with the absorption of other species in the pulse radiolysis experiments, since it has a very low molar extinction coefficient in the ultraviolet region.

Figure 37 shows the prompt formation of e_{aq}^- following pulse radiolysis and its decay, monitored at a wavelength of 480 nm, in Ar-saturated aqueous solutions of various concentrations of DAOx with 0.2 M t-butanol. While the observed buildup of the e_{aq}^- signal is limited by the response function of the FND-100 silicon photodiode detector, the decay represents the pseudo-first order reaction of e_{aq}^- with DAOx. It should be mentioned that e_{aq}^- signal would be larger if it was monitored at 720 nm, since e_{aq}^- has its maximum absorption there. However, 480 nm was used in these experiments in an attempt to observe the absorption spectrum of the $(DAOx)^{\bullet-}$ anion, eq. 27:

$$e_{aq}^- + DAOx \rightarrow (DAOx)^{\bullet-+} \qquad (27)$$

It should be noted that Figure 37 shows that the decay after the pulses at a monitoring wavelength of 480 nm does not reach a zero value, suggesting that the $(DAOx)^{\bullet-}$ anion has a weak absorption around this wavelength region. More investigation needs to be done on the pulse radiolysis transient spectroscopy of this system.

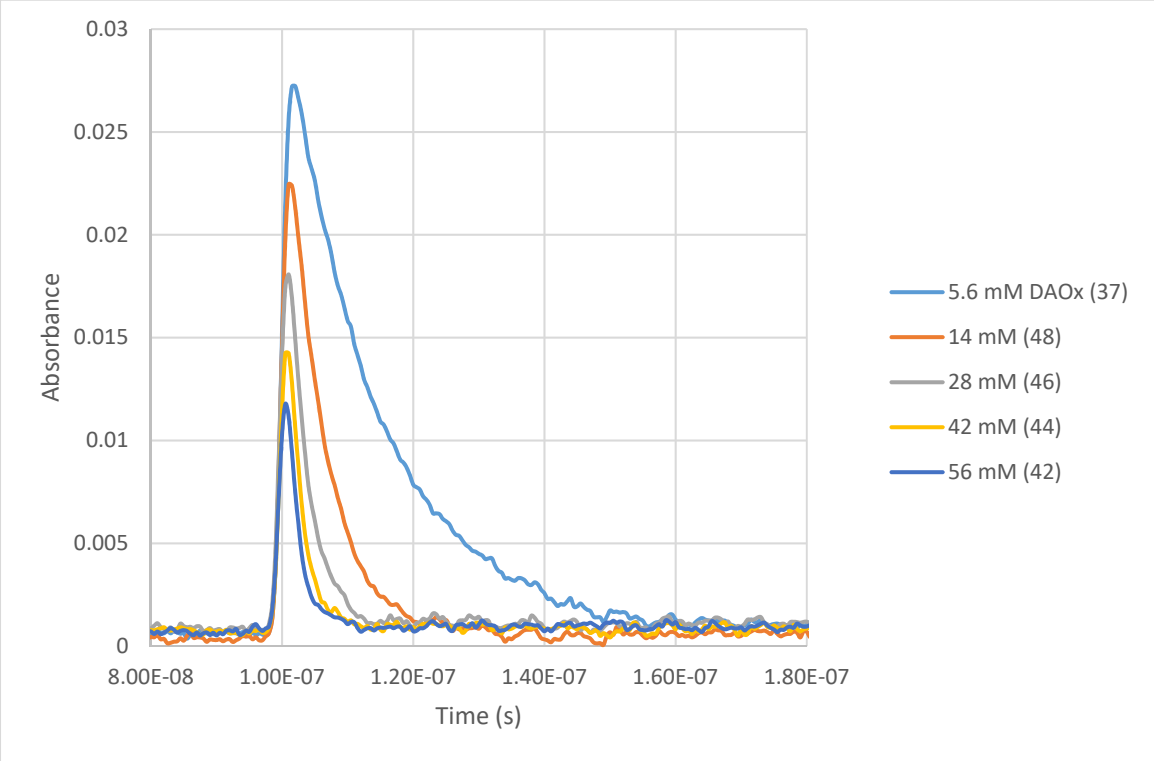

Figure 37 – The decay behavior of the absorbance of the aqueous electron at 480 nm with varying concentrations of DAOx.

Figure 38 shows the observed pseudo-first-order rate constants for the pseudo-first order reaction of e_{aq}^- with DAOx as a function of DAOx concentration. The slope of the linear fit to the fitted line data represents the second-order rate constant for the reaction of e_{aq}^- with DAOx, with a value of $9 \times 10^9 \pm 9 \times 10^8\ M^{-1}s^{-1}$.

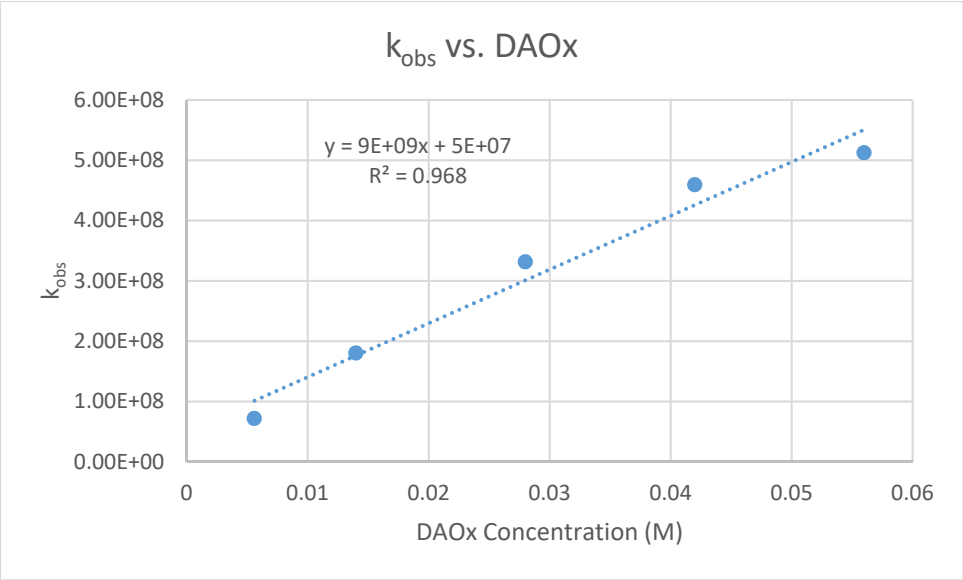

Figure 38 – The observed pseudo-first order rate constants for varying concentrations of DAOx. The derived second order rate constant from the linear regression of this graph gives a value of $9 \times 10^9 \pm 9 \times 10^8\ M^{-1}s^{-1}$.

As with any anion, the produced $(DAOx)^{\bullet -}$ anion undergoes a very rapid solvolysis reaction producing carbon-centered radicals, eq. 28:

$$(DAOx)^{\bullet -} + H_2O \rightarrow (H\text{-}DAOx)^{\bullet} + OH^- \qquad (28)$$

The $(H\text{-}DAOx)^{\bullet}$ carbon-centered radical initiates the polymerization reaction of the DAOx.Lower doses of about 150 kGy were used for subsequent neat DAOx grafting experiments in order to reduce the DoG to about 100%, which is more on the order of the expected best uranium extraction performance. Heating of the DAOx samples during direct grafting resulted in improved DoGs although the extent to which direct heating improved grafting was unexpected. This high DoG could be the result of excess homopolymerization due to the increased diffusion as a result of the higher temperature. Lower temperatures and doses should result in more ideal grafting.

As shown in Figure 39, radiation induces the formation of the C-centered free radicals of nylon$^{\bullet}$ and DAOx$^{\bullet}$. These free radicals undergo various desired reactions (grafting through the formation of C-C bonds between DAOx and the nylon 6), as well as undesired reactions, consisting of DAOx homopolymerization and the crosslinking reactions of nylon$^{\bullet}$.

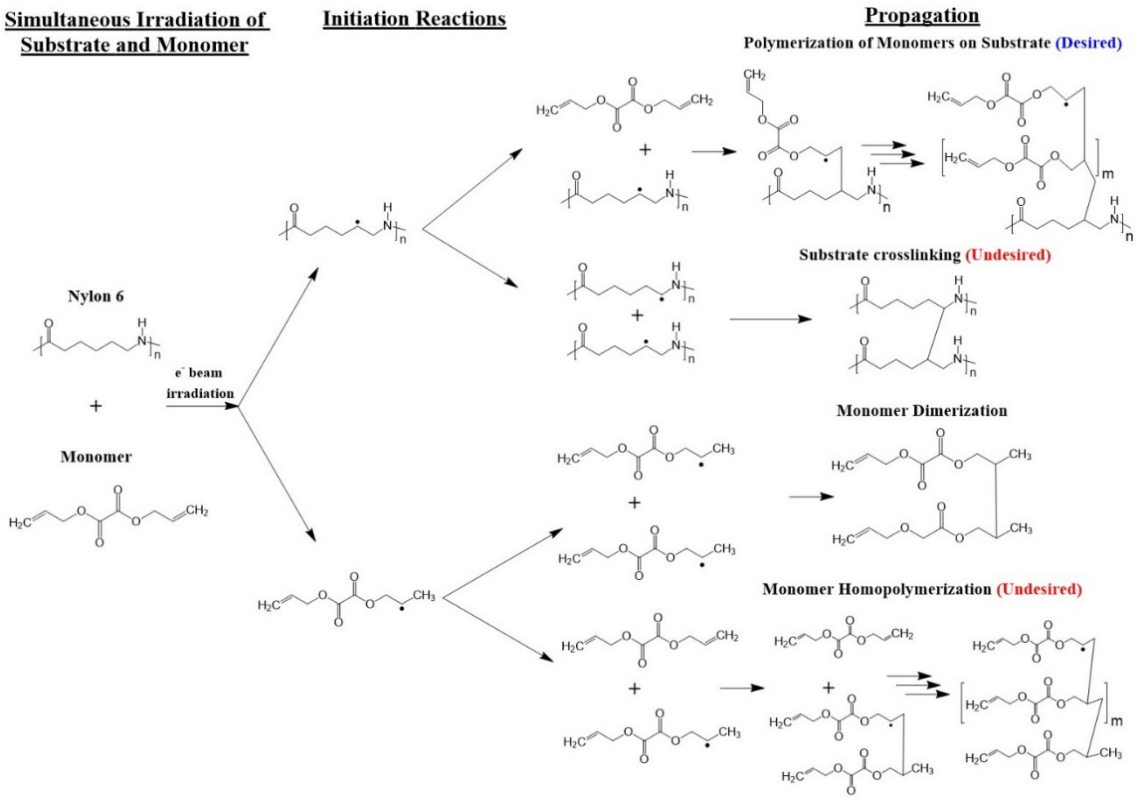

Figure 39 - Reaction of the graft polymerization reactions of neat monomer on the nylon 6 fabric in the absence of oxygen and solvent.

Therefore, under our experimental conditions, the decay rates of the DAOx• and nylon• can be expressed as follows, equations 29 and 30:

$$\frac{-d[DAOx\ ]}{dt} = k_1[nylon\ ][DAOx\ ] + 2k_2[DAOx\ ]^2 + k_3[DAOx\ ][DAOx] + k_4[nylon-(DAOx)n-DAOx\ ][DAOx\ ] \quad (29)$$

$$\frac{-d[nylon\ ]}{dt} = k_1[nylon\ ][DAOx\ ] + k_5[nylon\ ][DAOx] + 2k_6[nylon\ ]^2 \quad (30)$$

where k_1, k_2, k_3, k_4, k_5, k_6 are the rate constants of the desired grafting reaction, the undesired termination reaction of the DAOx• radicals, the undesired homopolymerization reaction of the DAOx, the termination reaction of the growing grafted DAOx• radicals, the desired grafting-addition reaction of the DAOx on nylon, and the undesired crosslinking reaction of the nylon, respectively.

In conclusion, these results demonstrate that radiation grafting polymerization of DAOx on nylon 6 through a solvent-free, single-step-direct process can be accomplished in the absence of oxygen. The desired reaction between the radiolytically produced nylon• and DAOx• C-centered radicals to form the grafting C-C bonds occurs despite the strong competition from the DAOx homo-polymerization reaction. These results also show that at radiation doses up to around 175 kGy, the undesirable homo-polymerization is the predominant reaction. However, as the viscosity increases due to the homo-polymerization reaction, the diffusion of the DAOx• C-centered radicals is slowed down. This hinders the homo-polymerization reaction and enhances

the local grafting reaction, and this allows reaching a grafting density of 140% at a dose level of 250 kGy.

Radiation grafting in aqueous solutions and in the presence of a surfactant:

Use of the TWEEN-20 surfactant can now be used as a viable grafting method if a stable monomer-surfactant solution can be obtained. Heat treating grafted samples also had a noticeable beneficial effect on the final DoGs. This is slightly surprising since the grafting reaction is an exothermic process so any additional heat energy should slow down the grafting reaction. However, it is possible that slowing the grafting reaction down allowed more time for radicals to diffuse into the material to graft.

In order to ensure that the surfactant TWEEN-20 was not being grafted to the surface of the winged nylon 6, grafting experiments were performed consisting solely of solutions containing TWEEN-20 in water. The low DoGs (<5%) obtained by TWEEN-20 support the notion that any amount of TWEEN-20 grafting that may have occurred is statistically insignificant especially in comparison to the grafting accomplished with DAOx-TWEEN-20 mixtures. There was a viable color change with a couple of the fabrics exposed to this compound while under irradiation; the origin of this change is unknown.

Degrees of grafting as high as 25 % have been reached in the aqueous, N_2O-saturated mixtures containing 0.11 M DAOx and 4.5 x 10^{-3} M TWEEN 20. Under these experimental conditions, water absorbed most of the electrons from the electron accelerator resulting in the formation of the following active species with their radiation chemical yields in micromole per joule:

$G(^{\bullet}OH) = G(e_{aq}^{-}) = G(H_3O^{+}) = 0.28$, $G(^{\bullet}H) = 0.062$, $G(H_2) = 0.042$, $G(H_2O_2) = 0.082$

Hydroxyl radicals ($^{\bullet}OH$) constitute a powerful oxidant, and they are highly reactive (through addition, abstraction or electron transfer). The $^{\bullet}OH$ radicals are responsible for initiating the grafting polymerization and other reactions in this system through the production of DAOx$^{\bullet}$ and nylon$^{\bullet}$ radicals upon reacting with nylon and DAOx. On the other hand, hydrated electrons (e_{aq}^{-}) are very strong reducing radicals and can be converted to $^{\bullet}OH$ radicals through the following reactions, eq. 31:

$$N_2O + e_{aq}^{-} + H_2O \rightarrow {}^{\bullet}OH + N_2 + OH^{-} \quad (31)$$

The above reaction is very fast, having a reaction rate constant of $k = 8 \times 10^9\ M^{-1}s^{-1}$ [31]. Hence, saturating the system with N_2O prior to irradiation, would double the $^{\bullet}OH$ yield to $G(^{\bullet}OH) = 0.56$ micromole per joules. In addition to $^{\bullet}OH$, H-atoms ($^{\bullet}H$) with $G(^{\bullet}H) = 0.062$ micromole per joule, also react with nylon and DAOx to produce DAOx$^{\bullet}$ and nylon$^{\bullet}$. Under these irradiation conditions and in the absence of oxygen, the radiolytically produced $^{\bullet}OH$ radicals and H-atoms add to the unsaturation site of DAOx and abstract H-atom from the backbone of the polymer substrate (nylon) producing OH—DAOx$^{\bullet}$, and H-DAOx$^{\bullet}$ radicals, and $^{\bullet}$nylon (-H) radicals, respectively. It should be mentioned that $^{\bullet}OH$ and $^{\bullet}H$ are also scavenged by the TWEEN surfactant, since the mixture contains, 4.2 x 10^{-3} M TWEEN, leading to a decrease in the concentrations of OH—DAOx$^{\bullet}$, H-DAOx$^{\bullet}$, and $^{\bullet}$nylon (-H) radicals. This also leads to the possibility of TWEEN being grafted on nylon 6. This can dramatically decrease the number of sites available for uranium adsorption.

Initial indirect grafting experiments with neat DAOx solutions yielded poor DoGs, even with the use of dry ice in an environmentally controlled chamber during the irradiations to maintain

the winged nylon 6 samples cold enough to preserve the radicals generated during the irradiations. On the other hand, direct grafting of DAOx to winged nylon 6 at elevated temperatures yielded extremely high DoGs (>400% in some cases).

These experiments showed that a DoG 25% can be achieved at dose of 250 kGy. This relatively low grafting density may be explained by the fact that the surfactant TWEEN also scavenges the •OH radicals, causing a decrease in the radiolytic yields of nylon• and DAOx• C-centered radicals, and thus its presence causes a decrease in the grafting density.

3.9.3.2 Characterization

In order to reinforce the hypothesis that the uranyl ion is binding to the negative oxalate group attached to the nylon 6 fabric, zeta potential measurements were performed on grafted and un-grafted nylon 6 fabric that had been chemically transformed into microparticles. An image of the solution of the microparticles can be seen in Fig. 40. The zeta potentials for both the grafted and ungrafted nylon 6 fabric were measured and the results are summarized in Table 3. These results show that at a pH of about 8 the surface of the oxalate-grafted fabric is negatively charged and thus suitable for extraction of UO_2^{2+} from the seawater.

Figure 40 - Nylon 6 particles suspended in solution.

Table 3 - The average sizes and zeta potentials of the grafted and non-grafted nylon 6 microparticles.

	Particles from grafted nylon 6	**Particles from non-grafted nylon 6**
Average Size	5.6 ± 1.6 μm	1.5 ± 0.12 μm
Zeta Potential in acidified deionized water (pH ~ 3)	26.4 ± 0.5 mV	40.1 ± 3.1 mV
Zeta Potential in acidified seawater (pH ~ 4.5)	-3.9 ± 0.3 mV	-3.9 ± 0.4 mV

Zeta Potential in Seawater with pH adjusted to ~8.3	-6.1 ± 0.9 mV	-4.6 ± 0.5 mV

3.9.3.3 Extraction Testing

Uranium Removal from Spiked Seawater

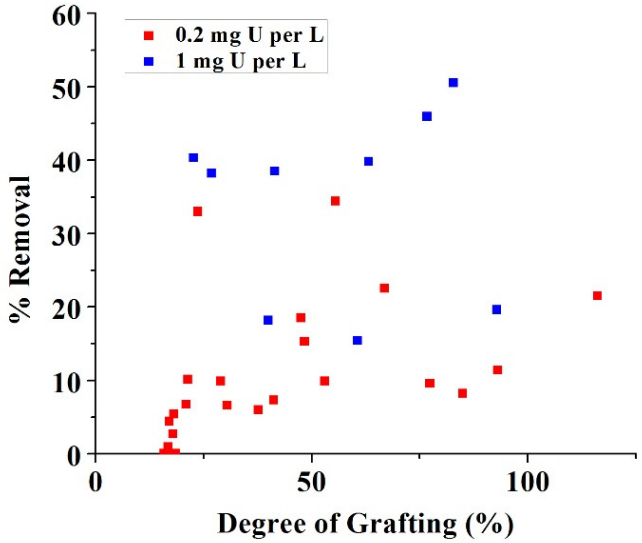

Figure 41 - The percent uranium removal of the fabrics from uranyl acetate and seawater solutions doped to the respective levels.

The results obtained for the removal of uranium from spiked seawater by means of nylon 6 fabrics grafted with neat DAOx are shown in Figure 41. The level of spiking was either 1.0 mg/L or 0.2 mg/L U (introduced as uranyl acetate). In each test, a sample weighing approximately 30 mg was rotated with 10 mL of the spiked seawater at 30 rpm for 7 days. The results show that significant removal of uranium from these solutions (>5%) took place when the DoG exceeded approximately 18%, and, in general, the percent removal of uranium from both the 1.0-mg/L and 0.2-mg/L U solutions increased with increasing DoG. The large scatter in the data can be ascribed to the non-uniform distribution of the grafted material on the nylon 6 fibers as observed by SEM (see below). Another reason for the scatter is associated with the fact that some of the adsorbent samples were subjected, following the radiation induced grafting, to heat treatment at 50°C for 7 days. The percent removal of uranium from the test solutions observed with these samples was generally higher than the corresponding percent removal observed with samples which did not undergo heat treatment. It should also be noted that the amounts of uranium in the test solutions were very small (0.01 or 0.002 mg, respectively) so that the results in Figure 41 cannot provide a realistic estimate of the maximum amount of uranium that can be removed by the fabric from large volumes of seawater.

As expected, Figure 41 shows that as the grafting density increases, the extraction of uranyl from spiked seawater increase. The scattering of the results of the percentage extraction can be

related to the non-uniformity of the grafting within the samples. This non-uniformity in the grafting is the principal disadvantage of the solvent-free grafting. Notwithstanding this disadvantage, removal of as much as 50% of the uranium from the test solution was achieved using adsorbent fabrics produced using this method. In general, it was observed that the measured extent of uranium uptake from the seawater, whether spiked with 1 mg/L or 0.2 mg/L of uranium, increased with the DoG of oxalate on the polymeric fabric.

TWEEN grafted fabrics did not perform as well in extraction tests, achieving <5% uranium removal, most likely due to the small amount of grafted TWEEN on the surface of the fabrics limiting uranyl access to the DAOx.

3.9.4 Azo Compounds

3.9.4.1 Selection

Following the implementation of the spectrophotometric method for the determination of the amount of uranium removed from seawater, it was hypothesized that chemicals with similar functional groups to the one used in the spectrophotometric method would be able to extract uranium very efficiently. The monomer repertoire tested includes a number of pyridylazo compounds, such as those shown in Fig. 42.

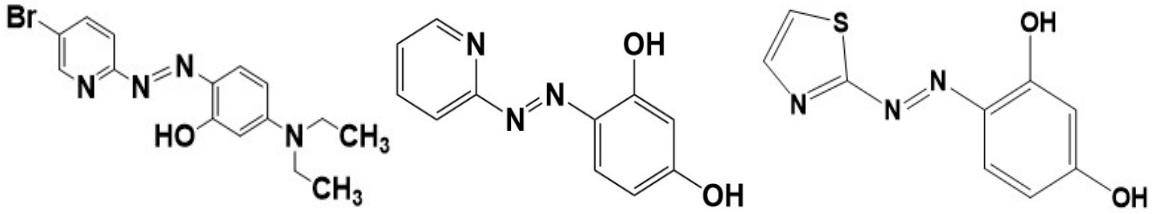

Figure 42– The compounds shown are B2MP, left, PAR, middle, and TAR, right.

Unfortunately, the compounds by themselves were not readily graftable as they contained no allyl or vinyl functional groups. However, TAR and PAR can be chemically altered to include an allyl group without affecting the functional groups that are believed to contribute to the binding of uranyl (the azo group, the nearest hydroxyl group, and the nitrogen in the thiazole ring). Through the reactions mechanism outlined in Fig. 43, two different allyl-functionalized compounds were created.

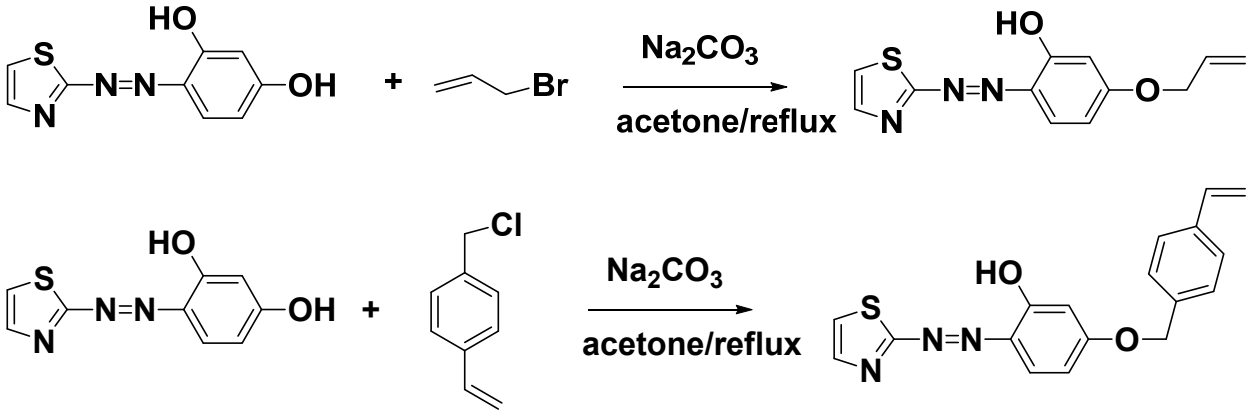

Figure 43 – The synthesis mechanisms for the allyl-functionalized TAR: allyl-TAR is on top and vinylbenzyl-TAR (VB-TAR) is on the bottom.

3.9.4.2 Grafting

2-(5-Bromo-2-pyridylazo)-5-(diethylamino)phenol (Br-PADAP), allyl-TAR, and vinylbenzyl-TAR were all used as monomers in a basic solution in an attempt to directly graft the azo moiety to the surface of winged nylon 6. Using electron beam, samples were irradiated using direct grafting conditions at elevated temperature. Even with the concurrent heating and sample irradiations, statistically significant DoGs were not seen. A discoloration present on the surface of the vinylbenzyl-TAR and allyl-TAR samples and the lack of color in the post-irradiated solution are strong indications that some amount of grafting of the compounds to the surface has occurred with these samples.

Indirect grafting was attempted with solutions of allyl- and vinylbenzyl-TAR in methanol. The mass loss as a results of the indirect grafting process is within the same range of the previous attempt to graft the two TAR compounds using direct methods. From the experiment, there are a few possible parameters that might have caused the low DoGs. One possibility might be the introduction of oxygen into the fabric vial during the monomer solution injection process. However, the quantity of oxygen possibly injected, and the amount of time before the sample was covered in an oxygen purged solution seems unlikely. It might also be possible that the irradiation and temperature conditions are not conducive to grafting.

While the DoGs of the fabric samples were high enough to be distinguished from possible error, such that there was a small amount of grafting, the DoGs were far from the values expected. As such, it appears the use of the glove bag, while important is not the only factor preventing high degrees of grafting. Other parameters that can be altered to improve DoG include the monomer concentration, the solvent, dose, and the temperature and time of post irradiation heat treatment.

While numerous grafting techniques and parameters were attempted in an effort to graft these compounds, they were all mostly unsuccessful and the time and cost of synthesizing and purifying these two compounds made sample processing difficult. In order to improve on the economics and DoG of the thiazolylazo compound on the surface of the polymer fabric, a new order was devised for processing samples. Instead of performing the chemical attachment of the allyl group to the TAR compound first, the vinylbenzyl chloride (VBC) precursor was grafted to the surface of nylon fabric first. Degrees of grafting of 150% and higher were achieved. The relationship between DoG and dose for this compound is shown in Fig. 44.

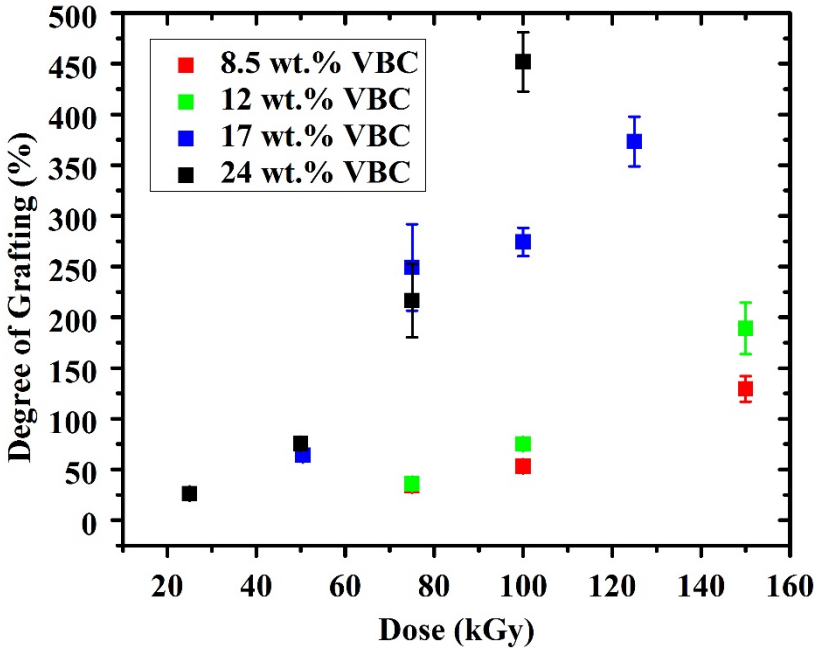

Figure 44 – The relationship between dose and DoG of VBC on nylon 6 under electron beam irradiation at a dose rate of 250 kGy/hr with two different concentrations of VBC in ethanol.

After the grafting step of the chemical precursor to the surface of the nylon fabric, the now chlorine functionalized fabric can have the TAR or PAR compound chemically attached to its surface. A scheme for this method of attaching PAR to the surface of the fabric is shown in Fig. 45. This method has several procedural improvements over the previous method. For example, the fabric grafting can be optimized prior to chemical attachment of the PAR or TAR groups, thereby reducing the amount of the more expensive azo compound necessary to optimize the system. This method will also serve to improve the exposure of the azo compounds to the seawater environment, as the chemically attached PAR or TAR will only be attached at the surface of any homopolymer, versus being trapped inside homopolymer if the allyl-functionalized azo compound had been grafted instead.

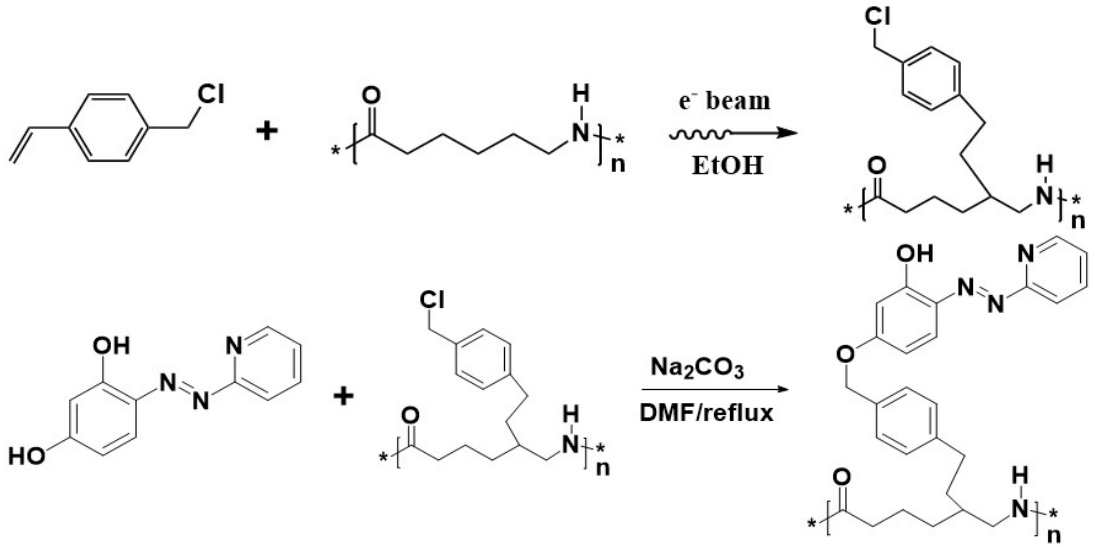

Figure 45 – The grafting and reaction mechanism for first attaching VBC to the surface of the nylon 6 using electron beam irradiation and then chemically attaching TAR to the grafted VBC.

Direct grafting of VBC was carried out in solutions of ethanol and methanol. In both cases, significant grafting was obtained. In methanol, a DoG of 56.6% was obtained and in ethanol DoGs of over 100% were obtained.

An attempt at indirectly grafting both VBC and allyl-bromide as chemical precursors to azo attachment were unsuccessful, though the initial failure was unexpected as the injections of monomer solution appeared to be successful.

The use of dichloromethane (DCM) was extremely effective in removing any VBC homopolymer from the surface of the fabric. The caveat to this was that for samples with higher doses, it appears the monomer had polymerized to the point where the DCM could no longer dissolve it effectively even after sonication. Based off TAR-attached fabric performance, the optimum DoG can be obtained for VBC that results in the highest uranium extraction.

While a number of experimental errors associated with the irradiations of the fabrics resulted in high error values for the total dose received for some fabric sets, there was a clear trend between concentrations of VBC and doses which followed the trend previously seen with earlier experiments. For the 24 wt. % VBC samples, the trend of DoG vs. dose shows a large widening in DoG deviation at higher doses most likely due to a large buildup of homopolymerization. At lower doses for the 24 wt. % VBC solution, the deviation between DoGs was much smaller. The attempt at indirect grafting of VBC proved fruitful as the indirect DoG reached values as high as 38%, and with an average around 10% for all samples. The main differences between this experiment and previous indirect grafting experiments are the higher concentration of monomer in solution and the fact that all samples were irradiated in a constant dose rate environment, i.e. the turntable was not on for a portion of the initial irradiation and the turntable was not used at all during the second irradiation. Assuming concentration is the minor cause of the indirect grafting, we can examine why the lack of turntable rotation might have impacted the amount of indirect grafting. Without rotation, all samples would receive a constant dose rate and will reach a plateau of radical concentration. In a variable dose rate environment, it is probably that the maximum radical concentration will be based on a time average dose rate across all points in the rotation. As such, it may be necessary to restrict the rotation for indirect irradiation and to re-do dosimetry measurements for future indirect experiments.

MAA was incorporated into the grafting procedure was begun in an attempt to improve the hydrophilicity of the surface of the fabrics. Indirect grafting was successfully achieved and while the DoGs achieved were not as high as those published in literature, they were nonetheless higher than any previous indirect grafting results and hold promise for improving DoGs in future experiments. A scheme for the different radical mechanisms that occur during the radiation grafting of VBC and MAA to the surface of nylon 6 is shown in Fig. 46.

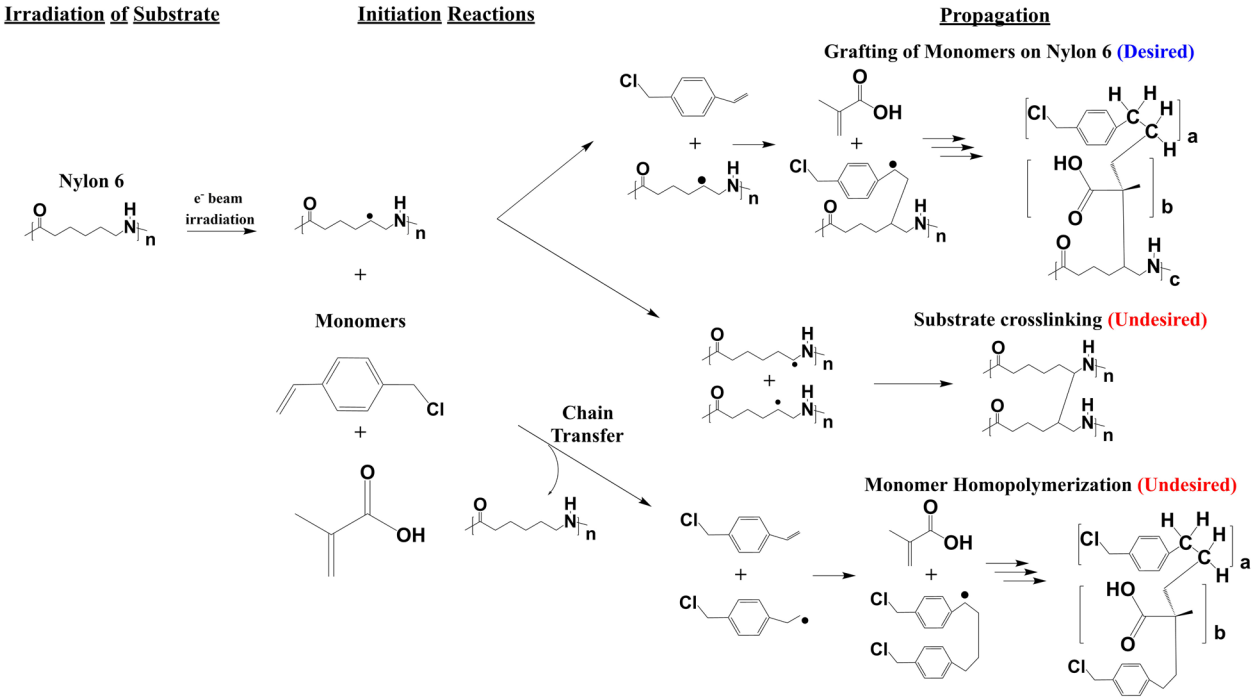

Figure 46 – Upon irradiation, the radicals on the backbone of the nylon 6 polymer are able to proceed through a number of different reactions either with the selected monomers, VBC and MAA, or with itself. Grafting of the monomers onto the nylon 6 is the preferred reaction, whereas crosslinking and homopolymerization following chain transfer are not desired.

Between the VBC and VBC/MAA samples of winged nylon-6, there did not appear to be a clear difference in DoGs which might indicate that the total wt. % of monomer in the solution plays a more important role than the concentration of each monomer individually in this case, though more experiments involving different monomers and concentrations will be required to prove this. The 3M nylon 6 (non-winged) exhibited lower DoGs as compared to its winged nylon 6 counterpart, but not significantly lower, as seen in Fig. 47. This might have been caused by the higher surface area of the winged fabric. The winged PET fabric should negative degrees of grafting. This might have been due to a loss of material during the initial washing of the fabric in acetone prior to irradiation. The dose used on the fabric might also have been too high for effective grafting to occur on this material.

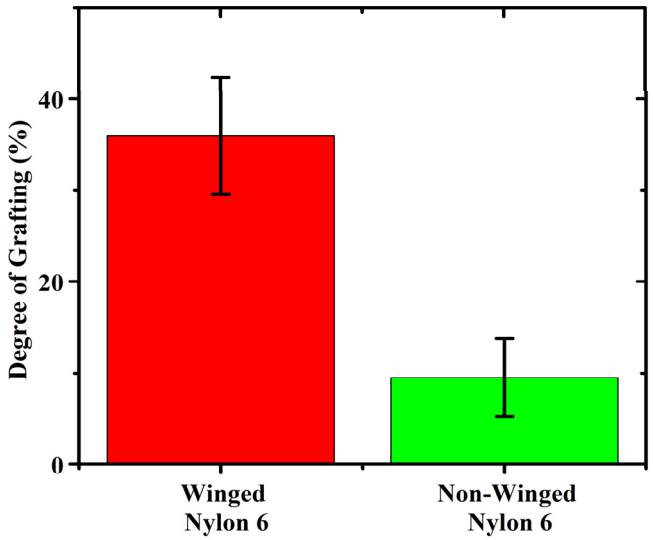

Figure 47 – A significant difference in DoG for indirectly grafted nylon was seen between the winged and non-winged varieties of the polymer.

Different wt. % of VBC and MAA dissolved in DMSO provided DoGs on the same order of magnitude as seen in Fig. 48. The grafting of these solutions as a follow-up to previous indirect grafting experiments showed that the procedure could allow for relative consistency of DoGs.

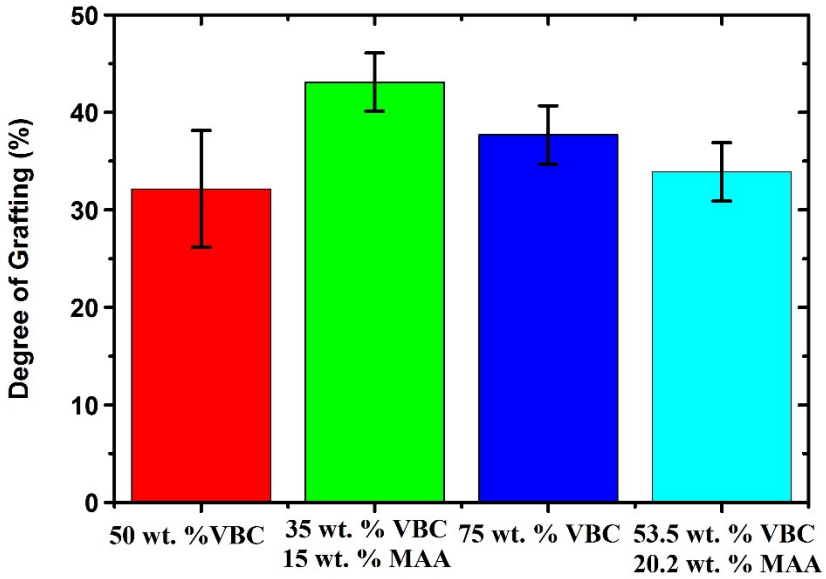

Figure 48 – Even at different monomer ratios, the total DoG of the indirectly grafted winged nylon 6 fabric irradiated under the same conditions was relatively consistent. This provides the opportunity to tune the VBC:MAA ratio without worrying about a decrease in DoG for these monomer concentrations.

Additional indirect radiation grafting of VBC and MAA experiments were performed using a 2 MeV Van de Graaff accelerator at NIST. These experiments yielded DoGs below 10 wt% for equivalent doses compared to previous experiments using the MIRF. The lower electron energy of the Van de Graaff and the longer time required before monomer solution could be added to the irradiated fabrics could have attributed to the low DoGs.

3.9.4.3 Characterization

XPS techniques were utilized to investigate the binding of azo compounds to the uranyl ion. Four different azo compounds, Br-PADAP, PAR, 1-(2-Pyridylazo)-2-naphthol (PAN), and 2-(2-Pyridylazo)-1-naphthol (ISOPAN), were independently mixed with uranyl acetate in methanol in 1:1 molar ratios as this was the expected molar ratio between azo and uranyl that would form in an aqueous environment. The azo compound and the uranyl acetate were dissolved in methanol separately then mixed together and stirred. The methanol was allowed to evaporate and the four azo-uranyl mixtures were collected for XPS analysis. Based on the XPS analysis results, the creation of a uranyl-chelated pyridylazo compound outside of solution appeared to be a success. Both physical characteristics and XPS data of the chelated compounds suggested this. The uniformity of the crystals and the presence of uranium in the XPS data were the main supporting observations respectively for this conclusion. From the XPS data, the most informative characteristic that suggested a 1:1 binding motif for uranium to the pyridylazo group/compound was the similar atomic percentage between the bromine and uranium atoms in the U-chelated Br-PADAP compound as shown in Fig. 49. The slightly higher U concentration could be due to the overlapping of the N_{1s} peak at ~400 eV with the U_{4f} peak.

Unfortunately, due to the lack of an atom of similar atomic percentage to U in PAR, PAN, and ISOPAN, this evaluation is not possible. However, the atomic % of U in PAR is on the correct order of magnitude in comparison to the three nitrogens present per pyridylazo group, as shown in Fig. 50.

Again, the overlap of the U_{4f} and N_{1s} peaks could explain any discrepancies. One important caveat to these conclusions is that in this experiment, the uranyl acetate and chelating monomer were mixed in 1:1 molar concentrations, which would result in the atomic percentages seen in the XPS results. Therefore, in order to more fully determine whether or not the uranium was actually bound to the monomer, the uranium bound monomer must be examined. Unfortunately again, the nitrogen functional groups that bind to uranium have overlapping peaks with the uranium which means their energy shift cannot be evaluated. This leaves the energy shift of the hydroxyl group. In both Br-PADAP and PAR, the unchelated compound shows a O_{1s} peak around 532.5 eV. When these compounds are chelated to uranium however, the peaks shift to lower energies by about 1 eV. This weakening of the binding energy would suggest that the oxygen is sharing its electron density through a chelation to the uranyl ion.

(a)

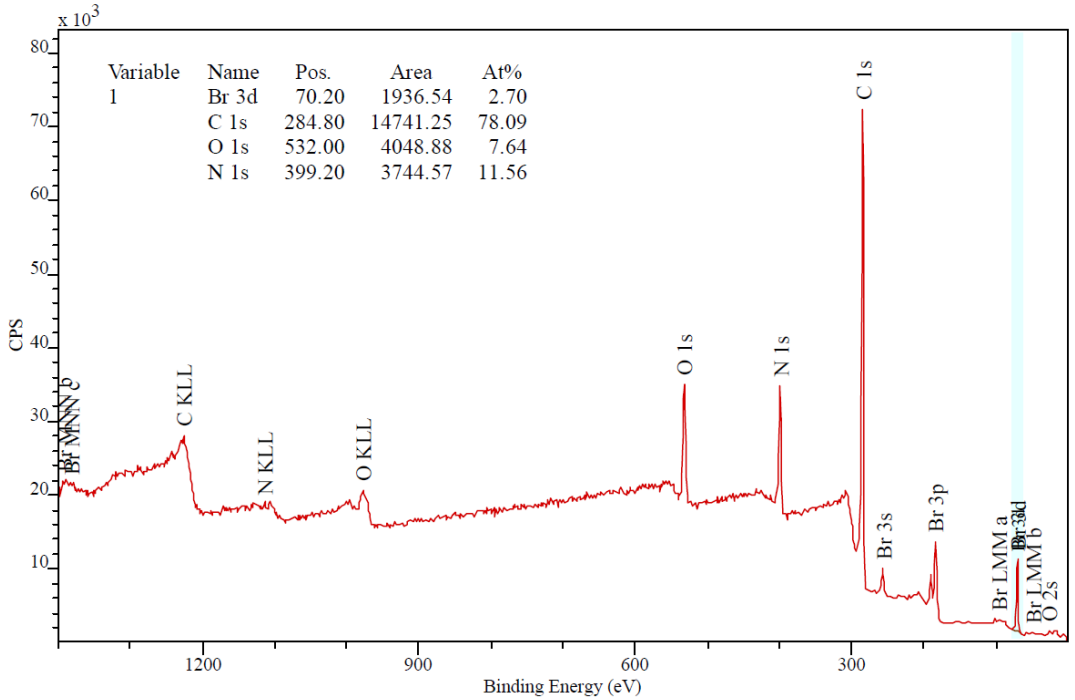

(b)

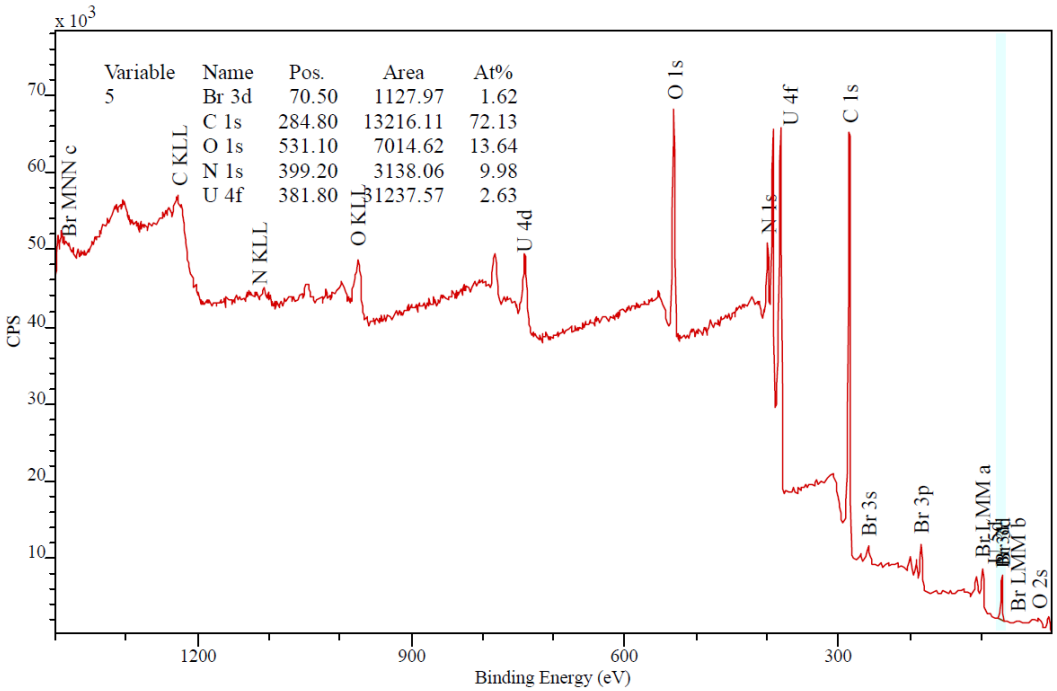

Figure 49 – (a) XPS spectra of Br-PADAP, (b) XPS spectra of Br-PADAP chelated to uranyl acetate.

(a)

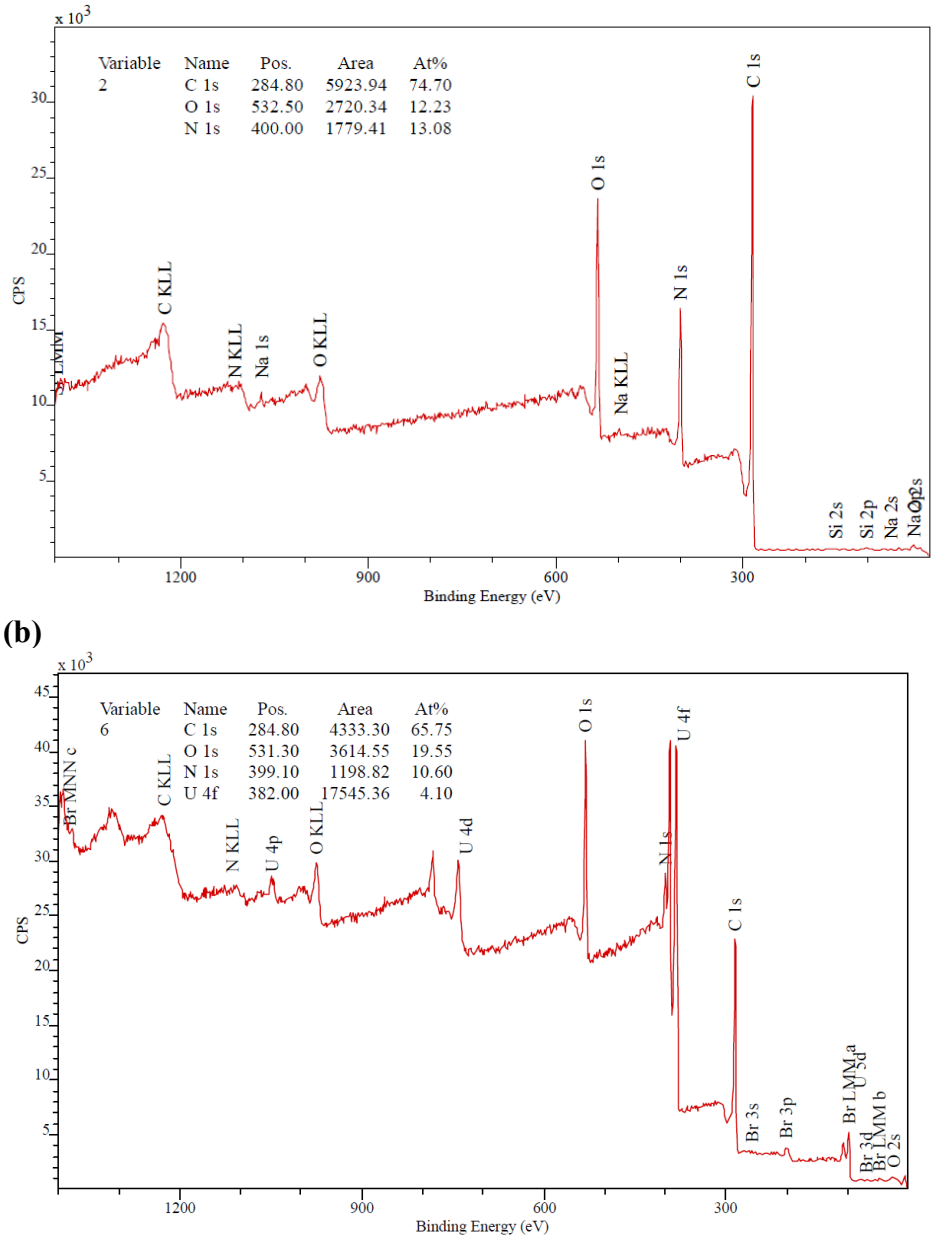

Figure 50 – (a) XPS spectra of PAR, (b) XPS spectra of PAR chelated to uranyl acetate.

The attachment of the azo compound to the surface of the grafted polymer was confirmed through the use of FTIR-ATR and SEM-EDS. Both techniques were able to observe an initial increase in C-Cl bonds or the atomic percent of chlorine on the surface of the fabric, respectively. Examples of the FTIR-ATR and the SEM-EDS data are shown in Figs. 51 and 52 respectively. Table 4 includes the EDS data from Fig. 52. Fig. 53 and Table 5 illustrate the effect of PAR attachment to a VBC grafted fabric. Following PAR attachment, as expected the chlorine content of the fabric decreases indicating a successful attachment.

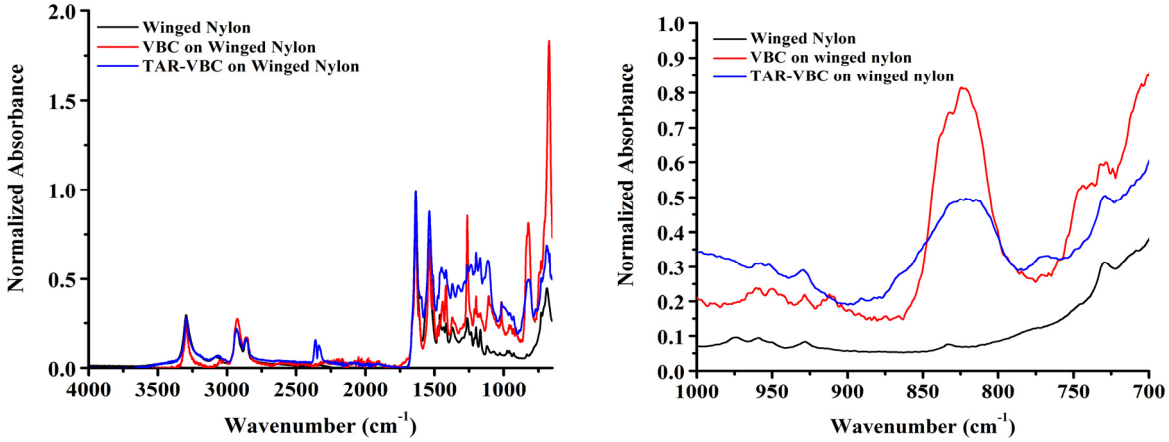

Figure 51 – FTIR-ATR scans of clean winged nylon, winged nylon grafted with VBC, and VBC-grafted winged nylon that has been chemically functionalized with the TAR monomer. The full spectrum is on the left and the right spectrum shows the peak associated with the C-Cl stretching vibration.

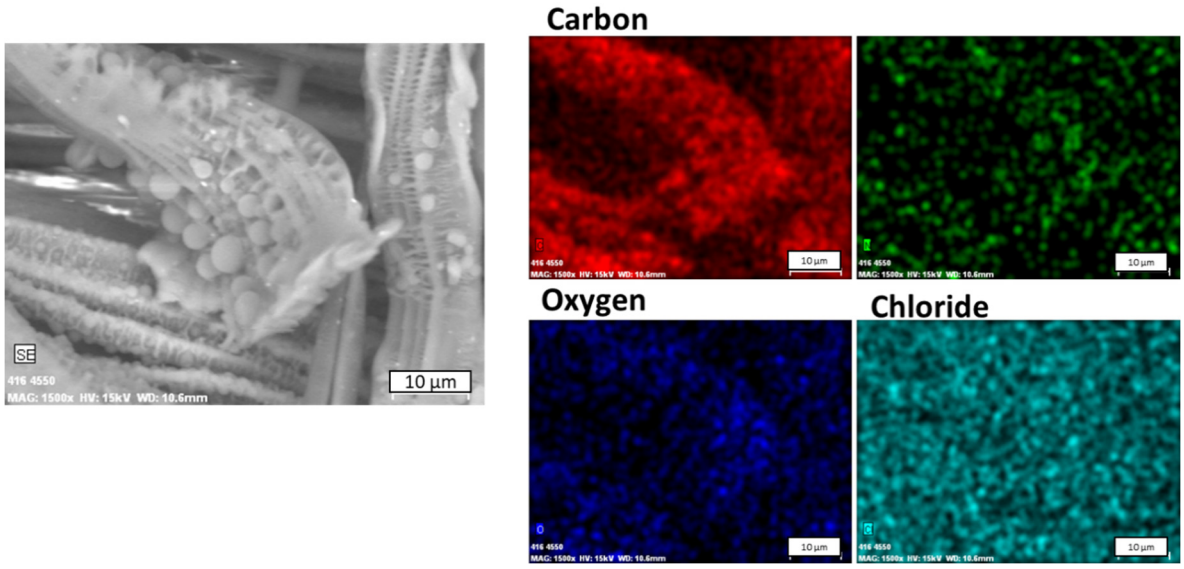

Figure 52 - SEM-EDS of directly grafted winged nylon 6 with VBC.

Table 4 Tabulated EDS results from the fabric in Fig. 46.

Element	Unn. C [wt. %]	Norm. C [wt. %]	Atom. C [at. %]	Error (1 σ) [wt. %]
Carbon	78.39	78.39	83.38	10.15
Nitrogen	8.74	8.74	7.97	2.61

Oxygen	**9.16**	**9.16**	**7.31**	**1.95**
Chloride	**3.71**	**3.71**	**1.34**	**0.17**
Total	***100.0***	***100.0***	***100.0***	

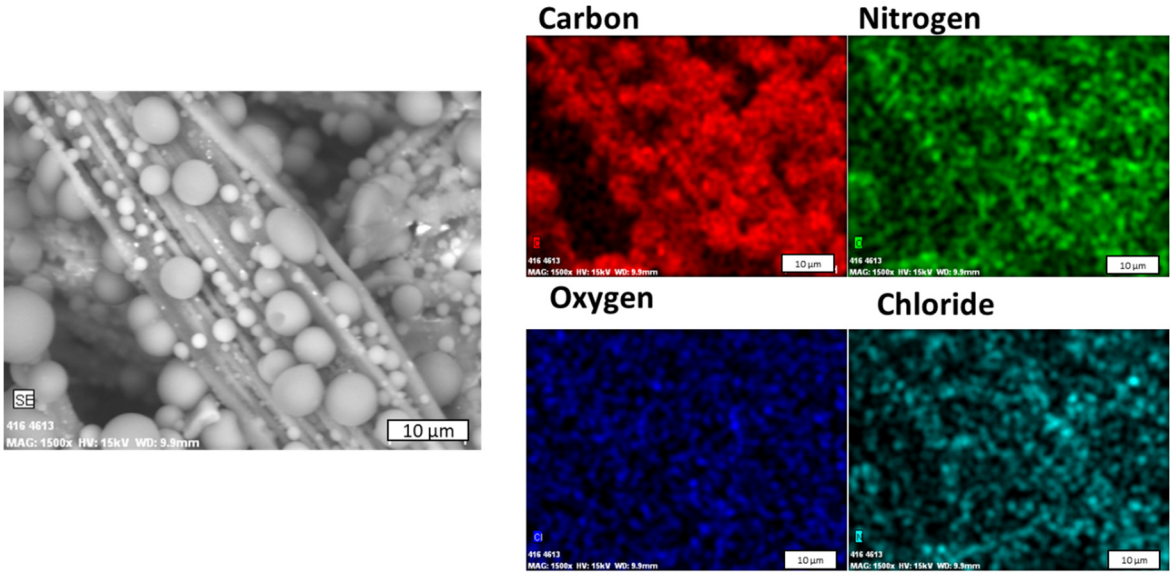

Figure 53 SEM-EDS of the same fabric as previous figure post-PAR attachment.

Table 5 Tabulated EDS results from the fabric in Fig. 47.

Element	Unn. C [wt. %]	Norm. C [wt. %]	Atom. C [at. %]	Error (1 σ) [wt. %]
Carbon	**77.35**	**77.35**	**80.99**	**8.75**
Nitrogen	**11.90**	**11.90**	**10.68**	**2.22**
Oxygen	**10.44**	**10.44**	**8.20**	**1.62**
Chloride	**0.24**	**0.24**	**0.08**	**0.04**
Total	***100.0***	***100.0***	***100.0***	

The loss in chlorine as seen in SEM-EDS for directly grafted VBC samples upon conversion to PAR-grafted samples is also seen for indirectly grafted fabrics, see Fig. 48.

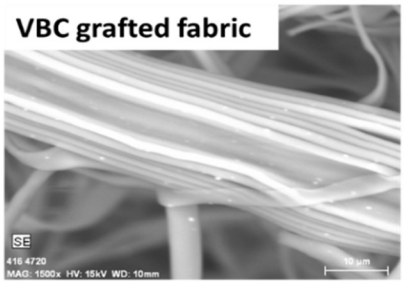

Element	Norm. C [wt. %]	Atom. C [at. %]	Error (1 σ) [wt. %]
Carbon	73.01	78.89	9.32
Nitrogen	10.82	10.01	2.71
Oxygen	11.91	9.65	2.20
Chlorine	4.26	1.56	0.18

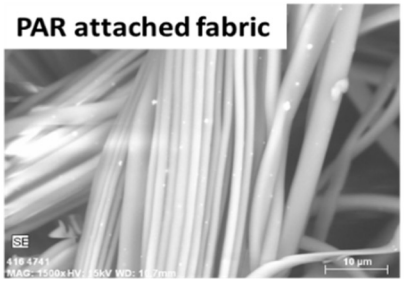

Element	Norm. C [wt. %]	Atom. C [at. %]	Error (1 σ) [wt. %]
Carbon	71.33	75.87	8.74
Nitrogen	12.63	11.52	2.92
Oxygen	15.26	12.19	2.63
Chlorine	0.05	0.02	0.03

Figure 54 – SEM-EDS analysis of both the VBC grafted (top) and PAR functionalized fabric (bottom).

3.9.4.4 Extraction Testing and Performance

The percent uranium removal of the grafted PAR fabric are promising, as shown in Fig. 55. However the amount of uranium removal seen for 0.2 ppm U in 10 mL seawater is still far below what was expected based on the charcoal tests. It is believed that the potential seen in the charcoal tests can be obtained by improving the DoG of the monomer and by increasing the surface area of the grafted polymer chains, which would in turn allow for a higher amount of PAR to be attached at their surface.

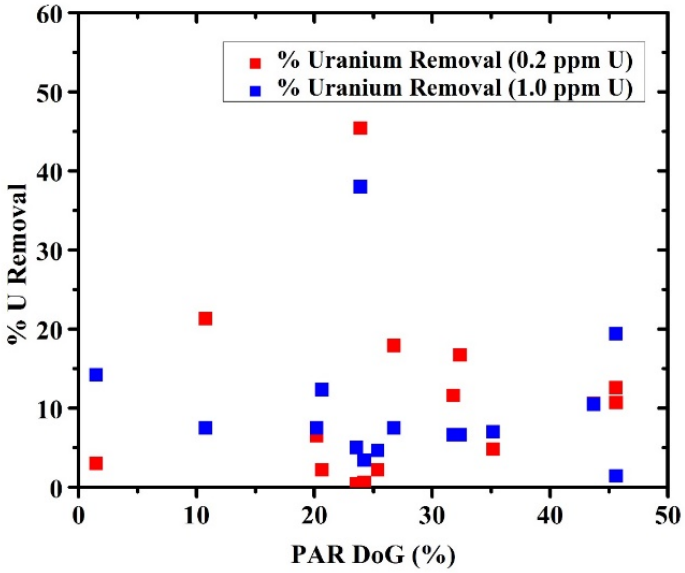

Figure 55 – A selection of samples produced by the irradiation grafting of VBC and then the chemical attachment of PAR with their % uranium removal from 10 mL of 0.2 ppm and 1.0 ppm U in seawater solution.

Unfortunately, these results were inconsistent with the ICP-MS based analysis of the fabrics after the fabrics were dissolved in 2% nitric acid as the amount of uranium on the surface of each fabric sample differed between the spectrophotometric and ICP-MS methods. This discrepancy is illustrated in Fig. 56. One reason for this difference could be that the incomplete dissolution of the nylon 6 fabric could have left some uranium trapped in the fabric. Due to the fact that acid and low pH solutions have been used to elute uranium off of fabrics in other research, this explanation is less likely and can be refuted with the implementation of perchloric dissolution. A more likely possibility is that the indirect nature of the spectrophotometric method resulted in an incorrect determination of the total uranium adsorbed by the fabrics, however refinement of the ICP-MS analysis for this particular system is required before this can be established.

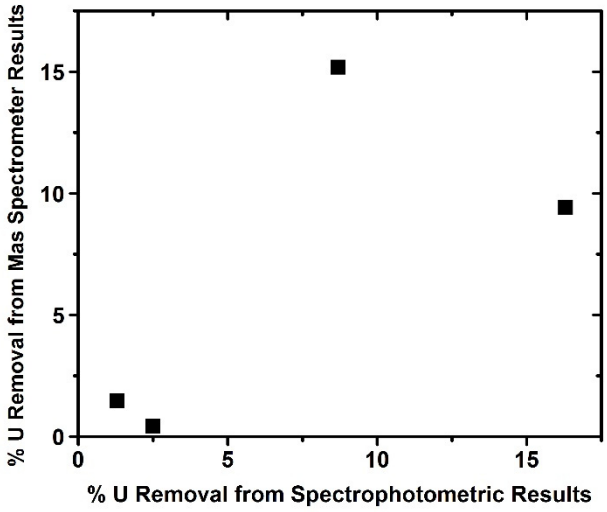

Figure 56 – The calculated % U removal by the spectrophotometric method did not correlate linearly with the ICP-MS method exhibited by the lack of linearity (the linear fit has an R^2 value of 0.19) in the distribution of the various samples.

To test if the azo grafted nylon 6 fabrics would be capable of extracting uranium from natural seawater, grafted fabric samples were placed in the seawater flow loop for seven days while being exposed to a flow rate of about 1.4 liters per minute, which is within the same range of flow rates used by Pacific Northwest National Laboratory in their flow-through column exposures.[25] Through the use of laser ablation ICP-MS, these fabrics were tested for the concentration of uranium on their surface.

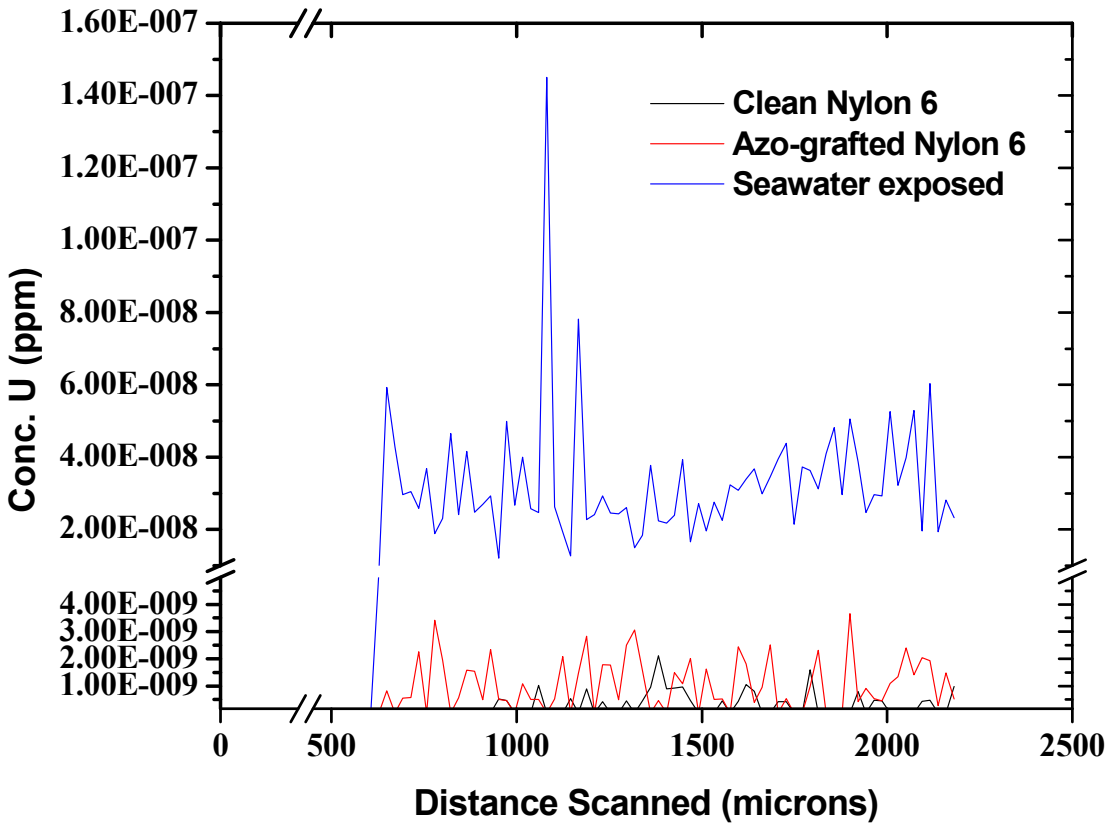

Figure 57 – Concentration of uranium on the surface of clean nylon 6, azo-grafted nylon 6, and seawater exposed nylon 6. The exposed nylon 6 sample was placed in the flow loop for one week, which contained natural concentrations of seawater.

The results of line scans of the laser over a distance of about 2 mm on the fabric, as shown in Fig. 57, show that the azo fabric was able to remove uranium from the seawater. The concentration of uranium however was extremely small and therefore it is difficult to ascertain if this uranium is merely residual uranium salts present on the surface of the fabric following the exposure that are not actually bound to the azo groups.

By using the laser ablation apparatus to drill a hole into the exposed fabric at two different locations and for different time periods, as shown in figure 58, it is clearly shown that the concentration of uranium on the fabric is limited mainly to the surface of the fabric.

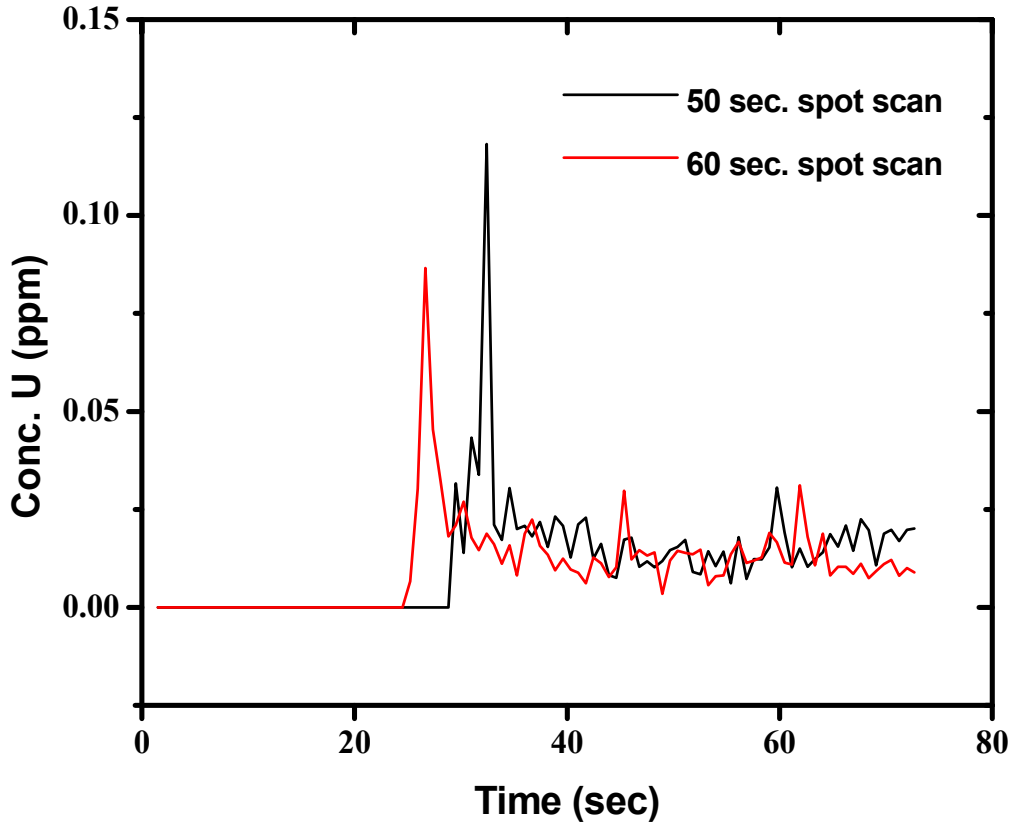

Figure 58 – Laser ablation of the seawater exposed, azo grafted fabric in a single location with an 80 µm beam diameter. The 0 ppm concentration shown in the first 20-25 seconds was performed to obtain a background as the laser was not on in this time frame.

Non-Radiation Synthesis of Uranium Extracting Materials Using Artificial Polymers

Non-radiation synthesis methods were also employed to attach the uranium extracting monomers to the surface of polymer fabrics. Specifically, nitroxides were chosen as the radical initiators for the grafting process. The nitroxide free radical chosen is the 4-hydroxy-2,2,6,6-tetramethylpiperidin-1-oxyl (TEMPOL). The hydroxy functional group ensures that this dissolves in polar solvents like DMSO and water. B2MP was the monomer selected for non-radiation grafting with artificial polymer fabrics. 0.636M B2MP solution was mixed with solutions of nitroxide to initiate and propagate the grafting of B2MP on winged nylon fabric.

DoGs as high as 56% were obtained for B2MP-grafted fabrics using non-radiation based, nitroxide grafting methods. It was found that higher reaction temperatures led to higher DoGs, though the trend was not statistically strong, as shown in Fig. 59. These fabrics were exposed to the reaction temperatures shown in Fig. 59 in solutions of TEMPOL and B2MP dissolved in 5 mL of ultra-high purity DI H_2O. The fabrics were subsequently washed using methanol and water rinses, and dried to a constant mass.

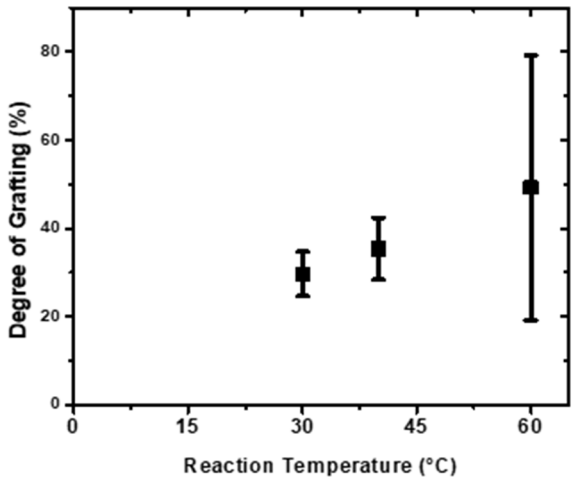

Figure 59 – The dependence of DoG on the temperature of the monomer and nitroxide solution that the winged nylon 6 fabrics were exposed to.

Further increasing the reaction temperature of the solution could lead to improved uranium extraction.

Non-Radiation Synthesis of Uranium Extracting Materials Using Natural Polymers

In additional to using artificial polymer fabrics, natural plant-based fibers have also been examined for the ability to extract uranium from seawater following attachment of uranium absorbing groups such as B2MP. Natural plant-based fibers contain cellulose, hemicellulose, and lignin. Plant-based fibers are naturally hydrophilic. Hydrophilicity of the backbone fiber is crucial in U-adsorption, because the more hydrophilic the adsorbent the greater the diffusion of seawater into the material, resulting to higher probability of interaction between uranyl and the grafted ligands. Hence, higher U-adsorption. Coir fibers shall serve as the backbone fiber in this adsorbent concept because it is hydrophilic, biodegradable, and demonstrates resilience against salt water and sunlight damages.[32] In fact, preliminary work had revealed that raw coir has a natural ability to adsorb U at approximately 0.008g-U/kg-ads. Free radical reactions shall be used for grafting ligand-monomers onto the backbone fibers. And because plant fibers are susceptible to decomposition upon irradiation, this thesis shall utilize persistent free radicals (e.g. nitroxide free radicals) and hydroxyl free radicals for the grafting process. A consequential benefit in not using irradiation chemistry is the savings in the synthesis cost.

Evidence of grafting

A noticeable difference between the two synthesis methods is that B2MP-coir via hydroxyl free radicals form products with B2MP gel coatings. This is not entirely unexpected because hydroxyl free radicals are strong electrophiles that strongly favors to undergo addition reaction to unsaturated aliphatic compounds and aromatic molecules. This means that it is possible for free

radical reactions to occur on the unsaturated tips of the B2MP-monomers. This may result in 2 different products: (1) grafted B2MP are crosslinked resulting to the coating of fibers or (2) formation of ungrafted crosslinked B2MP byproducts. Long durations of sonication did not remove these B2MP gel coatings. Also, these gel coatings appear to be very difficult to remove the closer it is on the surface of the fibers, without breaking off some of the fiber. This gelation is not observed in DAOx-coir adsorbents synthesized in the same free radicals.

FTIR spectra of raw coir fibers show the absence of phosphate and oxalate signatures. And FTIR spectra of B2MP-coir adsorbents confirm the addition of the phosphate signature as shown in Fig. 60, indicating successful grafting. This confirmation is observed for both synthesis methods. FTIR of DAOx-coir adsorbents, also confirms the addition of the oxalate signature as shown in Fig. 61, indicating successful grafting. However, this confirmation is only observed in DAOx-coir adsorbents synthesized via hydroxyl free radicals. In addition, both B2MP- and DAOx-coir adsorbents show an additional alkene (from the alkenyl C-H bond), and this suggests that the products do not polymerize on both unsaturated ends of the ligand-monomers.

SEM and EDS images of B2MP-coir adsorbents synthesized via NMP and hydroxyl free radicals are shown in Fig. 62 and Fig. 63, respectively. EDS images of both adsorbents show high concentrations of carbon and oxygen. The conclusion from these EDS images is that B2MP-coir adsorbents synthesized via NMP form uniform grafting on the surface of the fibers, as shown in Fig. 62(d). While synthesis via hydroxyl free radicals do not, as shown in Fig. 63(d).

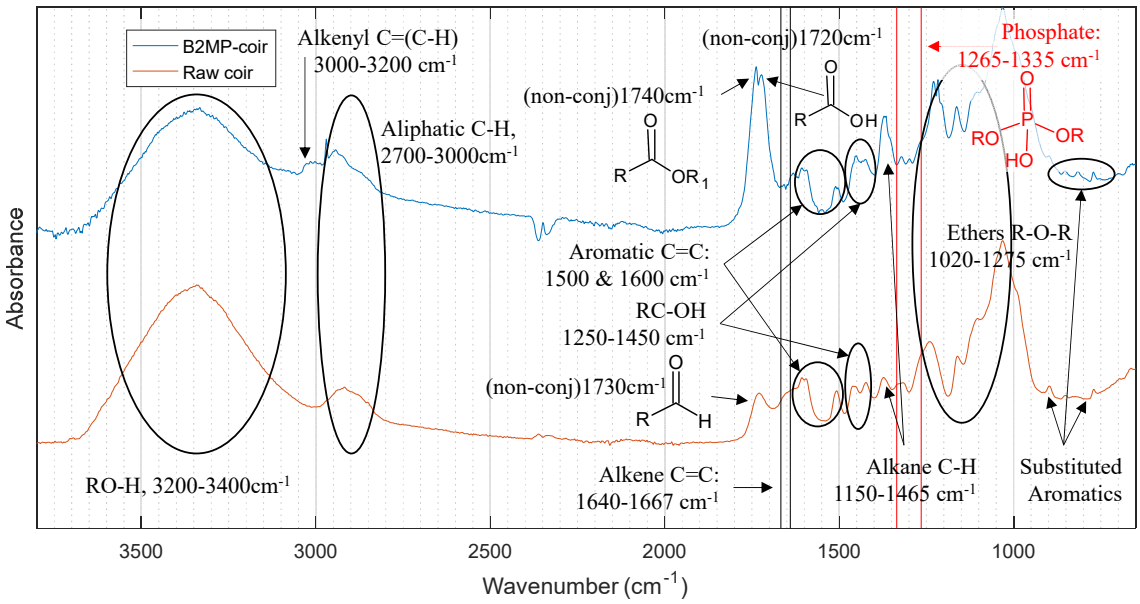

Figure 60 - FTIR of raw coir and B2MP-coir.

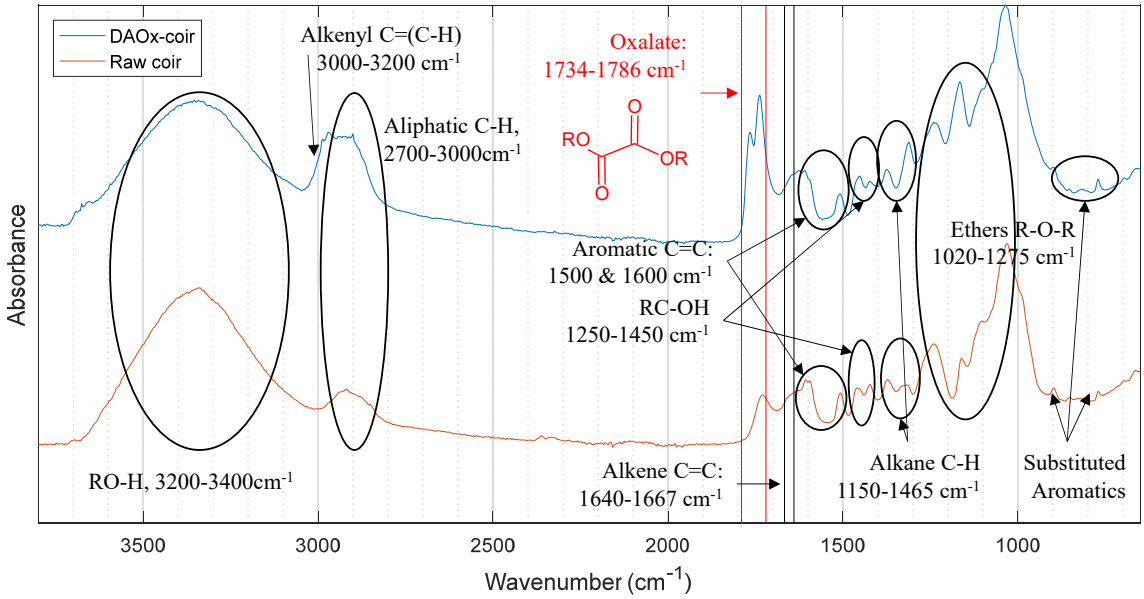

Figure 61 - FTIR of raw coir and DAOx-coir.

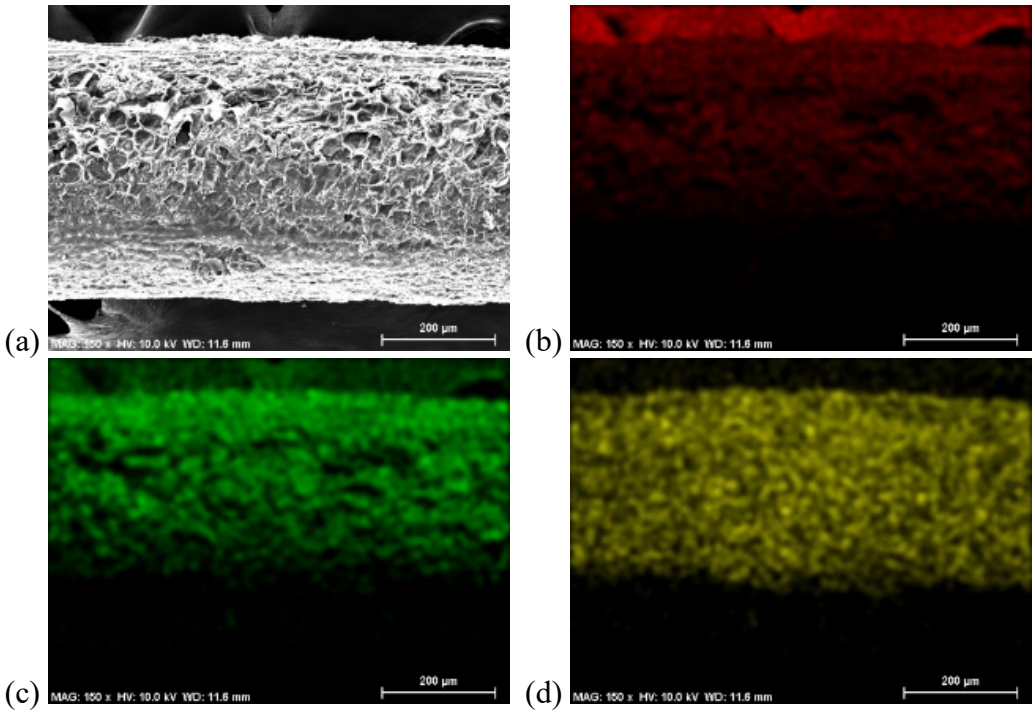

Figure 62 - (a) SEM and (b)-(d) EDS images of B2MP-coir synthesized via NMP. (b) carbon, (c) oxygen, (d) phosphorus content. **Image MAG: 150x, HV: 10.0kV**

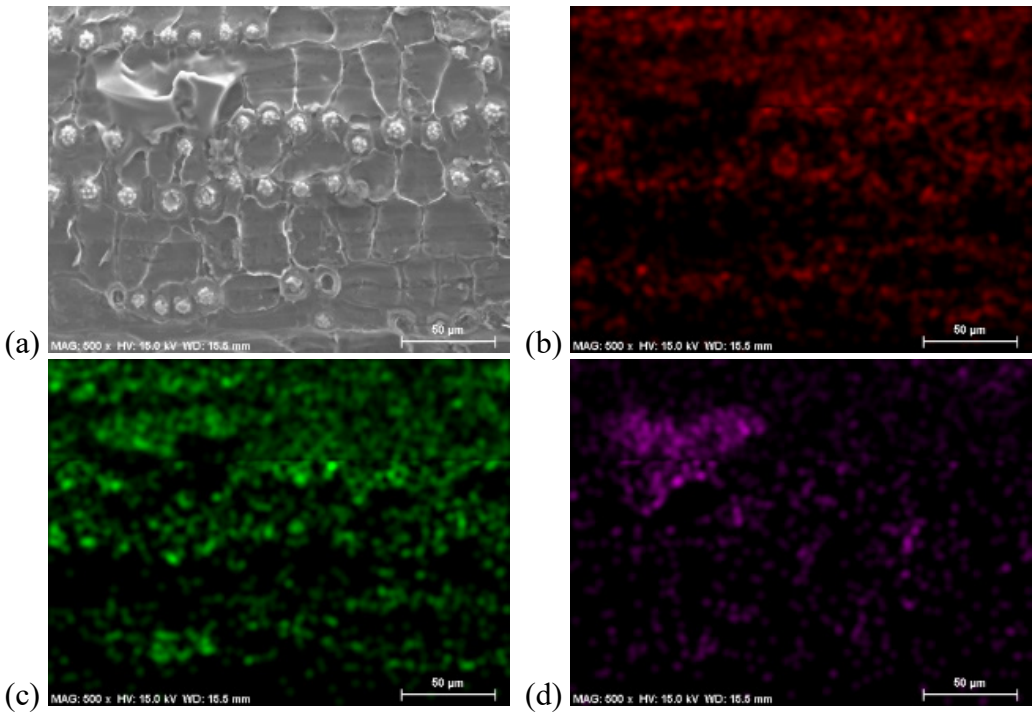

Figure 63 - (a) SEM and (b)-(d)EDS images of B2MP-coir synthesized via hydroxyl free radicals. (b) carbon, (c) oxygen, (d) phosphorus content. **Image MAG: 500x, HV: 15.0kV**

Uranium adsorption in seawater results

B2MP- and DAOx-coir adsorbents were tested in real seawater conditions at PNNL's marine testing facility in Sequim Bay, WA. The adsorbents were exposed to freshly pumped seawater from the bay at 250-300 mL/min at room temperature with an average salinity of 31.5 parts per thousand. The adsorbents were exposed to seawater at various durations to determine their optimal exposure times. The test sample size was quite low and no meaningful statistical information may be derived from the results, however, it reveals that U-adsorption is possible at normal concentrations of U in seawater, as shown in Fig. 64 below. And it is obvious that more work needs to be done to determine the kinetics of U-adsorption of the synthesized adsorbents in seawater conditions.

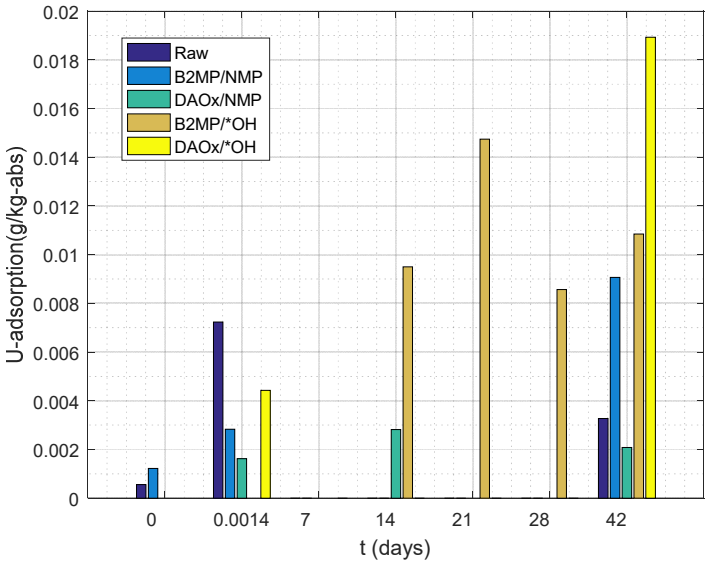

Figure 64 - U-uptake in real seawater normalized to salinity of 35 parts per thousand.

IV. Achieving Multi-Cycle Loading Capacity of ≥20 mg/g

The final milestone activity for this project was obtaining a multi-cycle uranium loading capacity of ≥20 mg U/g adsorbent. Multicycle uranium extracting testing was performed using fabrics grafted with B2MP using nitroxide, non-radiation based grafting. The fabrics were exposed to 20 mL of 26 ppm U in artificial seawater for 2 days in a rotator operating at 30 rpm. Following each exposure cycle, the fabrics were removed from solution, the solution was tested for uranium concentration change using the spectrophotometric method, the fabrics were washed three times with 0.26 M ammonium oxalate solution in an attempt to strip the fabrics of their chelated uranyl ions, and the fabrics were put back into solution for another cycle. While the fabrics used in these experiments were not able to obtain ≥20 mg U/g adsorbent per cycle, as shown in Fig. 65, it is believe that the fabrics under the same conditions except with additional 26 ppm U solution would be able to reach 20 mg/g loading capacities per cycle.

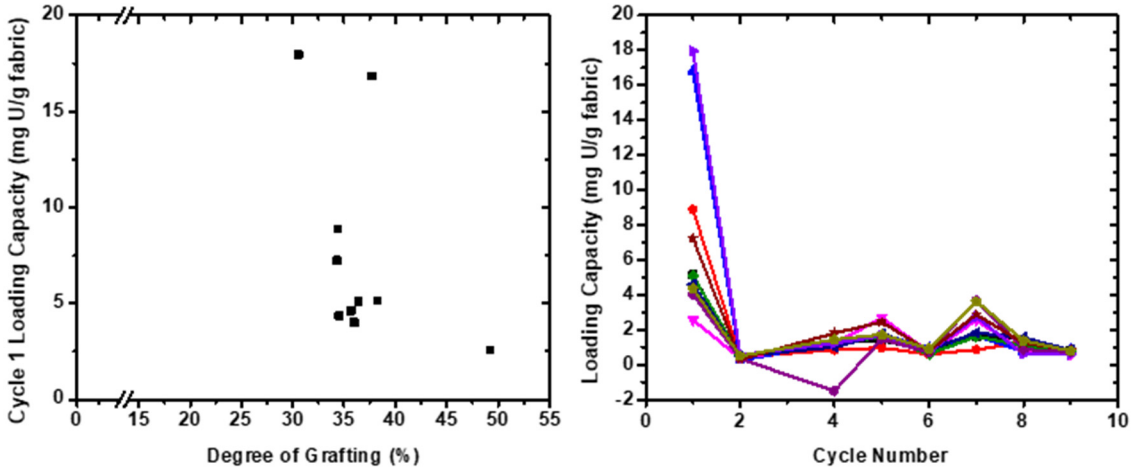

Figure 65 – The initial loading capacities of the fabrics (right) and the per-cycle loading capacities of the various fabrics tested (left).

Taking the highest performing fabric, this fabric had about 5.51 mg of B2MP grafted to its surface (the fabric had an initial mass of 18.03 mg and a final grafted mass of 23.54 mg with a DoG of 35.7%), which is equivalent to 1.71×10^{-5} mol of phosphate groups on the surface. Assuming that at least two phosphate groups are required for chelating the uranyl ions, the theoretical maximum moles of uranyl that can be bound to this fabric is 8.55×10^{-6} mol, which is equivalent to 2.03 mg of uranyl. Therefore the theoretical maximum loading capacity for uranium on this example B2MP fabric is 86.2 mg U/g adsorbent.

These conditions and considerations would indicate that the fabrics produced under this project are capable of achieving the ≥20 mg U/g adsorbent multicycle loading capacities. Using novel uranyl stripping methods developed by Pan, et al., along with the observation that the fabrics experienced no observable physical degradation at least during the initial five extraction cycles, the fabrics should be capable of achieving ≥20 mg U/g adsorbent multi-cycle loading capacities.[33]

V. Summary of Major Achievements

- Fabrics capable of extracting uranium from seawater have been created through the use of novel functional groups and radiation grafting techniques. More specifically:
  - Optimal radiation grafting methods based on predicted grafting mechanisms for phosphate, oxalate, and azo ligands have been established
  - Pulse radiolysis measurements have elucidated the kinetics and polymerization behavior of DAOx and B2MP in aqueous solution
  - Nylon 6 radical kinetics for winged nylon 6 fabrics have been established
- The various grafted fabrics, following the confirmation of the attachment of the functional group, are capable of extracting uranium from a seawater environment
- The various grafted fabrics, following the confirmation of the attachment of the functional group, are capable of extracting uranium from a seawater environment
- Nitroxide free radicals are implemented for grafting and not only for polymerization.

- Hydroxyl free radicals are implemented for synthesis of novel materials, as opposed to using it as an oxidizer, sanitizer, and disinfectant.
- Enhanced understanding of B2MP-uranyl and DAOx-uranyl coordinations and how well these ligands compete against carbonate ions in aqueous media.
- Made uranium extraction more economical than uranium mining, resulting to dramatic cost savings in the generation of electricity

VI. Publications and Presentations

Publications

1. Dietz, T.C., Al-Sheikhly, M. Two-step, Covalent Attachment of 4-(2-Pyridylazo) Resorcinol to Winged Nylon 6 Fabric for the Extraction of Uranium from Seawater. *In preparation.*
2. Dietz, T.C., Tsinas, Z., Pazos, I., Poster, D. Cumberland, L. Bateman, F.B., Grills, D., Wishart, J., Al-Sheikhly M. Radiation Grafting of Bis[2-(methacryloxy)ethyl] phosphate onto Nylon 6 for the Extraction of Uranium from Seawater. *In preparation.*
3. Dietz, T. C. Synthesis of Novel Co-Polymers Using Ionizing Radiation Grafting Methods for the Extraction of Uranium from Seawater. **2017**. https://doi.org/https://doi.org/10.13016/M2FB4WN79.
4. Dietz, T.C., Tomaszewski, C.E., Tsinas, Z., Poster, D., Barkatt, A., Adel-Hadadi, M., Bateman, F.B., Cumberland, L.T., Schneider, E., Gaskell, K., LaVerne, J., Al-Sheikhly, M. Uranium Removal from Seawater by Means of Polyamide 6 Fibers Directly Grafted with Diallyl Oxalate through a Single-Step, Solvent-Free Irradiation Process. Ind. Eng. Chem. Res. **2016**, *55* (15), 4179-4186. doi: 10.1021/acs.iecr.5b03401

Presentations

1. T.C. Dietz, et al. “Radiation Grafted Fabrics for the Extraction of Uranium From Seawater." 2017 ANS Winter Meeting & Expo, Washington, D.C., November, 2017.
2. T.C. Dietz, et al. \Azo Functionalized, Hydrophilic Fabrics for the Extraction of Uranium from Seawater.” 254th ACS National Meeting & Exhibition, Washington, D.C., August, 2017.
3. T.C. Dietz. “Radiation Grafted, Copolymerized Fabrics for the Extraction of Uranium from Seawater.” Materials Research Society Spring Meeting, Phoenix, AZ, April, 2017.
4. T.C. Dietz, A. Barkatt, M. Al-Sheikhly. “Azo Functionalized Fabrics for the Extraction of Uranium from Seawater.” American Nuclear Society Student Conference, Pittsburgh, PA, April, 2017.
5. T.C. Dietz. “Azo Functionalized Fabrics for the Extraction of Uranium From Seawater.” Graduate Research Appreciation Day, College Park, MD, April, 2017. Awarded First place for oral presentation in Environmental Chemistry session.
6. T.C. Dietz. “Azo and Oxalate Functionalized Fabrics for the Extraction of Uranium from Seawater.” International Conference on Ionizing Processes, Upton, NY, October, 2016.
7. T.C. Dietz, D. M. Bartels, M. Al-Sheikhly.”Method to Determine the Critical Hydrogen

Concentration in α-particle Irradiated Water." ANS Student Conference 2016, Madison, WI, April, 2016.
8. T.C. Dietz, et al. "Improvement of the radiation grafting of selective ligands onto polymeric substrates to produce high-capacity adsorbents for harvesting uranium from seawater." The Council on Ionizing Radiation Measurements and Standards Annual Conference 2015, Gaithersburg, MD, March, 2015.

VII. Acknowledgements

- The Radiation Physics Division of the National Institute of Science and Technology, specifically Dr. Lisa Karam, Dr. Fred Bateman, and Dr. Lonnie Cumberland
- Maryland NanoCenter
- Tim Maugel with The Laboratory for Biological Ultrastructure at UMD
- Dr. Karen Gaskell with the Materials Research Science and Engineering Center at the University of Maryland
- Dr. Gary Gill at Pacific Northwest National Laboratory
- Dr. Kim Morehouse at Food and Drug Administration
- Dr. Richard Ash for his help with ICP-MS measurements
- Dr. Jim Wishart, Dr. David Grills, and Mr. Bobby Layne at Brookhaven National Lab for their help with the pulse radiolysis measurements

VIII. References

(1) Seko, N.; Katakai, A.; Hasegawa, S.; Tamada, M.; Kasai, N.; Takeda, H.; Sugo, T.; Saito, K. Aquaculture of Uranium in Seawater by a Fabric-Adsorbent Submerged System. *Nucl. Technol.* **2003**, *144* (2), 274–278. https://doi.org/10.13182/NT03-2.

(2) Zhang, A.; Asakura, T.; Uchiyama, G. The Adsorption Mechanism of Uranium(VI) from Seawater on a Macroporous Fibrous Polymeric Adsorbent Containing Amidoxime Chelating Functional Group. *Reactive and Functional Polymers* **2003**, *57* (1), 67–76. https://doi.org/10.1016/j.reactfunctpolym.2003.07.005.

(3) Seko, N.; Katakai, A.; Tamada, M.; Sugo, T.; Yoshii, F. Fine Fibrous Amidoxime Adsorbent Synthesized by Grafting and Uranium Adsorption–Elution Cyclic Test with Seawater. *Separation Science and Technology* **2004**, *39* (16), 3753–3767. https://doi.org/10.1081/SS-200042997.

(4) Hou, Z.; Chen, S.; Sheng, K. Distribution of Acrylic Acid Grafted Chains Introduced into Polyethylene Film by Simultaneous Radiation Grafting with Water and Ethanol as Solvents. *J. Appl. Polym. Sci.* **2007**, *103* (3), 1570–1577. https://doi.org/10.1002/app.25351.

(5) Biswal, J.; Kumar, V.; Bhardwaj, Y. K.; Goel, N. K.; Dubey, K. A.; Chaudhari, C. V.; Sabharwal, S. Radiation-Induced Grafting of Acrylamide onto Guar Gum in Aqueous Medium: Synthesis and Characterization of Grafted Polymer Guar-g-Acrylamide. *Radiation Physics and Chemistry* **2007**, *76* (10), 1624–1630. https://doi.org/10.1016/j.radphyschem.2006.11.014.

(6) Yu, H.; Mo, X.; Peng, J.; Zhai, M.; Li, J.; Wei, G.; Zhang, X.; Qiao, J. Radiation-Induced Grafting of Multi-Walled Carbon Nanotubes in Glycidyl Methacrylate–Maleic Acid Binary

Aqueous Solution. *Radiation Physics and Chemistry* **2008**, *77* (5), 656–662. https://doi.org/10.1016/j.radphyschem.2007.11.010.
(7) Tamada, M. Current Status of Technology for Collection of Uranium from Seawater. *Japan Atomic Energy Agency* **2009**.
(8) Saito, T.; Brown, S.; Chatterjee, S.; Kim, J.; Tsouris, C.; Mayes, R. T.; Kuo, L.-J.; Gill, G.; Oyola, Y.; Janke, C. J.; et al. Uranium Recovery from Seawater: Development of Fiber Adsorbents Prepared via Atom-Transfer Radical Polymerization. *J. Mater. Chem. A* **2014**, *2* (35), 14674–14681. https://doi.org/10.1039/C4TA03276D.
(9) Johnson, D. A.; Florence, T. M. Spectrophotometric Determination of Uranium(vi) with 2-(5-Bromo-2-Pyridylazo)-5-Diethylaminophenol. *Analytica Chimica Acta* **1971**, *53* (1), 73–79. https://doi.org/10.1016/S0003-2670(01)80072-6.
(10) Hoon Seun Chang; Young Kun Kong; Chong Kwang Lee; Jae Ho Choi. Radiation-Induced Graft Copolymerization of Acrylic Acid onto Polyester. *Journal of the Korean Nuclear Soceity* **1977**, *9* (2), 65.
(11) Hu, J.; Ma, H.; Xing, Z.; Liu, X.; Xu, L.; Li, R.; Lin, C.; Wang, M.; Li, J.; Wu, G. Preparation of Amidoximated Ultrahigh Molecular Weight Polyethylene Fiber by Radiation Grafting and Uranium Adsorption Test. *Industrial & Engineering Chemistry Research* **2015**. https://doi.org/10.1021/acs.iecr.5b03175.
(12) Das, S.; Oyola, Y.; Mayes, R. T.; Janke, C. J.; Kuo, L.-J.; Gill, G.; Wood, J. R.; Dai, S. Extracting Uranium from Seawater: Promising AF Series Adsorbents. *Industrial & Engineering Chemistry Research* **2016**, *55* (15), 4110–4117. https://doi.org/10.1021/acs.iecr.5b03136.
(13) Das, S.; Oyola, Y.; Mayes, R. T.; Janke, C. J.; Kuo, L.-J.; Gill, G.; Wood, J. R.; Dai, S. Extracting Uranium from Seawater: Promising AI Series Adsorbents. *Industrial & Engineering Chemistry Research* **2016**, *55* (15), 4103–4109. https://doi.org/10.1021/acs.iecr.5b03135.
(14) Brown, S.; Chatterjee, S.; Li, M.; Yue, Y.; Tsouris, C.; Janke, C. J.; Saito, T.; Dai, S. Uranium Adsorbent Fibers Prepared by Atom-Transfer Radical Polymerization from Chlorinated Polypropylene and Polyethylene Trunk Fibers. *Industrial & Engineering Chemistry Research* **2016**, *55* (15), 4130–4138. https://doi.org/10.1021/acs.iecr.5b03667.
(15) Chemical Compatibility http://www.spectrumlabs.com/dialysis/Compatibility.html (accessed May 13, 2016).
(16) Chappas, W.; Pourdeyhimi, B. United States Patent: 8410006 - Composite Filter Media with High Surface Area Fibers. 8410006, April 2, 2013.
(17) Overview Alanine Dosimeter Reader EPR - Radiation dosimetry and EPR dosimetry for free radicals detection | Bruker https://www.bruker.com/products/mr/epr/e-scan/alanine-dosimeter-reader/overview.html (accessed Aug 31, 2017).
(18) Grills, D. C.; Cook, A. R.; Fujita, E.; George, M. W.; Preses, J. M.; Wishart, J. F. Application of External-Cavity Quantum Cascade Infrared Lasers to Nanosecond Time-Resolved Infrared Spectroscopy of Condensed-Phase Samples Following Pulse Radiolysis. *Applied spectroscopy* **2010**, *64* (6), 563–570.
(19) Baxendale, J. H.; Stott, D. A. Pulse Radiolysis of Aqueous CNS–Solutions and the Rates of Hydroxyl-Radical Reactions. *Chemical Communications (London)* **1967**, No. 14, 699–700.
(20) Baxendale, J. H.; Bevan, P. L. T.; Stott, D. A. Pulse Radiolysis of Aqueous Thiocyanate and Iodide Solutions. *Transactions of the Faraday Society* **1968**, *64*, 2389–2397.

(21) Spinks, J. W. T.; Woods, R. J. *An Introduction to Radiation Chemistry*; Wiley: New York, 1964.
(22) Espenson, J. H. *Chemical Kinetics and Reaction Mechanisms*, 2nd ed.; McGraw-Hill, Inc., 1995; Vol. 102.
(23) Kasser, M. J. THE PHOTOCHEMISTRY OF POLYENYL RADICALS AND ITS APPLICATION TO UHMWPE FOR USE IN ARTIFICIAL CARTILAGE. **2009**.
(24) Instruments | Electron Paramagnetic Resonance (EPR) Facility https://epr.chem.wisc.edu/content/instruments (accessed Oct 22, 2017).
(25) Gill, G. A.; Kuo, L.-J.; Janke, C. J.; Park, J.; Jeters, R. T.; Bonheyo, G. T.; Pan, H.-B.; Wai, C.; Khangaonkar, T.; Bianucci, L.; et al. The Uranium from Seawater Program at the Pacific Northwest National Laboratory: Overview of Marine Testing, Adsorbent Characterization, Adsorbent Durability, Adsorbent Toxicity, and Deployment Studies. *Industrial & Engineering Chemistry Research* **2016**, *55* (15), 4264–4277. https://doi.org/10.1021/acs.iecr.5b03649.
(26) Takigami, S.; Matsumoto, I.; Nakamura, Y. Electron Spin Resonance Study of γ-Irradiated Nylon 6. *J. Appl. Polym. Sci.* **1981**, *26* (12), 4317–4330. https://doi.org/10.1002/app.1981.070261229.
(27) Verma, G. S. P.; Peterlin, A. Electron Spin Resonance Study of Mechanically Stretched Nylon-6 Fibers. *Kolloid-Z.u.Z.Polymere* **1970**, *236* (2), 111–115. https://doi.org/10.1007/BF02086622.
(28) Beltrami, D.; Cote, G.; Mokhtari, H.; Courtaud, B.; Moyer, B. A.; Chagnes, A. Recovery of Uranium from Wet Phosphoric Acid by Solvent Extraction Processes. *Chem. Rev.* **2014**, *114* (24), 12002–12023. https://doi.org/10.1021/cr5001546.
(29) Jang, J.; Jeong, Y.-K. Synthesis and Flame-Retardancy of UV-Curable Methacryloyloxy Ethyl Phosphates. *Fibers and Polymers* **2008**, *9* (6), 667–673.
(30) Wentrup-Byrne, E.; Grøndahl, L.; Suzuki, S. Methacryloxyethyl Phosphate-Grafted Expanded Polytetrafluoroethylene Membranes for Biomedical Applications. *Polymer International* **2005**, *54* (12), 1581–1588. https://doi.org/10.1002/pi.1902.
(31) Dainton, F. S.; Logan, S. R. Radiolysis of Aqueous Solutions Containing Nitrite Ions and Nitrous Oxide. *Trans. Faraday Soc.* **1965**, *61* (0), 715–722. https://doi.org/10.1039/TF9656100715.
(32) Coir - International Year of Natural Fibres http://naturalfibres2009.org/en/fibres/coir.html (accessed Dec 31, 2018).
(33) Pan, H.-B.; Wai, C. M.; Kuo, L.-J.; Gill, G.; Tian, G.; Rao, L.; Das, S.; Mayes, R. T.; Janke, C. J. Bicarbonate Elution of Uranium from Amidoxime-Based Polymer Adsorbents for Sequestering Uranium from Seawater. *Chemistry Select* **2017**, *2* (13), 3769–3774. https://doi.org/10.1002/slct.201700177.